RECUEIL DES ACTIVITES 2019 DU THEME "ARCHIVES & TRACEURS"

Sommaire

Avant-propos

2019 ….

LISTE DES PUBLICATIONS 2019

Publications dans des revues de rang A

- Publication donnant lieu à une fiche ci-après

Agosta C., Amory C., Kittel C., **Orsi** A., Favier V., Gallee H., van den Broeke M.R., Lenaerts J.T.M., van Wessem J.M., van de Berg W.J. ,Fettweis X. (2019) Estimation of the Antarctic surface mass balance using the regional climate model MAR (1979-2015) and identification of dominant processes. *Cryosphere* 13, 281-296.

- Albert P.G., Giaccio B., Isaia R., Costa A., Niespolo E.M., **Nomade** S., **Pereira** A., Rennes P.R., Hinchliffe A., Mark D.F., Brown R.J. ,Smith V.C. (2019) Evidence for a large-magnitude eruption from Campi Flegrei caldera (Italy) at 29 ka. *Geology* 47, 595-599.
- Alexandre A., Webb E., **Landais** A., Piel C., Devidal S., Sonzogni C., Couapel M., Mazur J.-C., **Pierre** M., **Prié** F., Vallet-Coulomb C., Outrequin C., Roy J. (2018) Effects of grass leaf anatomy, development and light/dark alternation on the triple oxygen isotope signature of leaf water and phytoliths: insights for a new proxy of continental atmospheric humidity. *Biogeosciences* 16, 4613-4625
- Antoine P., Lagroix F., Jordanova D., Jordanova N., Lomax J., Fuchs M., Debret M., Rousseau D.-D., **Hatté** C., Moine O. (2019) A remarkable Late Saalian loess (dust) accumulation in the Lower Danube at Harletz (Bulgaria). *Quaternary Science Reviews*, 207, 80-100

Bartl I., Hellemann D., **Rabouille** C., Schulz K., Tallberg P., Hietanen S. ,Voss M. (2019) Particulate organic matter controls benthic microbial N retention and N removal in contrasting estuaries of the Baltic Sea. *Biogeosciences* 16, 3543-3564.

- **Bazin** L., **Govin** A., **Landais** A., Lemieux-Dudon B., Genty D., **Michel** E., Siani G., **Nomade** S. (2019) Construction of a Tephra-Based Multi-Archive Coherent Chronological Framework for the Last Deglaciation in the Mediterranean Region. *Quaternary Science Reviews* 216, 47-57
- Beaumet J., Déqué M., Krinner G., **Agosta** C., Alias A. (2019) Effect of prescribed sea surface conditions on the modern and future Antarctic surface climate simulated by the ARPEGE atmosphere general circulation model. *The Cryosphere*, 13, 3023-3043.

Bréant C., **Dos Santos** C.L., **Agosta** C., **Casado** M., **Fourré** E., **Goursaud** S., **Masson-Delmotte** V., Favier V., **Cattani** O., **Prié** F., Golly B., **Orsi** A., Martinerie P. ,**Landais** A. (2019) Coastal water vapor isotopic composition driven by katabatic wind variability in summer at Dumont d'Urville, coastal East Antarctica. Earth and Planetary Science Letters 514, 37-47.

Bréant C., **Landais** A., **Orsi** A., Martinerie P., **Extier** T., **Prié** F., Stenni B., **Jouzel** J., **Masson-Delmotte** V., Leuenberger M. (2019) Unveiling the anatomy of Termination 3 using water and air isotopes in the Dome C ice core, East Antarctica. Quat. Sci. Rev. 211, 156-165.

Camino-Serrano M., Tifafi M., Balesdent J., **Hatté** C., Peneulas J., Cornu S., Guenet B. (in press) Including stable carbon isotopes to evaluate the dynamics of soil carbon in the land-surface model ORCHIDEE. *Journal of Advances in Modeling Earth Systems*. doi: 10.1029/2018MS001392.

Chaabane S., Lopez Correa M., Ziveri P., Trotter J., Kallel N., **Douville** E., McCulloch M., Taviani M., Linares C., Montagna P. (2019) Elemental systematics of the calcitic skeleton of Corallium rubrum and implications for the Mg/Ca temperature proxy. *Chemical Geology* 524, 237-258.

Chauvet F., Geoffroy L., **Guillou** H., Maury R.C., Le Gall B., Agranier A., Viana A. (2019) Eocene ocntinental breakup in Baffin Bay. *Tectonophys*. 757, 170-186.

Colin C., **Tisnérat-Laborde** N., Mienis F., Collart T., **Pons-Branchu** E., Dubois-Dauphin Q., Frank N., **Dapoigny** A., Ayache M., Swingedouw D., Dutay J.C., Eynaud F., Debret M., **Blamart** D., **Douville** E. (2019) Millenial-scale variations of the Holocene North Atlantic mid-depth gyre inferred from radiocarbon and neodymium isotopes in cold water corals. *Quat. Sci. Rev.* 211, 93-106.

Columbu A., Drysdale R., Hellstrom J., Woodhead J., Cheng H., Hua Q., Zhao J.-x., Montagna P., **Pons-Branchu** E , Edwards R.L. (2019) U-Th and radiocarbon dating of calcite speleothems from gypsum caves (Emilia Romagna, North Italy). *Quaternary Geochronology* 52, 51-62.

Coogan L.A., **Daëron** M., Gillis K.M. (2019) Seafloor weathering and the oxygen isotope ratio in seawater: Insight from whole-rock $\delta^{18}O$ and carbonate $\delta^{18}O$ and Δ_{47} from the Troodos ophiolite. Earth Planet. Sci. Lett. 508, 41-50.

- **Cuny-Guirriec** K., **Douville** E., Reynaud S., Allemand D., Bordier L., **Canesi** M., Mazzoli C., Taviani M., Canese S., McCulloch M., Trotter J., Damian Rico-Esenaro S., Sanchez-Cabeza J.-A., Carolina Ruiz-Fernandez A., Carricart-Ganivet J.P., Scott P.M., Sadekov A., Montagna P. (2019) Coral Li/Mg thermometry: Caveats and constraints. *Chemical Geology* 523, 162-178.

Daëron M., Drysdale R.N., **Péral** M., Huyghe D., **Blamart** D., Coplen T.B., Lartaud F., Zanchetta G. (2019) Most Earth-surface calcites precipitate out of isotopic equilibrium. *Nature Communications* 10, 429 – doi: 10.1038/s41467-019-08336-5

Damian Rico-Esenaro S., Sanchez-Cabeza J.-A., Carricart-Ganivet J.P., **Montagna** P., Carolina Ruiz-Fernandez A. (2019) Uncertainty and variability of extension rate, density and calcification rate of a hermatypic coral (Orbicella faveolata). *Science of the Total Environment* 650, 1576-1581.

Dang H., Wang T., Qiao P., **Bassinot** F., Jian Z. (2019) The B/Ca and Cd/Ca of a subsurface-dwelling foraminifera Pulleniatina obliquiloculata in the tropical Indo-Pacific Ocean: implications for the subsurface carbonate chemistry estimation. *Acta Oceanologica Sinica* 38, 138-150.

Daujeard C., Vettese D., Britton K., Béarez P., Boulbes N., Crégut-Bonnoure E., Desclaux E., Lateur N., Pike-Tay A., Rivals F., Allué E., Chacon M.G., Puaud S., Richard M., Courty M.A., Gallotti R., Hardy B., Bahain J.J., Falguères C., **Pons-Branchu** E., **Valladas** H., Moncel M.H. (2019). Neanderthal selective hunting of reindeer? The case study of Abri du Maras (south-eastern France). *Archaeological and Anthropological Sciences* 11, 985-1011.

Drugat L., **Pons-Branchu** E., **Douville** E., **Foliot** L., Bordier L., Roy-Barman M. (2019) Rare earth and alkali elements in stalagmites, as markers of Mediterranean environmental changes during Termination I. *Chemical Geology* 525, 414-423.

Dubois-Dauphin Q., Colin C., Elliot M., **Dapoigny** A., **Douville** E. (2019) Holocene shifts in sub-surface water circulation of the North-East Atlantic inferred from Nd isotopic composition in cold-water corals. *Marine Geology* 410, 135-145.

- **Durier** M.-G., Bruguière P., **Hatté** C., Vaiedelich S., **Gauthier** C., **Thil** F., **Tisnérat-Laborde** N. (2019) Radiocarbon dating of legacy music instrument collections: example of traditional Indian vina from the Musée de la Musique, Paris. *Radiocarbon*, 61(5), 1357-1366, doi: 10.1017/RDC.2019.71

Ehn J.K., Reynolds R.A., Stramski D., Doxaran D., **Lansard** B., Babin M. (2019) Suspended Particulate Matter in Canadian Beaufort Sea. *Biogeosciences* 16, 1583-1605.

Elliot M., Colin C., Douarin M., **Pons-Branchu** E., **Tisnerat-Laborde** N., Schmidt F., **Michel** E., Dubois-Dauphin Q., **Dapoigny** A., **Foliot** L., Miska S., **Thil** F., Long D., **Douville** E. (2019) Onset and demise of coral reefs, relationship with regional ocean circulation on the Wyville Thomson Ridge. *Marine Geology* 416, 105969.

Fauquembergue, K., Fournier, L., Zaragosi, S., **Bassinot, F., Kissel, C.,** Malaize, B., Caley, T., Moreno, E., Bachelery, P. (2019) Factors controlling frequency of turbidites in the Bengal fan during the last 248 kyr cal BP: Clues from a presently inactive channel. *Marine Geology*, 414, 105965. 10.1016/j.margeo.2019.105965

Ferranti L., Pace B., Valentini A., Montagna P., **Pons-Branchu** E., **Tisnerat-Laborde** N., Maschio L. (2019) Speleoseismological Constraints on Ground Shaking Threshold and Seismogenic Sources in the Pollino Range (Calabria, Southern Italy*). Journal of Geophysical Research-Solid Earth* 124, 5192-5216.

- Finke P., Opolot E., Balesdent J., Berhe A.A., Boeckx P., Cornu S., Harden J., **Hatté C.**, Trumbore S., Willians E., Doettrl S. (2019) Can SOC modelling be improved by accounting for pedogenesis? *Geoderma*, 338, 513-524. doi: 10.1016/j.geoderma.2018.10.018

Gandois L., Hoyt A., **Hatté** C., Jeanneau L., Teisserenc R., Liotaud M., Tananaev N. (in press) Contribution of peatland permafrost to dissolved organic matter along a thaw gradient in North Siberia. *Environmental Science and Technology*

Gao J., Yao T., **Masson-Delmotte** V., Steen-Larsen H.C., Wang W. (2019) Collapsing glaciers threaten Asia's water supplies. *Nature* 565, 19-21.

Giaccio B., Leicher N., Mannella G., Monaco L., Regattieri E., Wagner B., Zanchetta G., Gaeta M., Marra F., **Nomade S.**, Palladino D.M., **Pereira** A., Scheidt S., Sottili G., Wonik T., Wulf S., Zeeden C., Ariztegui D., Cavinato G.P., Dean J.R., Florindo F., Leng M.J., Macrì P., Niespolo E., Renne P., Rolf C., Sadori L., Thomas C., Tzedakis P.C. (2019) Extending the tephra and palaeoenvironmental record of the Central Mediterranean back to 430 ka: A new core from Fucino Basin, central Italy. *Quaternary Science Reviews* 225, 106003 – doi: 10.1016/j.quascirev.2019.106003

Goursaud S., **Masson-Delmotte** V., Favier V., Preunkert S., Legrand M., **Minster** B., Werner M. (2019) Challenges associated with the climatic interpretation of water stable isotope records from a highly resolved firn core from Adélie Land, coastal Antarctica. *The Cryosphere* 13, 1297-1324.

Gray W.R., Evans D., (2019) Non-thermal influences on Mg/Ca in planktonic foraminifera: A review of culture studies and application to the last glacial maximum. Paleoceanography and Paleoclimatology. 34, 306-315.

- **Guillou** H., **Scao** V., **Nomade** S., Van Vliet-Lanoë B., Liorzou C., Guomundsson A. (2019) 40Ar/39Ar dating of the Thormork ignimbrite and Icelandic sub-glacial rhyolites. Quaternary Science Reviews 209, 52-62.
- Hajdas I., Jull A.J.T., Huysecom E., Mayor A., Jean Renold M.-A., Synal H.-A., **Hatté C.**, Hong W., Chivall D., Beck L., Liccoli L., Fedi M., Friedrich R., Maspero F., Sava T. (2019) Radiocarbon dating and the protection of cultural heritage. *Radiocarbon*, 61(5), 1133-1134.

Isola I., Ribolini A., Zanchetta G., Bini M., Regattieri E., Drysdale R.N., Hellstrom J.C., Bajo P., Montagna P., **Pons-Branchu** E. (2019) Speleothem U/Th age constraints for the Last Glacial conditions in the Apuan Alps, northwestern Italy. *Palaeogeography Palaeoclimatology Palaeoecology* 518, 62-71.

Jean-Baptiste P., **Fontugne** M., **Fourré** E., Charmasson S., Marang L., Siclet F. (2019) Organically bound tritium (OBT) and carbon-14 accumulation in the sediments off the mouth of the Rhone river. *Environmental Earth Sciences* 78 – doi: 10.1007/s12665-019-8081-y.

Jean-Baptiste P., Genty D., **Fourré** E., **Régnier** E. (2019) Tritium dating of dripwater from Villars Cave (SW-France). *Applied Geochemistry* 107, 152-158.

Jenkins W.J., Doney S.C., Fendrock M., Fine R., Gamo T., **Jean-Baptiste** P., Key R., Klein B., Lupton J.E., Newton R., Rhein M., Roether W., Sano Y., Schlitzer R., Schlosser P. ,Swift J. (2019) A comprehensive global oceanic dataset of helium isotope and tritium measurements. *Earth System Science Data* 11, 441-454.

- Jourdan F., **Nomade** S., Wingate M.T.D., Eroglu E., Deino A. (2019) Ultraprecise age and formation temperature of the Australasian tektites constrained by $^{40}Ar/^{39}Ar$ analyses. *Meteoritics & Planetary Science* 54, 2573-2591.

Klein F., Abram N.J., Curran M.A.J., Goosse H., **Goursaud** S., **Masson-Delmotte** V., Moy A., Neukom R., **Orsi** A., Sjolte J., Steiger N., Stenni B., Werner M. (2019) Assessing the robustness of Antarctic temperature reconstructions over the past 2 millennia using pseudoproxy and data assimilation experiments. *Climate of the Past* 15, 661-684.

- Lahaye C., Guérin G., Gluchy M., **Hatté** C., **Fontugne** M., Clemente-Conte I., Santos J.C., Villagran X., Da Costa A., Borges C., Guidon N., Boeda E. (2019) Another site, same old song: the Pleistocene-Holocene archaeological sequence in Toca da Janela da Barra do Antonião-North, Piauí, Brazil. *Quaternary Geochronology*, 49, 223-229. doi: 10.1016/j.quageo.2018.03.006

Laruelle G.G., Marescaux A., Le Gendre R., Garnier J., **Rabouille** C., Thieu V. (2019) Carbon Dynamics Along the Seine River Network: Insight From a Coupled Estuarine/River Modeling Approach. *Frontiers in Marine Science* 6 – doi: 10.3389/fmars.2019.00216

Leng W., von Dobeneck T., Just J., **Govin A.,** St-Onge G., Piper D.J.W. (2019) Compositional changes in deglacial red mud event beds off the Laurentian Channel reveal source mixing, grain-size partitioning and ice retreat. *Quaternary Science Reviews*. 215, 98-115, doi: 10.1016/j.quascirev.2019.04.031.

- Lomax J., Fuchs M., Antoine P., Rousseau D.-D., Lagroix F., **Hatté** C., Taylor S., Till J., Debret M., Moine O., Jordanova D. (2019) Luminescence chronology of the Harletz loess sequence, Bulgaria. Boreas. 49(1), 179-184. doi: 10.1111/bor.12348

Lougheed B.C., Obrochta S.P. (2019) A rapid, deterministic age-depth modelling routine for geological sequences with inherent depth uncertainty. *Palaeoceanography and Palaeoclimology*. 34, 122-133.

Ma R., Sepulcre S., Licari L., **Bassinot** F., Liu Z., **Tisnérat-Laborde** N., Kallel N., Yu Z., Colin C. (2019) Changes in intermediate circulation in the Bay of Bengal since the Last Glacial Maximum as inferred from benthic foraminifera assemblages and geochemical proxies. Geochem. Geophys. Geosyst. 20, 1592-1608.

- Mannella G., Giaccio B., Znachetta G., Regattieri E., Niespolo E.M., **Pereira** A., Renne P.R., **Nomade** S., Leicher N., Perchiazzi N., Wagner B. (2019) Palaeoenvironmental and palaeohydrological variability of mountain areas in the central Mediterranean region: A 190 ka-long chronicle from the independently dated Fucino palaeolake record (central Italy). *Quaternary Science Reviews* 210, 190-210.

Marra F., Bahain J-J., Jicha B. R., **Nomade S.,** Palladino D.M., Pereira, A. Tolomei C., Voinchet P., Anzidei M., Aureli D., Ceruleo P., Falguères C., Florindo F., Gatta M., Ghaleb B., La Rosa M., Peretto C., Petronio C., Rocca R., Rolfo M. F., Salari L., Smedile A., Tromblet O. (2019) Reconstruction of the MIS 5.5, 5.3 and 5.1 coastal terraces in Latium

(central Italy): a re-evaluation of the sea-level history in the Mediterranean Sea during the Last Interglacial. *Quaternary International* 525, 54–77.

- Marra F., Florindo F., Jicha B.R., **Nomade** S., Palladino D.M., Pereira A., Sottili G., Tolomei C. (2019) Volcano-tectonic deformation in the Monti Sabatini Volcanic District at the gates of Rome (central Italy): evidence from new geochronologic constraints on the Tiber River MIS 5 terraces. *Scientific Reports* 9, 11496 – doi: 10.1038/s41598-019-47585-8.
- Menviel L., Capron E., **Govin** A., Dutton A., Tarasov L., Abe-Ouchi A., Drysdale R.N., Gibbard P.L., Gregoire L., He F., Ivanovic R.F., Kageyama M., Kawamura K., **Landais** A., Otto-Bliesner B.L., Oyabu I., Tzedakis P.C., Wolff E., Zhang X. (2019) The penultimate deglaciation: protocol for Paleoclimate Modelling Intercomparison Project (PMIP) phase 4 transient numerical simulations between 140 and 127 ka, version 1.0. *Geoscientific Model Development* 12, 3649-3685.
- **Missiaen** L., **Waelbroeck** C., Pichat S., Jaccard S.L., Eynaud F., Greenop R., Burke A. (2019) Improving North Atlantic Marine Core Chronologies Using Th-230 Normalization. *Paleoceanography and Paleoclimatology* 34, 1057-1073.
- Moncel M.-H., Santagata C., **Pereira** A., **Nomade** S., Bahain J.-J., Voinchet P., Piperno M. (2019) A biface production older than 600 ka ago at Notarchirico (Southern Italy) contribution to understanding early Acheulean cognition and skills in Europe. *Plos One* 14(10), e02224603 – doi: 10.1371/journal.pone.0224603.

Montaggioni L.F., Salvat B., Aubanel A., **Pons-Branchu** E., Martin-Garin B., Dapoigny A., Goeldner-Gianellla L. (2019) New insights into the Holocene development history of a Pacific, low-lying coral reef island: Takapoto Atoll, French Polynesia. *Quaternary Science Reviews* 223, 105947. doi: 10.1016/j.quascirev.2019.105947

Nave S., Lebreiro S., **Michel** E., **Kissel** C., Figueiredo M. O., A., **Labeyrie** L., Alberto A. (2019) The Atlantic Meridional Overturning Circulation as productivity regulator of the North Atlantic Subtropical Gyre. *Quaternary Research* 91(1), 399-413. doi : 10.1017/qua.2018.88.

- **Nomade** S., **Bassinot** F., Marino M., Simon Q., **Dewilde** F., Maiorano P., **Isguder** G., **Blamart** D., Girone A., **Scao** V., **Pereira** A., Toti F., Bertini A., Combourieu-Nebout N., **Péral** M., Bourlès D.L., Petrosino P., Gallicchio S., Ciaranfi N. (2019) High-resolution foraminifer stable isotope record of MIS19 at Montalbano Jonico, southern Italy : a window into Mediterranean climatic variability **Guihou** during a low-eccentricity interglacial. *Quaternary Science Reviews* 205, 106-125.

Pang H., Hou S., **Landais** A., **Masson-Delmotte** V., **Jouzel** J., Steen-Larsen H.C., Risi C., Zhang W., Wu S., Li Y., An C., Wang Y., **Prié** F., **Minster** B., **Falourd** S., Stenni B., Scarchilli C., Fujita K. ,Grigioni P. (2019) Influence of Summer Sublimation on delta D, delta O-18, and delta O-17 in Precipitation, East Antarctica, and Implications for Climate Reconstruction From Ice Cores. *Journal of Geophysical Research-Atmospheres* 124, 7339-7358.

Paul A., Balesdent J., **Hatté** C. (in press) ^{13}C-^{14}C relations reveal that soil 13C-depth gradient is linked to historical changes in vegetation ^{13}C. *Plant and Soil*

- **Paterne** M., Evrard O., **Hatté** C.**,** Laceby J. P., Nouet J., Onda Y. (2019) Radiocarbon and radiocesium in litter fall at Kawamata, 45km NW from the Fukushima Dai-Ichi nuclear power plant (Japan). Journal of Radioanalytical and Nuclear Chemistry, 319 (3), 1093-1101. doi: 10.1007/s10967-018-6360-9

Paterne M., **Michel** E., Héros V. (2019) Variability of marine ^{14}C reservoir ages in the Southern Ocean highlighting circulation changes between 1910 and 1950. *Earth and Planetary Science Letters* 511, 99-104.

Planes S., Allemand D., Agostini S., Banaigs B., Boissin E., Boss E., Bourdin G., Bowler C., **Douville** E., Flores J.M., Forcioli D., Furla P., Galand P.E., Ghiglione J.-F., Gilson E., Lombard F., Moulin C., Pesant S., Poulain J., Reynaud S., Romac S., Sullivan M.B., Sunagawa S., Thomas O.P., Trouble R., de Vargas C., Vega Thurber R., Voolstra C.R., Wincker P., Zoccola D., Tara Pacific Cruise members (2019) The Tara Pacific expedition-A pan-ecosystemic approach of the "-omics" complexity of coral reef holobionts across the Pacific Ocean. *PLoS biology* 17, e3000483-e3000483.

- **Rabouille**, C., Dennielou, B., Baudin, F., Raimonet, M., Droz, L., Khripounoff, A., Martinez, P., Mejanelle, L., Michalopoulos, P., Pastor, L., Pruski, A., Ragueneau, O., Reyss, J.L., Ruffine, L., Schnyder, J., Stetten, E., Taillefert, M., Tourolle, J., Olu, K. (2019) Carbon and silica megasink in deep-sea sediments near the Congo Canyon. *Quaternary Science Reviews*, 222, 105854 - doi: 10.1016/j.quascirev.2019.07.036.

Rapuc W., Sabatier P., Arnaud F., Palumbo A., Develle A.L., Reyss J.L., Augustin L., **Régnier** E., Piccin A., Chapron E., Dumoulin J.P., **von Grafenstein** U. (2019) Holocene-long record of flood frequency in the Southern Alps (Lake Iseo, Italy) under human and climate forcing. *Global Planetary Change* 175, 160-172.

- Regattieri E., Giaccio B., Mannella G., Zanchetta G., **Nomade** S., Tognarelli A., Perchiazzi N., Vogel H., Boschi C., Drysdale R.N., Wagner B., Gemelli M., Tzedakis P.C. (2019) Frequency and dynamics of millennial-scale variability

during Marine Isotope Stage 19: Insights from the Sulmona Basin (central Italy). *Quaternary Science Reviews* 214, pp.28-43

Richard M., Falguères C., **Pons-Branchu** E., **Foliot** L., Guillem P.M., Martinez-Valle R., Eixea A., Villaverde V. (2019) ESR/U-series chronology of early Neanderthal occupations at Cova Negra (Valencia, Spain). *Quaternary Geochronology* 49, 283-290.

Richard M., Falguères C., **Pons-Branchu** E., Richter D., Beutelspacher T., Conard N.J., Kind C.J. (2019) The Middle to Upper Palaeolithic transition in Hohlenstein-Stadel cave (Swabian Jura, Germany): A comparison between ESR, U-series and radiocarbon dating. *Quaternary International* - doi: 10.1016/j.quaint.2019.04.009

Richard M., Falgueres C., **Valladas** H., Ghaleb B., **Pons-Branchu** E., Mercier N., Richter D., Conard N.J. (2019) New electron spin resonance (ESR) ages from Geissenklosterle Cave: A chronological study of the Middle and early Upper Paleolithic layers. *Journal of Human Evolution* 133, 133-145.

Rico-Esenaro S.D., Sanchez-Cabeza J.A., Carricart-Ganivet J.P., **Montagna** P., Ruiz-Fernandez A.C. (2019) Uncertainty and variability of extension rate, density and calcification rate of a hermatypic coral (Orbicella faveolata). *Science of the Total Environment* 650(1), 1576-1581.

Rochette P., Alaç R., Beck P., Brocard G., Cavosie A.J., Debaille V., Devouard B., Jourdan F., Mougel B., Moustard F., **Nomade** S., Osinski G.R., Renard B., Cornec J. (2019) Pantasma: evidence for a Pleistocene circa 14km diameter impact crater in Nicaragua. Meteoritics and Planetary Science 54(3) – doi : 10.111/maps.13244

Roy-Barman M., **Thil** F., Bordier L., **Dapoigny** A., **Foliot** L., Ayrault S., Lacan F., Jeandel C., Pradoux C. ,Garcia-Solsona E. (2019) Thorium isotopes in the Southeast Atlantic Ocean: Tracking scavenging during water mass mixing along neutral density surfaces. *Deep-Sea Research Part I-Oceanographic Research Papers* 149, 103042.

Sagnotti L., Giaccio B., Liddicoat J.C., Carrichi C., **Nomade S.,** Renne P.R., On the reliability of the Matuyama-Brunhes record in the Sulmona Basin – Comment to "A reappraisal of the proposed rapid Matuyama-Brunhes geomagnetic reversal in the Sulmona Basin, Italy" by Evans and Muxworthy (2019). *Journal of Geophysical International* 216, 296-301

Schmitt A., Elliot M., Thirumalai K., La C., **Bassinot** F., Petersen J., Movellan A., Jorry S.J., Borgomano J. (2019) Single foraminifera Mg/Ca analyses of past glacial-interglacial temperatures derived from G. ruber sensu stricto and sensu lato morphotypes. *Chemical Geology* 511, 510-520.

Taviani M., Angeletti L., Cardone F., **Montagna** P., Danovaro R. (2019) A unique and threatened deep water coral-bivalve biotope new to the Mediterranean Sea offshore the Naples megalopolis. *Scientific Reports* 9, 3411 – doi: 10.1038/s41598-019-39665-8.

Taviani M., Angeletti L., Foglini F., Corselli C., Nasto I., **Pons-Branchu** E., **Montagna** P. (2019) U/Th dating records of cold-water coral colonization in submarine canyons and adjacent sectors of the southern Adriatic Sea since the Last Glacial Maximum. *Progress in O*ceanography 175, 300-308.

Thiebault T., Fougere L., Destandau E., Rety M., **Jacob** J. (2019) Impact of meteorological and social events on human-excreted contaminant loads in raw wastewater: From daily to weekly dynamics. *Chemosphere* 230, 107-116.

- Thöle L.M., Amsler H.E., Moretti S., Auderset A., Gilgannon J., Lippold J., Vogel H., Crosta X., **Mazaud** A., **Michel** E., Martinez-Garcia A., Jaccard S.L. (2019) Glacial-interglacial dust and export production records from the Southern Indian Ocean. Eart and Planetary Science Letters, 525, 115716.

Valet J.P., **Bassinot** F., Simon Q., Savranskaia T., Thouveny N., Bourles D.L., **Villedieu** A. (2019) Constraining the age of the last geomagnetic reversal from geochemical and magnetic analyses of Atlantic, Indian, and Pacific ocean sediments. *Earth and Planetary Science Letters* 506, 323-331.

Verfaillie D., Favier V., Gallée H., Fettweis X., Agosta C., Jomelli V. (2019) Regional modeling of surface mass balance on the Cook Ice Cap, Kerguelen Islands (49°S, 69°E). Clim. Dyn. 53, 5909-5925.

Waelbroeck C., **Lougheed** B.C., **Vazquez Riveiros** N., **Missiaen** L., Pedro J., Dokken T., Hajdas I., Wacker L., Abbott P., Dumoulin J.P., **Thil** F., Eynaud F., Rossignol L., **Fersi** W., Albuquerque A.L., Arz H., Austin W.E.N., Came R., Carlson A.E., Collins J.A., Dennielou B., Desprat S., Dickson A., Elliot M., Farmer C., Giraudeau J., Gottschalk J., Henderiks J., Hughen K., Jung S., Knutz P., Lebreiro S., Lund D.C., Lynch-Stieglitz J., Malaizé B., Marchitto T., Martinez-Mendez G., Mollenhauer G., Naughton F., Nave S., Nurnberg D., Oppo D., Peck V., Peeters F.J.C., Penaud A., Portilho-Ramos R.C., Repschlager J., Roberts J., Ruhlemann C., Salgueiro E., Sanchez-Goni M.F., Schonfeld J., Scussolini P., Skinner L.C., Skonieczny C., Thornalley D., Toucanne S., Van Rooij D., Vidal L., Voelker A.H.L., Wary M., Weldeab S., Ziegler M, (2019) Consistently dated Atlantic sediment cores over the last 40 thousand years. *Scientific Data* 6, 165 – doi: 10.1038/s41597-019-0173-8.

- Wagner B., Vogel H., Francke A., Friedrich T., Donders T., Lacey J.H., Leng M.J., Regattieri E., Sadori L., Wilke T., Zanchetta G., Albrecht C., Bertini A., Combourieu-Nebout N., Cvetkoska A., Giaccio B., Grazhdani A., Hauffe T., Holtvoeth J., Joannin S., Jovanovska E., Just J., Kouli K., Kousis I., Koutsodendris A., Krastel S., Lagos M., Leicher N., Levkov Z., Lindhorst K., Masi A., Melles M., Mercuri A.M., **Nomade** S., Nowaczyk N., Panagiotopoulos K., Peyron O., Reed J.M., Sagnotti L., Sinopolo G., Stelbrink B., Sulpizio R., Timmermann A., Tofilovska S., Torri P., Wagner-Cremer F., Wonik T., Zhang X. (2019) Mediterranean winter rainfall in phase with African monsoons during the past 1.36 million years. Nature (2019) 573, 7773, 256-260. https://doi.org/10.1038/s41586-019-1529-0
- Wang F., Shi W., **Guillou** H., Zhang W., Yang L., Wu L., Wang Y., Zhu R. (2019) A new unspiked K-Ar dating approach using laser fusion on microsamples. Rapid Communications in Mass Spectrometry 33, 587-599.

Wei Z., Lee X., Aemisegger F., Benetti M., Berkelhammer M., **Casado** M., Caylor K., Christner E., Dyroff C., Garcia O., Gonzalez Y., Griffis T., Kurita N., Liang J., Liang M.-C., Lin G., Noone D., Gribanov K., Munksgaard N.C., Schneider M., Ritter F., Steen-Larsen H.C., Vallet-Coulomb C., Wen X., Wright J.S., Xiao W., Yoshimura K. (2019) A global database of water vapor isotopes measured with high temporal resolution infrared laser spectroscopy. *Scientific Data* 6, 180302.

- Wille J., Favier V., Dufour A., Gorodetskaya I.V., Turner J., **Agosta** C., Codron F. (2019) West Antarctic surface melt triggered by atmospheric rivers. *Nature Geoscience*, 12, 911-916.

Autres publications

(Corrigendum, Addendum, articles EGU en "discussion", chapitre, article de rang B)

Ouvrages

Juillet-Leclerc A. (2019) Could coral skeleton oxygen isotopic fractionation be controlled by biology? in "Isotopes applications in Earth Sciences". IntechOpen – doi : 10.5772/intechopen.89146.

Nomade S. (2019) Argon-Argon dating. In "The Encyclopedia of Archaeological Sciences", S.L. Lopez Varela (Ed.) – doi : 10.1002/9781119188230.saseas0042.

Corrigendum, Addendum, Responses

Sagnotti L., Giaccio B., Liddicoat J.C., Carrichi C., Nomade S., Renne P.R. (2019) On the reliability of the Matuyama-Brunhes record in the Sulmona Basin – Comment to “A reappraisal of the proposed rapid Matuyama-Brunhes geomagnetic reversal in the Sulmona Basin, Italy” by Evans and Muxworthy (2019). Journal of Geophysical International 216, 296-301.

Journaux EGU (en discussion)

Metcalfe B., Lougheed B. C., **Waelbroeck** C., Roche D.M. (2019) On the validity of foraminifera-based ENSO reconstructions. Climate of the Past Discussion, doi.org/10.5194/cp-2019-9.

Missiaen L., Bouttes N., Roche D.M., Dutay J-C., Quiquet A., **Waelbroeck** C., Pichat S., Peterschmidtt J-Y. (2019) Carbon isotopes and Pa/Th response to forced circulation changes: a model perspective, Climate of the Past Discussion, doi : 10.5194/cp-2019-45.

Rousseau D.D., Antoine P., Boers N., Lagroix F., Ghil M., Lomax J., Fuchs M., Debret M., Hatté C., Moine O., Gauthier C., Jordanova D., Jordanova N. (2019) DO-like events of the penultimate climate cycle: the loess point of view. Climate of the Past Discussion.

Autres valorisations

- Jacob J. (2019) Ça m'intéresse

Thèses et Habilitations soutenues en 2019

Thèse de doctorat

- thèse donnant lieu à une fiche ci-après

Lise MISSIAEN soutenue le 18 janvier 2019
Quantification des changements de la circulation océanique profonde de l'Atlantique au cours des changements climatiques rapides des derniers 40 ka.

- Xiaolei PANG soutenue le 14 octobre 2019
Transport de chaleur et de salinité à travers l'archipel indonésien au cours des 270 000 dernières années: nouveaux enregistrements de la dynamique orbitale et millénaire du flux indonésien et de la zone de convergence intertropicale.

- Thomas EXTIER soutenue le 18 octobre 2019
Variations climatiques et variations du cycle hydrologique aux basses latitudes au cours du Quaternaire: une approche combinant modèle et données

Habilitation à diriger les recherches

Jérémy JACOB soutenue le 28 mai 2019
Biomarqueurs moléculaires des interactions passées entre le climat, les écosystèmes, et les sociétés : de l'allégorie de la caverne d'Ali Baba à la géochimie organique du ressenti et des sens

Cafés-science de 2019

sous l'impulsion de l'équipe 2019 d'organisation des Cafés Sciences:
Romain Euverte, Cécile Agosta, Tiphaine Penchenat et Marie-Gabrielle Durier

Café Science = Moldeling animation "PiCO session"
Omar Alaoui, Jonathan Barichivich, Camille Contoux, Thomas Extier, Fabienne Maignan, Olivier Marti, Claude Mugler, Catherine Ottlé, Aurélien Quiquet, Elodie Salmon, Jérôme Servonnat, Nicolas Viovy
le 12 février 2019

Café Manip "géochimie organique"
Jérémy Jacob, Aurélie Diacre, Caroline Gauthier, Christine Hatté
le 12 mars 2019

Café Science "Antarctique"
Amaëlle Landais et Christophe Leroy-Dos Santos
le 2 avril 2019

Café Manip "Equipe CLIMAG"
Catherine Kissel, Aline Govin, Aurélie van Toer, Camille Wandres
le 7 mai 2019

Café Science "Spécial stagiaires"
le 4 juin 2019

Café Science "Spécial doctorants"
le 3 novembre 2019

FICHES ILLUSTRANT LES ACTIVITÉS 2019

… publications 2019

Estimation of the Antarctic surface mass balance using the regional climate model MAR (1979–2015) and identification of dominant processes

Agosta C., Amory C., Kittel C., Orsi A., Favier V., Gallée H., van den Broeke M.R., Lenaerts J.T.M., van Wessem J.M., van de Berg W.J., Fettweis X.

The Cryosphere (2019) 13, 281-296

The Antarctic ice sheet mass balance is a major component of the sea level budget and results from the difference of two fluxes of a similar magnitude: ice flow discharging in the ocean and net snow accumulation on the ice sheet surface, i.e. the surface mass balance (SMB). Separately modelling ice dynamics and SMB is the only way to project future trends. In addition, mass balance studies frequently use regional climate models (RCMs) outputs as an alternative to observed fields because SMB observations are particularly scarce on the ice sheet.

Here we evaluate new simulations of the polar RCM MAR forced by three reanalyses, ERA-Interim, JRA-55, and MERRA-2, for the period 1979–2015, and we compare MAR results to the last outputs of the RCM RACMO2 forced by ERA-Interim. We show that MAR and RACMO2 perform similarly well in simulating coast-to-plateau SMB gradients, and we find no significant differences in their simulated SMB when integrated over the ice sheet or its major basins. More importantly, we outline and quantify missing or underestimated processes in both RCMs. Along stake transects, we show that both models accumulate too much snow on crests, and not enough snow in valleys, as a result of drifting snow transport fluxes not included in MAR and probably underestimated in RACMO2 by a factor of 3. Our results tend to confirm that drifting snow transport and sublimation fluxes are much larger than previous model-based estimates and need to be better resolved and constrained in climate models. Sublimation of precipitating particles in low-level atmospheric layers is responsible for the significantly lower snowfall rates in MAR than in RACMO2 in katabatic channels at the ice sheet margins. Atmospheric sublimation in MAR represents 363 Gt yr−1 over the grounded ice sheet for the year 2015, which is 16% of the simulated snowfall loaded at the ground. This estimate is consistent with a recent study based on precipitation radar observations and is more than twice as much as simulated in RACMO2 because of different time residence of precipitating particles in the atmosphere. The remaining spatial differences in snowfall are attributed to differences in advection of precipitation with snowfall particles being likely advected too far inland in MAR.

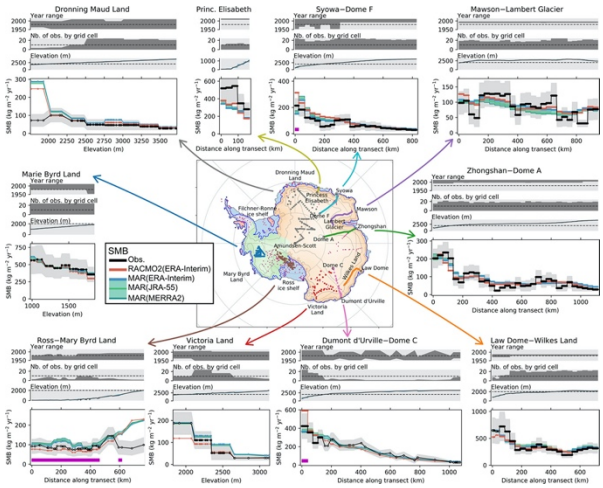

Fig. 1. Modelled vs. observed SMB for sectors and transects over Antarctica. MAR SMB is in blue and green and observed SMB is in black. SMB values are first averaged on MAR grid cells then along a chosen grid direction or by elevation bins. Distance along the transect starts at the coast.

Evidence for a large-magnitude eruption from Campi Flegrei caldera (Italy) at 29 ka

Albert P.G., Giaccio B., Isaai R., Costa A., Niespolo E.M., Nomade S., Pereira A., Renne P.R., Hinchliffe A., Mark D.F., Brown, R.J., Smith V.C.

Geology (2019) 47(7) 595-599

The 40 ka caldera-forming eruption of Campi Flegrei (Italy) is the largest known eruption in Europe during the last 200 k.y., but little is known about other large eruptions at the volcano prior to a more recent caldera-forming event at 15 ka. At 29 ka a widespread volcanic ash layer, termed the Y-3 tephra, covered >150,000 km^2 of the Mediterranean. The glass compositions of the layer are consistent with Campi Flegrei being the source (Fig. 1), but no prominent proximal equivalent in the appropriate chrono-stratigraphic position had been previously identified. Here we report new glass chemistry data and ^{40}Ar/^{39}Ar ages (29.3 ± 0.7 ka [2σ], Fig. 2)) that reveal the near-source Y-3 eruption deposit in a sequence at Ponti Rossi and a nearby borehole (S-19) in Naples. The dispersal and thickness of the deposits associated with this eruption, herein named the Masseria del Monte Tuff, were simulated using a tephra sedimentation model. The model indicates that ~16 km^3 dense rock equivalent of the magma erupted was deposited as fall. This volume and the areal distribution suggest that the Masseria del Monte Tuff resulted from a magnitude (M) 6.6 eruption (corresponding to volcanic explosivity index [VEI] 6), similar to the 15 ka caldera-forming Neapolitan Yellow Tuff (M 6.8) eruption at Campi Flegrei. However, the lack of coarse, thick, traceable, near-vent deposit suggests peculiar eruption dynamics. Our reconstruction and modeling of the eruption show the fundamental role that distal tephrostratigraphy can play in constraining the scale and tempo of past activity, especially at highly productive volcanoes.

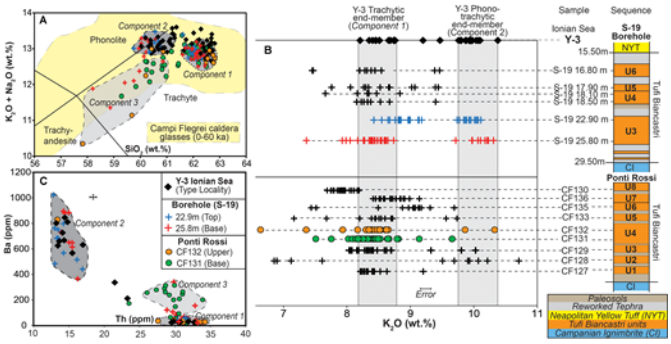

Fig. 1. Geochemical characterization of distal Y-3 tephra consistent with Campi Flegrei caldera (Italy) glasses.

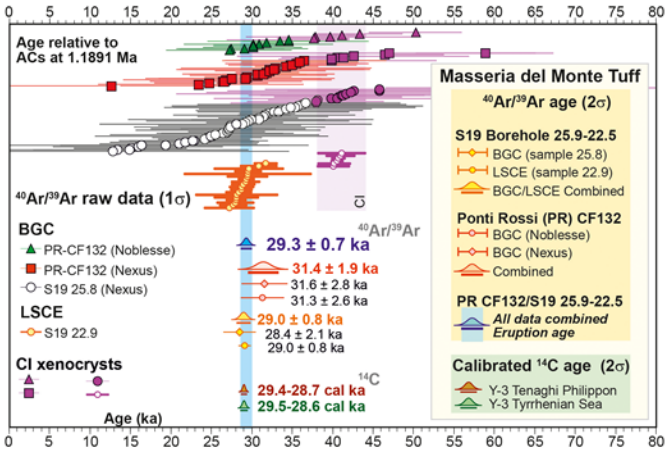

Fig. 2: 40Ar/39Ar dates obtained for the Y3 tephra

Effects of grass leaf anatomy, development and light/dark alternation on the triple oxygen isotope signature of leaf water and phytoliths: insights for a new proxy of continental atmospheric humidity

Alexandre A., Webb E., Landais A., Piel C., Devidal S., Sonzogni C., Couapel M., Mazur J.C., Pierre M., Prié F., Vallet-Coulomb C., Outrequin C., Roy J.

Biogeosciences 16, 4613-4625, 2019

Continental relative humidity (RH) is a key-climate parameter. However, there is a lack of quantitative RH proxies suitable for climate model-data comparisons. Recently, a combination of climate chamber and natural transect calibrations laid the groundwork for examining the robustness of the triple oxygen isotope composition ($\delta^{18}O$, $\delta^{17}O$) of phytoliths as a new proxy for past changes in RH. However, it was recommended that besides RH, additional factors that may impact $\delta^{18}O$ and $\delta^{17}O$ of plant water and phytoliths be examined. Here, the effects of grass anatomy, leaf development stage and day/night alternations are addressed from the growth of the grass species F. arundinacea in climate chambers. Plant water and phytoliths are analyzed in d18O and ^{17}O-excess. Silicification patterns are examined using light and scanning electron observation of phytoliths. Progressions with length of $\delta^{18}O$ and 17O-excess of F. arundinacea leaf water and phytoliths were observed and modeled using the Farquhar and Gan (2003) model and considering a fractionation between leaf water and silica depicted by $\lambda_{Phyto\text{-}LW}$ which evolves from 0.522 to 0.520. Despite of these progressions, the average triple oxygen isotope compositions of leaf water and phytoliths can be estimated and is not length-dependent. Heterogeneity in stem vs leaf biomass among grasses should neither impact the average isotope composition of phytoliths. Day/night alternations (RH being set constant) do not modify the triple oxygen isotope composition of leaf water. However, when RH changes, silica is expected to form rather when transpiration is high at low RH. Thus, daytime conditions should be considered when interpreting ^{17}O-excessPhyto values as a RH proxy. Last, as most of silica polymerizes at the end of the elongation stage (58 % in the present case), RH conditions leading to generalized leaf senescence in nature should be considered when interpreting ^{17}O-excess$_{Phyto}$. This study contributes to a more precise identification of the parameters to take into consideration when interpreting ^{17}O-excess$_{Phyto}$ as a proxy of RH.

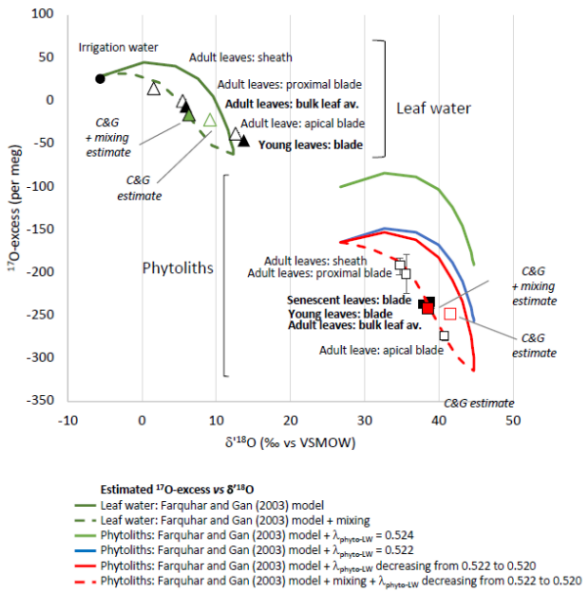

Fig. 1. Observed ^{17}O-excess vs $\delta^{18}O$ for leaf water (triangles) and phytoliths (squares) in young, adult and senescent leaves (black symbols) and along adult leaf (sheath, proximal blade, apical blade) (white symbols)

A remarkable Late Saalian (MIS 6) loess (dust) accumulation in the Lower Danube at Harletz (Bulgaria)

Antoine P., Lagroix F., Jordanova D., Jordanova N., Lomax J., Fuchs M., Debret M., Rousseau D.-D., Hatté C., Gauthier C., Moine O., Taylor S.N., Till J.L., Coutard S.

Quaternary Science Reviews (2019), 2017, 80-100, doi : 10.1016/j.quascirev.2019.01.005

While numerous high-resolution studies concerning Last Glacial aeolian sequences are available for Europe, the approach of the penultimate glacial in this geographical area is still poorly developed. In order to bridge this gap, this study focuses on the Bulgarian sequence of Harletz, along the Danube River, where extremely high sedimentation rates allow the depiction of high-resolution signals during MIS 6. At Harletz in NW Bulgaria on the western bank of the Ogosta River (tributary of the Danube) a 20m thick loess-palaeosols section was cleaned and sampled for a multi-disciplinary study and detailed pedostratigraphic approach. High-resolution continuous bulk sampling (5 cm) was carried out to characterise sedimentary grain size, magnetic properties (including magnetic susceptibility and its frequency dependence), colour reflectance (1 cm), and organic carbon. Geochronological control is based on 16 samples collected for OSL and MET-pIRIR dating. Using a cyclo-stratigraphic approach of the sequence combined with dating constraints provided by both MET-pIRIR dates and the age of a tephra layer occurring at a depth of 12m within the main loess unit, we can demonstrate that the Harletz section exhibits a 10m thick Late Saalian (Marine Isotope Stage 6, MIS 6) loess accumulation unique in Europe. The lower part of the main loess unit is 4m thick and overlies a basal brown soil complex allocated to MIS 7, which includes an exceptionally thick (4 m) and detailed succession of loess and four incipient soil horizons never described in European loess until now. ….

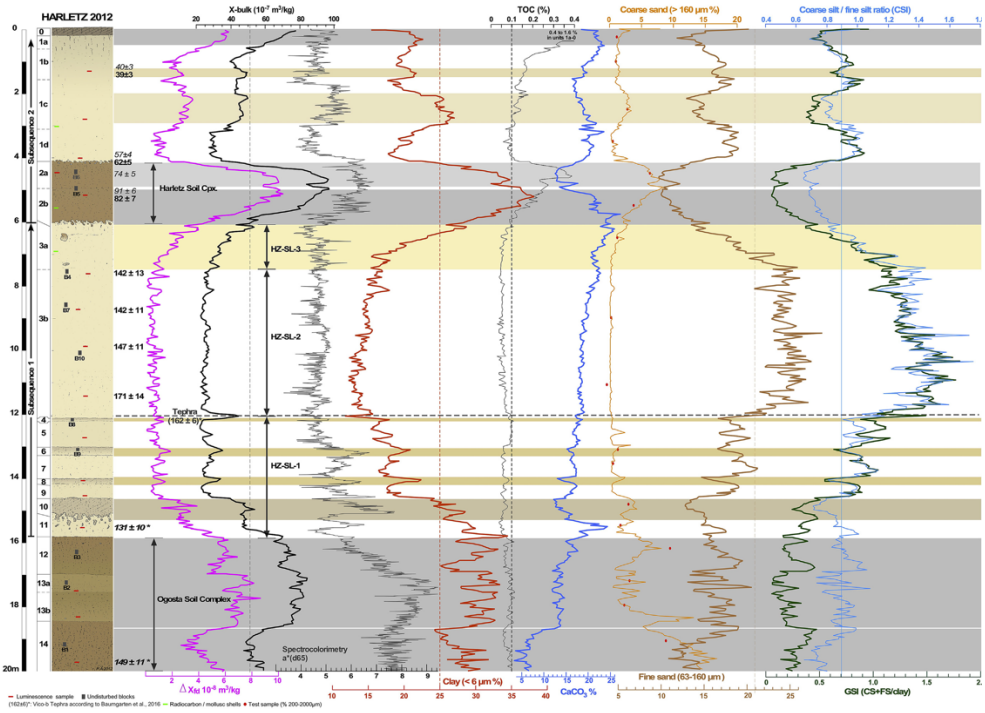

Figure 1 : Detailed stratigraphic log of the Harletz profile including the location of the various luminescence and micromorphological samples (blocks). High-resolution grain size data (clay, coarse and fine sand, grain-size ratios (GSI and CSI), TOC, carbonate, mass-specific magnetic susceptibility (c_{BULK} in $10^{-8}m^3/kg$) and absolute frequency dependence of mass-specific magnetic susceptibility (Dc_{FD} in $10^{-8}m^3/kg$), colour reflectance data and luminescence dating results from Lomax et al. (2019)) (black: feldspar coarse grain fraction, applying the MET-pIRIR protocol, grey italics: quartz fine grain fraction and SAR protocol).

Construction of a tephra-based multi-archive coherent chronological framework for the last deglaciation in the Mediterranean region

Bazin L., Lemieux-Dudon B., Siani G., Govin A., Landais A., Genty D., Michel E., Nomade S.

Quaternary Science Reviews (2019) 216, 47-57

Proxy records from different climate archives such as ice cores, speleothems or sediment cores are essential to define the sequence of events over to the last deglaciation. However, multi-archive comparison and compilation of data, necessary to assess the robustness of climate models, are rapidly limited by inconsistencies between archives' chronology.

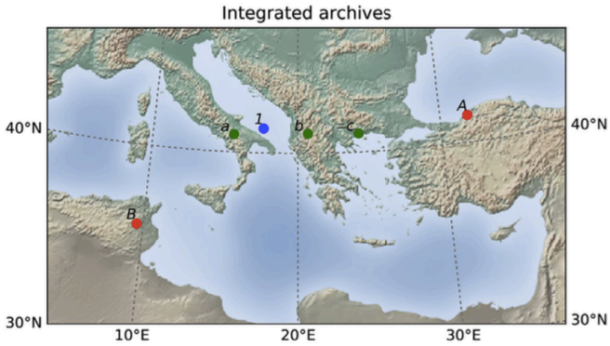

Fig. 1. Map of the sites included into the tephra-based coherent chronological framework for the last deglaciation in the Mediterranean region. The marine core is in blue, the continental sediment records are in green, and the speleothems are indicated by the red dots (1- MD90-917, a- Monticchio, b- Ohrid, C- Tenaghi Philippon, A- Sofular, B- La Mine).

Here we present the development and validation of the Datice chronological integration tool for the construction of multi-archive coherent chronologies. This chronology building tool, first developed to date ice cores only, can now integrate deposition-like archives such as sediment cores and speleothems, independently or coherently. The robustness of this dating method resides in its capacity to build coherent chronologies for multiple archives with a proper calculation of chronological uncertainties.

Using this tool, we were able to construct a coherent chronology for the last deglaciation in the Mediterranean region based on volcanic tephra layers correlation in terrestrial and marine sediment cores. We confirm the synchronicity, within chronological errors, of the sequence of events characterizing the last deglaciation between Greenland and the Mediterranean region, independently of any climatic alignment assumptions. Using this chronological framework, we however highlight some regional expression of this transition period in term of vegetation cover over the Mediterranean region.

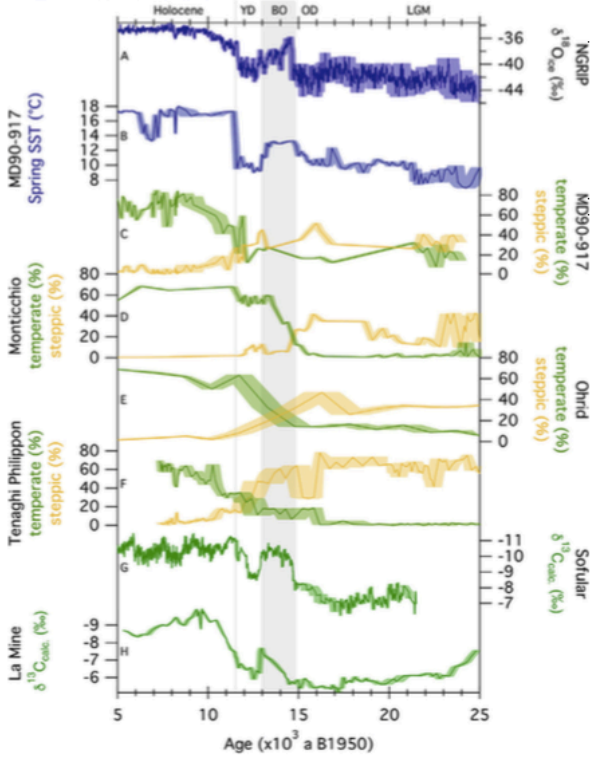

Fig. 2. Comparison of the last deglaciation records, presented on the Mediterranean coherent chronology between 5 ka and 25 ka B1950, with NGRIP reference record $\delta^{18}O_{ice}$ (GICC05 chronology; NGRIP community Members, 2004). All records are presented with their respective 1-sigma chronological uncertainty envelope. Shaded areas highlight the position of prominent events as recorded by the SST of MD90-917. Selected periods are indicated on top of the figure.

Effect of prescribed sea surface conditions on the modern and future Antarctic surface climate simulated by the ARPEGE atmosphere general circulation model

Beaumet J., Déqué M., Krinner G., Agosta C., Alias A.

The Cryosphere (2019) 13, 3023–3043

Owing to increase in snowfall, the Antarctic Ice Sheet surface mass balance is expected to increase by the end of the current century. Assuming no associated response of ice dynamics, this will be a negative contribution to sea-level rise. However, the assessment of these changes using dynamical downscaling of coupled climate model projections still bears considerable uncertainties due to poorly represented high-southern-latitude atmospheric circulation and sea surface conditions (SSCs).

This study evaluates the Antarctic surface climate simulated using a global high-resolution atmospheric model and assesses the effects on the simulated Antarctic surface climate of two different SSC data sets obtained from two coupled climate model projections. The two coupled models from which SSCs are taken, MIROC-ESM and NorESM1-M, simulate future Antarctic sea ice trends at the opposite ends of the CMIP5 RCP8.5 projection range. The atmospheric model ARPEGE is used with a stretched grid configuration in order to achieve an average horizontal resolution of 35 km over Antarctica. Over the 1981–2010 period, ARPEGE is driven by the SSCs from MIROC-ESM, NorESM1-M and CMIP5 historical runs and by observed SSCs. These three simulations are evaluated against ERA-Interim for atmospheric general circulation as well as the MAR regional climate model and in situ observations.

For the late 21st century, SSCs from the same coupled climate models forced by the RCP8.5 emission scenario are used both directly and bias-corrected with an anomaly method which consists in adding the future climate anomaly from coupled model projections to the observed SSCs with taking into account the quantile distribution of these anomalies. We evaluate the effects of driving the atmospheric model by the bias-corrected instead of the original SSCs. For the simulation using SSCs from NorESM1-M, no significantly different climate change signals over Antarctica as a whole are found when bias-corrected SSCs are used. For the simulation driven by MIROC-ESM SSCs, a significant additional increase in precipitation and in winter temperatures for the Antarctic Ice Sheet is obtained when using bias-corrected SSCs. For the range of Antarctic warming found (+3 to +4 K), we confirm that snowfall increase will largely outweigh increases in melt and rainfall. Using the end members of sea ice trends from the CMIP5 RCP8.5 projections, the difference in warming obtained (∼1 K) is much smaller than the spread of the CMIP5 Antarctic warming projections. This confirms that the errors in representing the Southern Hemisphere atmospheric circulation in climate models are also determinant for the diversity of their projected late 21st c. Antarctic climate change.

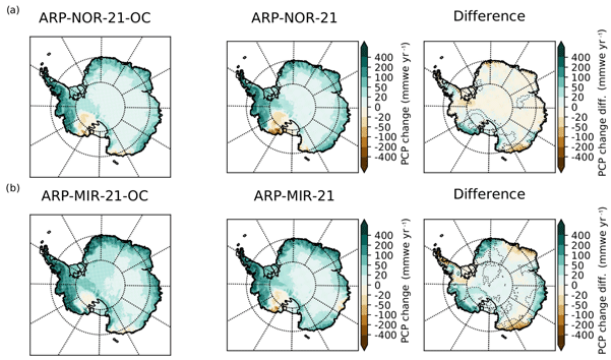

Fig. 1. Climate change signal in total precipitation (mm w.e. yr−1) for the late 21st century (reference period: 2071–2100) in the ARPEGERCP8.5 projection with bias-corrected SSCs (left), original SSCs (centre) and the difference (right). Results for projections with SSCs fromNorESM1-M are presented in panel(a)and from MIROC-ESM in panel(b). Dotted lines indicate where the difference is 50 % of theprecipitation change in the non bias-corrected SSC projection.

Coastal water vapor isotopic composition driven by katabatic wind variability in summer at Dumont d'Urville, coastal East Antarctica

Bréant C., Leroy Dos Santos C., Agosta C., Casado M., Fourré É., Goursaud S., Masson-Delmotte V., Favier V., Cattani O., Prié F., Golly B., Orsi A., Martinerie P., Landais A.

Earth and Planetary Science Letters (2019) 514, 37-47
Projet/financement: ERC Combiniso, LEFE ADELISE

Dumont d'Urville station, located on the East coast of Antarctica in Adélie Land, is in one of the windiest coastal region on Earth, due to katabatic winds downslope from the East Antarctic ice sheet. In summer, the season of interest in this study, coastal weather is characterized by well-marked diel cycles in temperature and wind patterns. Our study aims at exploring the added value of water vapor stable isotopes in coastal Adélie Land to provide new information on the local atmospheric water cycle and climate. An important application is the interpretation of water isotopic profiles in snow and ice cores recently drilled in Adélie Land. We present the first continuous measurements of $\delta^{18}O$ and d-excess in water vapor over Adélie Land. During our measurements period (26/12/2016 to 03/02/2017), we observed clear diel cycles in terms of temperature, humidity and isotopic composition. The cycles in isotopic composition are particularly large given the muted variations in temperature when compared to other Antarctic sites where similar monitoring have been performed. Based on data analyses and simulations obtained with the regional MAR model on the coastal Adélie Land, we suggest that the driver for $\delta^{18}O$ and d-excess diel variability in summer at Dumont d'Urville is the variations of the strength of the wind coming from the continent: the periods with strong wind are associated with the arrival of relatively dry air with water vapor associated with low $\delta^{18}O$ and high d-excess from the Antarctic plateau. Finally, in addition to the interpretation of snow and ice core isotopic profiles in the coastal regions, our study has implications for the evaluation of atmospheric models equipped with water isotopes.

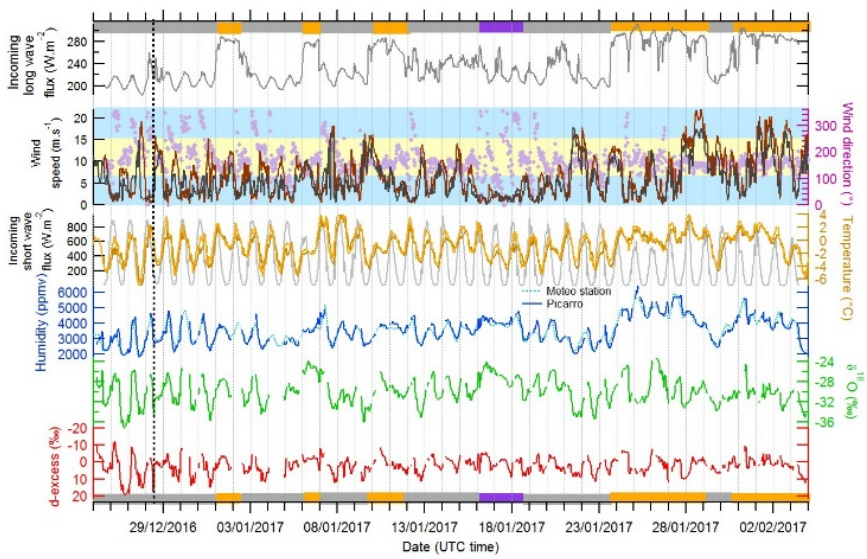

Figure: Evolution of incoming long wave flux (used here to differentiate cloudy from clear sky conditions), wind strength (bordeaux), wind direction (purple dots) and temperature (orange) from the Cap Prud'homme automatic weather station. Evolution of temperature (light orange), wind speed (black) and humidity from DDU meteorological station together with the evolution of humidity, $\delta^{18}O$ and d-excess (inverted axis) from DDU Picarro instrument. In the second upper panel, the horizontal blue and yellow bands stand for the range of direction winds originating from the ocean or from the continent respectively. The grey, orange and violet rectangles indicate the periods with different weather conditions (clear sky, cloudy, no wind). The snowy period (25th to 28th of January 2017) is included in the cloudy periods.

Unveiling the anatomy of Termination 3 using water and air isotopes in the Dome C ice core, East Antarctica

Bréant C., Landais A., Orsi A., Martinerie P., Extier T., Prié F., Masson-Delmotte V., Jouzel J., Leuenberger M.

Quaternary Science Reviews (2019) 211, 156-165
Projet/financement: ERC Combiniso, LEFE NEVE/CLIMAT

Each glacial – interglacial transition of the Quaternary occurs in a different orbital context leading to various timing for the deglaciation and sequence of high vs low latitudes events. Termination 3, 250 kiloyears before present (ka), is an unusual deglaciation in the context of the last 9 deglaciations recorded in the old EPICA Dome C (EDC) Antarctic ice core: it exhibits a three-phase sequence, two warming phases separated by a small cooling, the last phase suggesting a particularly rapid temperature increase. We present here new high resolution $\delta^{15}N$ and deuterium excess (d-excess) data from the EDC ice core to provide a detailed temperature change estimate during this termination. Then, we combined the δD and $\delta^{18}O$ to discuss the relationship between high and low latitude changes through the d-excess. We also provide the high vs low latitude sequence of events over this deglaciation without chronological uncertainty using low latitude ice core proxies. In agreement with previous studies based on speleothem analyses, we show that the first phase of Termination 3 (256 to 249 ka) is associated with small Heinrich like events linked to changes in ITCZ position, monsoon activity and teleconnections with Antarctica. In a context of minimum Northern Hemisphere insolation, this leads to a rather strong Antarctic warming, as observed in the $\delta^{15}N$ record in contrast to the relatively small δD increase. The second warming phase occurs during the rise of the Northern hemisphere insolation, with a large Heinrich like event leading to the characteristic Antarctic warming observed in the $\delta^{15}N$ and δD increase as for the more recent terminations.

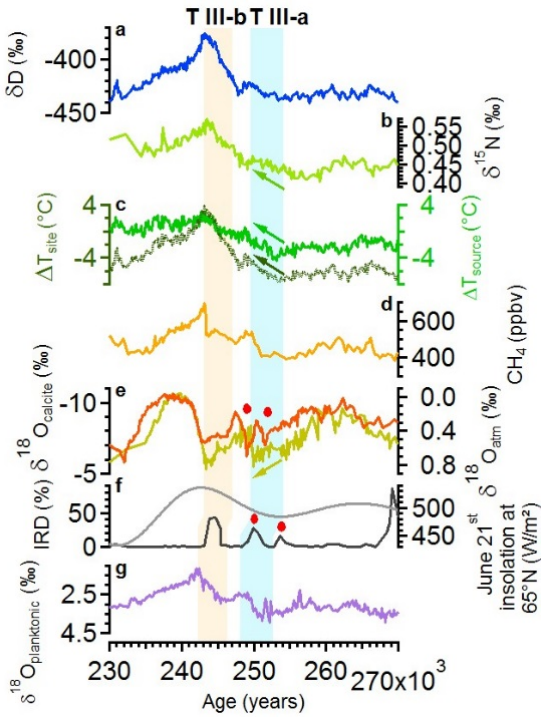

Figure: Millennial variability during the Terminations 3.a: EDC δD record. b: measured EDC $\delta^{15}N$. c: EDC $\Delta Tsite$ (dark green) and $\Delta Tsource$ (green) reconstructions. d: EDC CH_4. e: $\delta^{18}Ocalcite$ from East Asian speleothems in red and EDC $\delta^{18}O_{atm}$ in yellow. f: IRD percentage from site ODP980 in black and June 21st insolation at 65°N in grey. g: $\delta^{18}Oplanktonic$ of core MD97-2120.

Coral Li/Mg thermometry: caveats and constraints

Cuny-Guirriec K., Douville E., Reynaud S., Allemand D., Bordier L., Canesi M., Mazzoli C., Taviani M., Canese S., McCulloch M., Trotter J., Rico-Esenaro S.D., Sanchez-Cabeza J.A., Ruiz-Fernandez A.C., Carricart-Ganivet J.P., Scoot P.M., Sadekov A., Montagna P.

Chemical Geology, 523, 167-178, 2019

The coral Li/Mg temperature proxy is revisited through an in-depth trace element analysis of scleractinians collected live from tropical to polar environments. The dataset consists of Li/Ca, Mg/Ca, Sr/Ca and Li/Mg ratios of 64 coral specimens belonging to 8 different taxa, including both reef-building zooxanthellate and cold-water non-zooxanthellate species, from a wide range of water temperature (-1 to 29.5°C), salinity (34.71 to 38.61,) and depth (3 to 670m).

Our results showed that the reliability of the Li/Mg temperature proxy is strongly limited by the organic matter associated with the coral skeleton, which is most evident within the green bands observed in tropical corals. Organic-rich bands can double the Mg content otherwise present in the skeleton, which may ultimately lead to a temperature overestimation exceeding 15°C. We found that this bias can be overcome by the treatment of coral skeletons with a specific oxidizing cleaning protocol. We also detected the presence of calcite deposits within the aragonite skeleton of some Antarctic living coral specimens, which strongly affects the robustness of the Li/Mg proxy given its temperature sensitivity of ~1.5°C/1% calcite. Therefore, to obtain reliable reconstructions a correction needs to be applied when organic matter and/or calcite contamination is present.

The integrated results across a wide temperature range, from extreme cold to tropical shallow waters, yield to an overall precision for the Li/Mg-temperature proxy of ±1.0°C, with slight differences on the uncertainties depending on the environment: ±0.9°C, ±1.5°C and ±2.6°C for deep, intermediate, and tropical shallow water corals, respectively. However, the uncertainty for tropical corals can be reduced to ±0.6°C if a Li/Mg and Sr/Ca multi-regression approach is applied.

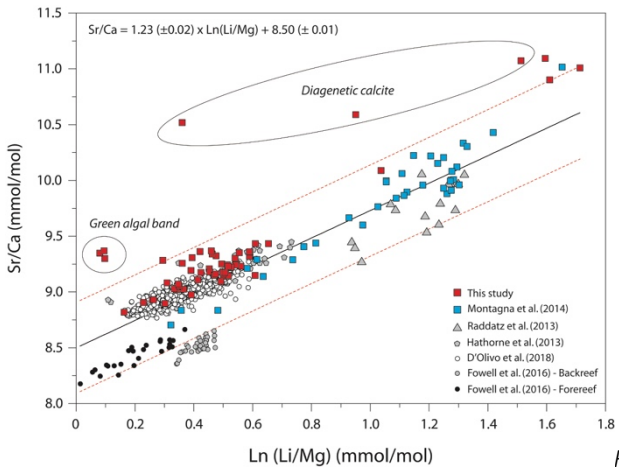

Fig. 1. Paired Sr/Ca vs ln (Li/Mg) values for all the chemically-cleaned samples analysed in the present study (red squares), plotted together with data from Hathorne et al (2013), Raddatz et al (2013), Montagna et al (2014), Fowell et al (2016) and D'Olivo et al (2018).

Radiocarbon dating of legacy music instrument collections : example of traditional Indian vina from the Musée de la Musique, Paris.

Durier M.-G., Bruguière P., Hatté C., Vaiedelich S., Gauthier C., Thil F., Tisnérat-Laborde N.

Radiocarbon (2019) 61(5), 1357-1366 - doi : 10.107/RDC.2019.71
Projet DATIM – DIM Patrimoine, Ile de France

Although radiocarbon (^{14}C) dating is commonly used for archeological music instruments, little research has been conducted on modern instruments (16th–19th centuries). New technology, based on the Mini Carbon Dating System (MICADAS), enables some of the recurring challenges (e.g. sampling size) to be circumvented and paves the way for a new field of investigation. We here address the Indian instrumentarium, about which very little is known. We investigate the making and the restoration phases of two *vina*, a *kinnari vina* (E.1444), and a *rudra vina* or bin (E.997.24.1). By comparing ^{14}C measurements made on several samplings of the instruments' elements with museological information, we were able to overcome the limits of the calibration curve on the historical times that might yield for several equiprobable interval of ages for a unique ^{14}C activity measurement. We were here able to specify a unique calibrated interval of ages [1666 AD – 1690 AD] for the *kinnari vina*, with a restoration phase [1678 AD – 1766 AD] for the upper nut. The bin is likely attributed to the [1650 AD – 1683 AD] interval.

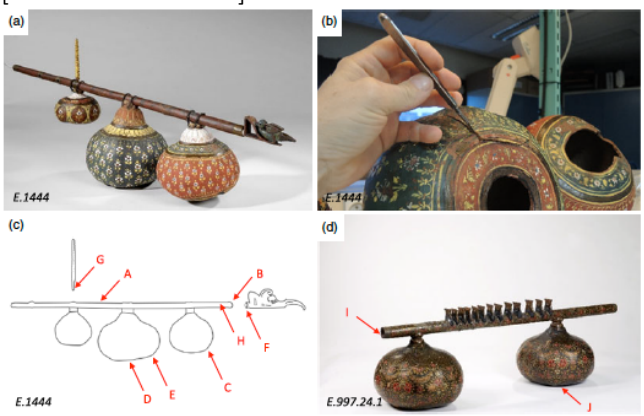

Figure 2 : Indian vina from the museum collections and sampling locations: (a) kinnari vina E.1444, (b) close up of sampling in a crack from kinnari vina E.1444, (c) schematic view of the kinnari vina E.1444 and location of the 8 samples, (d) bin or rudra vina E.997.24.1 and sample locations. Pictures by Claude Germain (a, d) and Stéphane Vaiedelich (b) © Musée de la musique-Philharmonie de Paris.

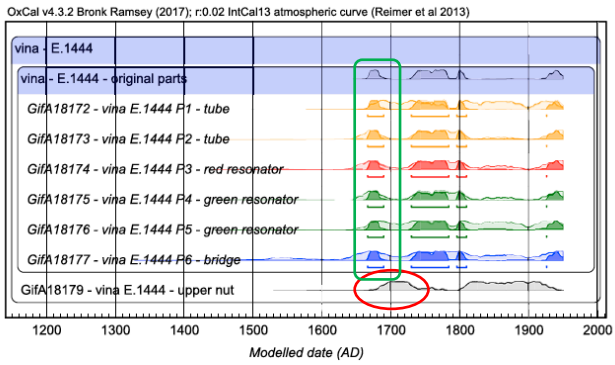

Figure 2 Calibrated 14C ages of the kinnari vina E.1444. The upper probability distribution diagram, underlined in blue corresponds to the Bayesian modeling of the combination of the vina's original parts. The probability distribution diagram of the restored piece (upper nut) is shown in the last line.
The instrument was acquired in 1892 and no restoration has been carried out since it entered the museum. Any replacement was thus done before. The use of terap in 19th-century Europe in cabinet making and instrument making is not attested and remains highly unlikely. European instrument makers of this era probably did not have the organological knowledge of traditional Indian instruments to accurately reproduce this part, either. It is very likely that the replacement was done while the instrument was still in India and was made by an Indian instrument maker. The only few slight traces of (musical) use on the upper nut seem to reveal that it was not played as much as the other parts of the vina. It is thus assumed that the nut was replaced during the [1678 AD – 1766 AD] interval (red ellipse in Figure 2), towards the end of the musical use of the vina. Consequently, the instrument was made (age of the original pieces) during the [1666 AD – 1690 AD] interval (green rectangular from in Figure 2). It appears that the instrument is a little older than initially thought by the curator, who expected it to date from the 18th century.

Factors controlling frequency of turbidites in the Bengal fan during the last 248 kyr cal BP: Clues from a presently inactive channel

Fauquembergue K., Fournier L., Zaragosi S., Bassinot F., Kissel C., Malaizé B., Caley T., Moreno E., Bachelery P.

Marine Geology (2019) 415, 105965.

The seafloor of the Bay of Bengal is covered by thick sediment deposits that constitute the largest turbiditic system in the world, fed primarily by the Ganges and Brahmaputra rivers draining the high Himalayan ranges. Sediment transfers from the delta to the deep-sea fan take place as turbidity currents in channel-levee systems. Most of these channels are now inactive and sealed by hemipelagic deposits but the evolution of the inactive channels during the last sea-level variations has never been described in detail.

Sedimentation in the currently active channel, the Active Valley, was particularly important during the last sea-level rise, which suggests a very good connection between the fluvial systems and the deep turbidite system at this time. During the MONOPOL cruise (2012), we retrieved a giant piston core (MD12-3412) near the currently inactive E4 channel assumed to be connected to the Swatch of No Ground canyon on the upper fan. The upper part of the core covers the last ~250 kyr. It reveals that, contrary to what is known about the Active Valley, the turbidite activity in E4 took place mainly during low sea-level phases (glacial stages), and stopped around 11.8 kyr cal BP. This different mode of activity suggests that (i) E4 was not abandoned but served as a secondary channel, and (ii) that the supply of turbidite material at the site of core MD12- 3412 was not related to past changes in summer monsoon strength. Periods of activation of the E4 channel observed on core MD12-3412 were previously identified on the shelf area as thick Forced Regression System Tracts (FRST) after a displacement of deltaic edifices. High turbidites record on the deep basin are mainly synchronous with sea-level fall and rise conditions, but mostly during low sea-level periods. This could be explained by a residual connection between the coastal system and the E4 channel during sea level low stands.

Fig. 1. Location map and physiography of the upper and middle fan of the Ganges-Brahmaputra sedimentary system. Fluvial systems are in light blue, and channelizations of the Bengal fan are in a shade of blue.

Can SOC modelling be improved by accounting for pedogenesis?

Finke P., Opolot E., Balesdent J., Behre A. A., Boeckxx P., Cornu S., Harden J., Hatté C., Williams E., Doetterl S.

Geoderma (2019) 388, 513-524

Recent findings suggest that soil organic carbon mineralization and stabilization depend to a substantial degree on the soil geochemistry and the degree of weathering. We hypothesized that this dependence can be translated to decay rate modifiers in a model context, and used data from the Merced chronosequence (CA, U.S.A., 100 yr – 3 Myr), representing a weathering sequence, to test, on a 1000-year time scale for model spin-up, a simple soil organic carbon (SOC) model based on the RothC26.3 model concepts. Model performance was tested for four levels of information: (1) known decay rates for each model SOC pool at individual chronosequence locations, obtained by calibrating the model to measured SOC-fractions and measured site-specific C-inputs; (2) average decay rates for each SOC-pool, corrected per location with rate modifiers based on geochemical proxies and measured site-specific C-inputs; (3) uncorrected average decay rates per SOC-pool and measured site-specific C-inputs; (4) uncorrected average decay rates per SOC-pool and averaged C-inputs. A lumped root mean square error (RMSE) statistic was calculated for each information level. We found that using local measurements of fresh C-input led to a decrease in RMSE of near 15% relative to information level (4). Applying geochemical rate modifiers led to a further reduction of 20%. Thus, we conclude that there is a benefit of including geochemical rate modifiers in this SOC-model. We repeated this analysis for a five-pool and a four-pool SOC model that either included or excluded an inert organic matter pool. In terms of the lumped RMSE both models performed similarly, but by comparing measured and simulated percentage Modern Carbon (pMC) for bulk SOC we concluded that measured pMC was best approximated using a four-pool SOC model (without an Inert Organic Matter pool). Furthermore, it is likely that a five-pool model including a very slowly decaying pool would further improve model performance.

$^{40}Ar/^{39}Ar$ dating of the Thorsmork ignimbrite and Icelandic sub-glacial rhyolites

Guillou H., Scao V., Nomade S., Van Vliet-Lanoé B., Liorzou C., Gudmundsson A.

Quaternary Science Reviews (2019) 209, 52-62.

Robust correlation of paleoclimatic archives (e.g. marine sediments, ice, speleothems) necessitates an increase of the number of independent and accurately dated stratigraphic markers using numerical methods. Icelandic rhyolitic volcanism has a strong chronological interest because these products are found as tephra in the North Atlantic marine archives as well as in Greenland ice cores.

In this study, we have dated, using the $^{40}Ar/^{39}Ar$ method, subglacial rhyolites of the Tindfjallajökull, Kerlingarfjöll and Torfajökull volcanoes which are the main sources of rhyolitic tephra identified in marine and glaciological records.

The Thorsmork ignimbrite (Tindfjallajökull) which correlates with the rhyolitic component (II-RHY-1) of the North Atlantic Ash Zone II (NAAZ II) layer is dated at 55.6 ± 2.4 ka, an age that agrees with the ones given by the ice core chronologies (GICC05: 55.4 ± 1.2 ka). The eruptions of Rauðfossafjöll and Fannborg are respectively dated at 77.0 ± 3.0 ka and 149.3 ± 3.4 ka (Fig. 1). These new ages along with the published ones confirm, as already concluded by Flude et al. (2010) that there is no clear evidence, at least at the latitude of Iceland, that climate warming is the main mechanism that triggered rhyolitic eruptions (Fig. 1).

Combining major and trace element compositions with our new age determinations, it appears that the Rauðfossafjöll and the Snaefell rhyolitic eruptions have not yet been discovered in marine sediment cores. Nevertheless, given the accuracy and precision of our dating, these rhyolitic eruptions have the potential to become chronostratigraphic markers, once tephra shards corresponding to these eruptions are discovered in ice and or marine sediment records. The Fannborg eruption might be recorded in the marine core LINK 16 during MIS 6 prior to the transition to MIS5e.

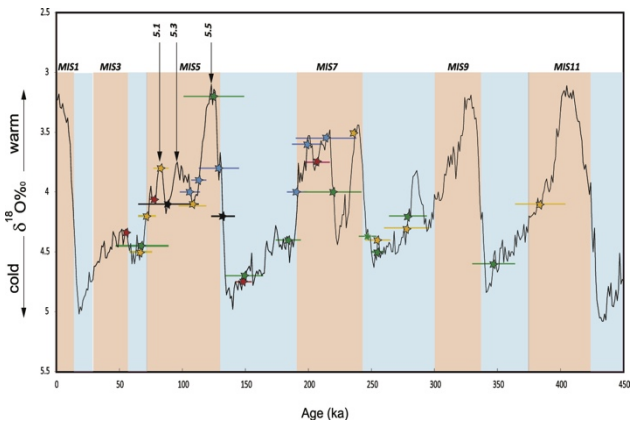

Fig.1 a) Lisieki and Raymo (2005) $\delta^{18}O$ benthic stack, with the timing of the 24 dated Icelandic rhyolitic eruptions. The error bars of individual rhyolitic eruptions are here reported at1 sigma. MIS refers to Marine Isotopic Stages. Substages 5.1, 5.3, 5.5 are pointed on the curve. Red stars are samples dated in this work. Orange stars are rhyolites from Torfajökull (McGarvie et al. (2006); Clay et al. (2015)), green stars: rhyolites from Kerlingarfjöll (Flude et al., 2010), blue stars: rhyolites from Ljosufjöll (Flude et al., 2008) and the black stars correspond to the Prestahnúkur rhyolite (dated at 132 ka in Clay et al. (2015) and at 89 ka in McGarvie et al. (2007))

Radiocarbon dating and the protection of cultural heritage

Hajdas I., Jull A.J.T., …, Hatté C., ….Beck L., ….

Radiocarbon (2019) 61(5), 1133-1134 - doi : 10.107/RDC.2019.100

ABSTRACT

The modern antiquities market uses radiocarbon (^{14}C) dating to screen for forged objects. Although this fact shows the potential and power of the method, **the circumstances where it is applied can be questionable and call for our attention**. Here we present an outline of a call to radiocarbon laboratories for due diligence and best practice approaches to the analysis of antique objects requested by non-research clients.

BACKGROUND

Protection of cultural heritage is considered one of the most important national and international goals. Each nation has the right to protect their past and present cultural goods, both tangible and intangible. The fact that international involvement is needed has been recognized since the early 20th century. The need for protection of culture is essential for building peace as it was stated by founders of the UNESCO when it was established in Nov.– Dec. 1945. In 1970 a UNESCO Convention on the protection of cultural heritage was adopted and ratified by most of the countries. Concerns of the post-WWII era were with the destruction of cultural heritage that wars and crises impose on whole communities (Gerstenblith 2008).

The present-day antiquities trade is operating in a world that is far from being free of conflicts and wars. It is a most striking fact that the remains of old cultures and civilizations are located and endangered by conflicts and looting. Illicit trade of antique objects is driven by the demand for antiquities in countries outside of conflicts. Huysecom *et al.* (2017) have shown that on the part of buyer this demand is accompanied by the need for a secure investment. Whenever possible, antiquities on the market are tested using scientific methods such as thermoluminescence (TL) and radiocarbon (^{14}C) dating. However, the use of the scientific techniques and involvement in authentication appears questionable and raises ethical issues similar to those faced by conservators (Sease 1998).

The radiocarbon community has recognized this problem and is committed to following due diligence protocols, which will help to minimize the involvement of laboratories in providing data for illegally displaced antiquities.

Here, we propose the first measures that can help to minimize access of the illicit market to radiocarbon analysis and to prevent misuse of ^{14}C ages in promotion of illicit trade and looting. This would also protect the radiocarbon laboratories. These procedures are proposed to be applied when the analysis is requested by private persons or for-profit organizations such as auction houses, antiquity dealers, and private collections (sometimes private museums).

Ultraprecise age and formation temperature of the Australasian tektites constrained by $^{40}Ar/^{39}Ar$ analyses

Jourdan F., Nomade S., Wingate M.T. D., Eroglu E., Deino A.

Meteoritics and Planetary Science (2019) 54(10) 2573–2591 – doi: 10.1111/maps.13305

The Australasian tektites are quench melt glass ejecta particles distributed over the Asian, Australian, and Antarctic regions resulting of the impact at high velocity of a meteorite. It is worth noticing that the source crater is currently elusive but probably localized in the Megong area. This tektites strewn field is currently the much widespread one known of earth

In this article we present new $^{40}Ar/^{39}Ar$ age data from four tektites: one each from Thailand, China, Vietnam, and Australia (Fig. 1) measured using three different instruments from two different laboratories (Univ. Curtin, Australia ; LSCE France). Combined with published $^{40}Ar/^{39}Ar$ data yield a weighted mean age of 788.1 ± 2.8 ka (±3.0 ka, including all sources of uncertainties) (P = 0.54) (Fig.2).

This new age is five times more precise compared to previous results thanks, in part, to the multicollection capabilities of the ARGUS VI noble gas mass spectrometer, which allows an improvement of almost fourfold on a single plateau age measurement.

Diffusion experiments on tektites combined with synthetic age spectra and Monte Carlo diffusion models suggest that the minimum temperature of formation of the Thai tektite is between 2350 °C and 3950 °C, hence a strict minimum value of 2350 °C.

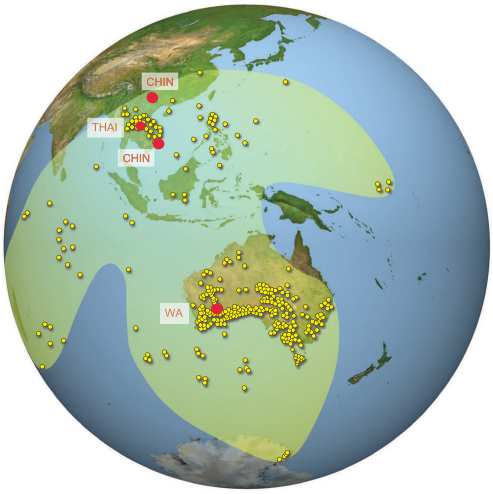

Fig. 1 : The Australasian tektite strewn field after Folco et al. (2009). Western Canada has been reported to contain Australasian tektites that could result from ballistic transport. However, it still remains to be confirmed that they were not brought by humans (Schwarz et al. 2016), hence are not included in this map at this stage.

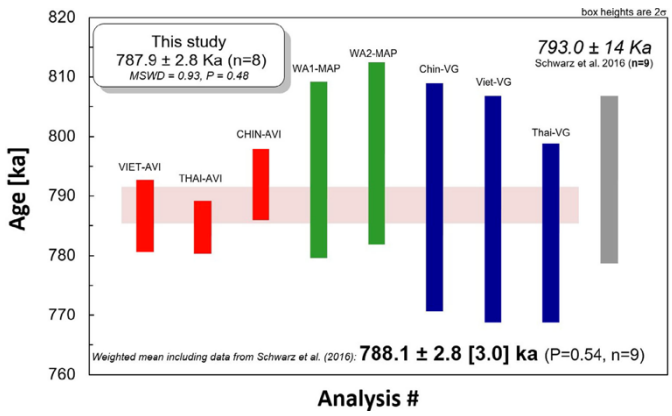

Fig. 2. Plot of all the 40Ar/39Ar plateau age results obtained in this study using an ARGUS VI (AVI, red), a MAP-215(MAP, green), a VG5400 (VG, blue). Weighted mean age calculated for all data obtained in this study shown as a horizontal pink box. The weighted mean age (gray) of Schwarz et al. (2016) is shown for comparison. Grand weighted mean including the data from Schwarz et al. (2016) results in an age of 788.1 ± 2.8 ka [± 3.0ka].

Assessing the robustness of Antarctic temperature reconstructions over the past 2 millennia using pseudoproxy and data assimilation

Klein F., Abram N.J., Curran M.A.J, Goosse H., Goursaud S., Masson-Delmotte V., Moy A., Neukom R., Orsi A., Sjolte J., Steiger N., Stenni B., Werner M.

Climate of the Past (2019) 15, 661-684 – doi : 10.5194/cp-15-661-2019

[…] Here, we use climate model results, pseudoproxy experiments and data assimilation experiments to assess the potential for reconstructing the Antarctic temperature over the last 2 millennia [...]. The well-known covariance between δ^{18}O and temperature is reproduced in the two isotope-enabled models used (ECHAM5/MPI-OM and ECHAM5-wiso), but is generally weak over the different Antarctic regions, […] *and* displays large variations over the past millennium, further affecting the potential skill of temperature reconstructions based on statistical methods which rely on the assumption that the last decades are a good estimate for longer temperature reconstructions. Using a data assimilation technique allows, in theory, for changes in the δ^{18}O–temperature link through time and space to be taken into account. Pseudoproxy experiments confirm the benefits of using data assimilation methods instead of statistical methods that provide reconstructions with unrealistic variances in some Antarctic subregions. They also confirm that the relatively weak link between both variables leads to a limited potential for reconstructing temperature based on δ^{18}O. However, the reconstruction skill is higher and more uniform among reconstruction methods when the reconstruction target is the Antarctic as a whole rather than smaller Antarctic subregions. This consistency between the methods at the large scale is also observed when reconstructing temperature based on the real δ^{18}O regional composites. In this case, temperature reconstructions based on data assimilation confirm the long-term cooling over Antarctica during the last millennium, and the later onset of anthropogenic warming compared with the simulations without data assimilation, which is especially visible in West Antarctica. Data assimilation also allows for models and direct observations to be reconciled by reproducing the east–west contrast in the recent temperature trends. This recent warming pattern is likely mostly driven by internal variability given the large spread of individual Paleoclimate Modelling Intercomparison Project (PMIP)/Coupled Model Intercomparison Project (CMIP) model realizations in simulating it. As in the pseudoproxy framework, the reconstruction methods perform differently at the subregional scale, especially in terms of the variance of the time series produced. While the potential benefits of using a data assimilation method instead of a statistical method have been highlighted in a pseudoproxy framework, the instrumental series are too short to confirm this in a realistic setup

.

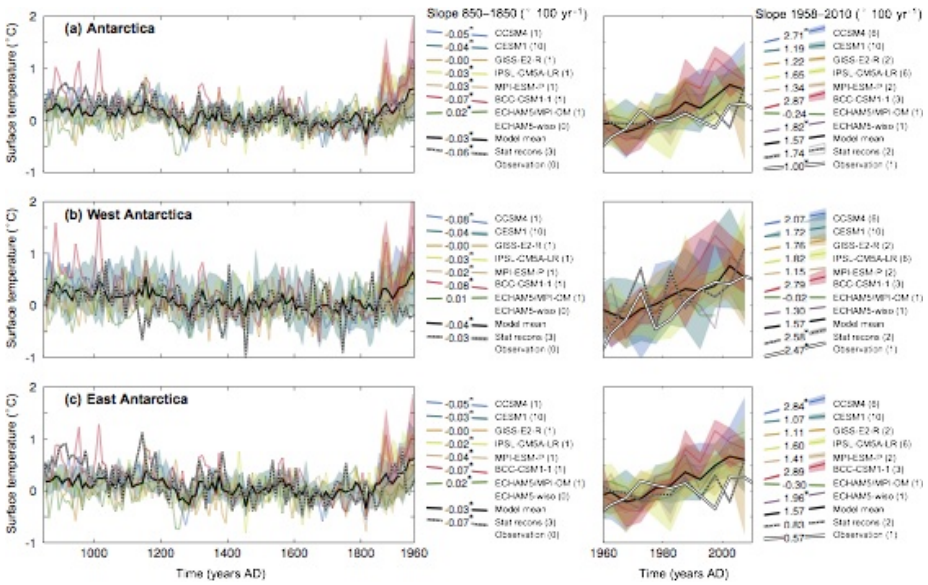

Figure Changes in 10- (left panels) and 5-year averaged (right panels) surface temperature over the 850–2000 CE period over (a) Antarctica, (b) West Antarctica and (c) East Antarctica

Another site, same old song: The Pleistocene-Holocene archaeological sequence of Toca da Janela da Barra do Antonião-North, Piaui, Brazil

Lahaye C., Guérin G., Gluchy M., Hatté C., Fontugne M., Clemente-Conte I., Santos J.-C., Villagran X.S., Da Costa A., Borges C., Guidon N., Boëda E.

Quaternary Geochronology (2019),49, 223-229 – doi: 10.1016/j.quageo.2018.03.006
Financé par projet Ministère des Affaires Européennes et Étrangères

Since 2013, new excavations have focused on the northern part of the Toca da Janela da Barra do Antonião - North rockshelter, which is located on the edge of the Serra da Capivara National Park in Brazil. Ten sediment samples were dated by multigrain quartz OSL and three samples by feldspar IRSL. Multigrain OSL ages on quartz were assessed using the Central Age Model (CAM) and a Bayesian model built with the R BayLum statistics package. Ages are in good stratigraphic agreement and ages from quartz and feldspars, when available, are internally consistent. Furthermore, we produced a Bayesian model (BayLum) based on OSL ages obtained for the six sediment samples of the main stratigraphy that included stratigraphic constraints and a covariance matrix of errors. Two gaps in sedimentation were detected and can be correlated with climatic changes during the MIS 3 and during the MIS 3 to MIS 2 transition. Finally, our results provide a chronological framework for a new important Pleistocene-Holocene sequence in the region.

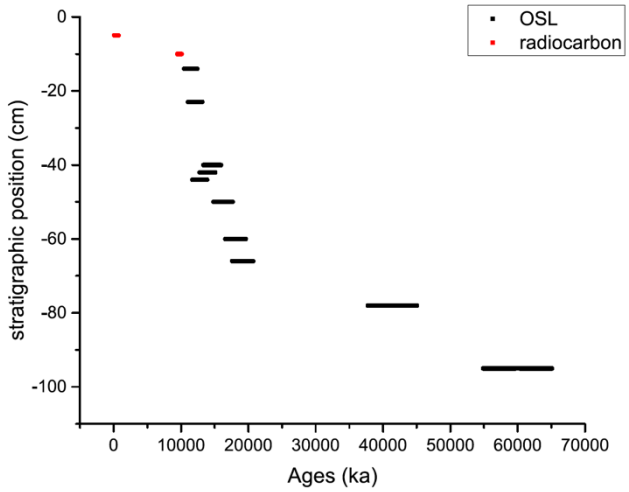

Fig: Summary of OSL and radiocarbon ages establishing the chronostratigraphic framework of the occupations of the Toca da Janela da Barra do Antoniaèo-Norht site (Brazil).

Compositional changes in deglacial red mud event beds off the Laurentian Channel reveal source mixing, grain-size partitioning and ice retreat

Leng W., von Dobeneck T., Just J., Govin A., St-Onge G., Piper D.J.W.

Quaternary Science Reviews (2019) 215, 98-115 - doi: 10.1016/j.quascirev.2019.04.031.

The 1400 km-long, 100-150 km wide and 300-550 m deep Laurentian Channel trough that winds from the St. Lawrence Estuary through the shallow basins of the Gulf of St. Lawrence to the edge of the Grand Banks Shelf, is among Canada's most remarkable bathymetric features. Between 22 and 17 thousand year before present, five large meltwater events from within the Laurentian Channel Ice Stream deposited mud beds meters thick across a large area of the Laurentian Fan and adjacent continental slopes.

This study determines the sources of these event beds and relates them to the glaciological evolution of the retreating Laurentian Ice Stream. We analyzed major element and magnetic mineral contents of these event beds and compare them with a new collection of 80 source reference samples from the Gulf of St. Lawrence area.

Element ratios suggest a steady compositional change from older to younger outburst event beds. Their magnetic properties place event beds on the source mixing trend of four reference samples groups: two magnetite-rich granitic sources (Canadian Shield and/or Southern Newfoundland, in blue and orange in Fig. 1) and two hematite-rich sources (Appalachian red beds, in red in Fig. 1). Using a deterministic linear source mixing model based on IRM100mT, HIRM and Ca%, we find that the earlier two outburst events (Fig. 1, top) had higher contributions from granitic and calcareous sources than the later three events (Fig. 1, bottom). Combining materials, timing and scenarios of the outburst events with ice-sheet retreat and ice-stream dynamics, we argue that the subglacial sediment depocenter of the earlier two event beds was located in the lower Laurentian Channel while that of the later three events was upstream from Cabot Strait (Fig. 1).

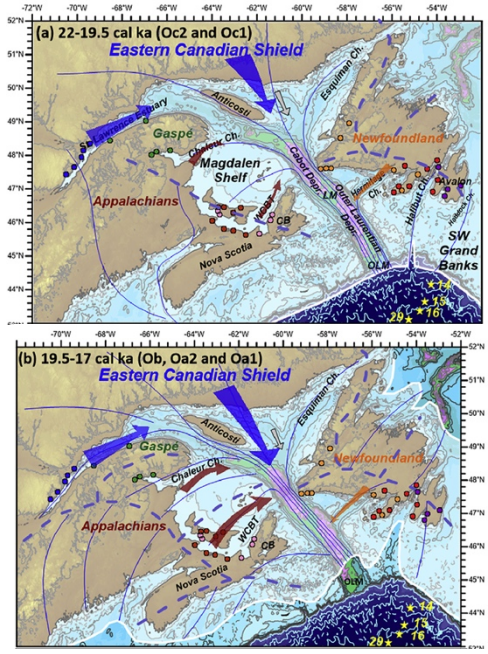

Fig. 1. Provenance of sediments during ice margin retreat in the Gulf of St. Lawrence area for (top) the early outburst events (Oc2, Oc1) and (bottom) the late three outburst events (Ob, Oa2, Oa1). Changing sediment provenance, from increased magnetic-rich granitic contribution (blue/orange arrows, top) to increased hematite-rich red bed input (red arrows, bottom), highlights the changing location of the subglacial sediment depocenters, from the lower Laurential channel (top) to further upstream in Cabot Depression (bottom).

A luminescence-based chronology for the Harletz loess sequence, Bulgaria

Lomax J., Fuchs M., Antoine P., Rousseau D.-D., Lagroix F., Hatté C., Taylor S.N., Till J.L., Debret M., Moine O., Jordanova D.

Boreas (2019) 48(1), 174-194 - doi : 10.1111/bor.12348

The Harletz loess-palaeosol sequence is located in northwestern Bulgaria and represents an important link between well studied loess sequences in eastern Romania and further sites to the west of the Carpathians (e.g. Serbia and Hungary). The aim of this study was to establish a chronostratigraphy of the deposits, using various methods of luminescence dating, together with basic stratigraphical field observations as well as magnetic properties. Luminescence dating was carried out using the quartz fine grain fraction and a SAR protocol, and the feldspar coarse grain fraction, applying the MET-pIRIR protocol. Due to underestimation of the quartz fine grain fraction in the lower parts of the sequence, the resulting chronology is mainly based on the feldspar ages, which are derived from the stimulation temperature at 150 °C. A comparison with nearby sequences from Serbia, Hungary and Romania, and interpretations obtained through the stratigraphical and sedimentological signature of the sequence, supports the established chronology. Our data suggest that the prominent palaeosol (soil complex) in the upper quarter of the sequence was formed during MIS 5. It would follow that large parts of the Last Glacial loess overlying this palaeosol were probably eroded, and that the thick loess accumulation underlying this soil complex can be allocated to the penultimate glacial (MIS 6). A prominent MIS 6 tephra, which has been reported from other sequences in the area, is also present at Harletz..

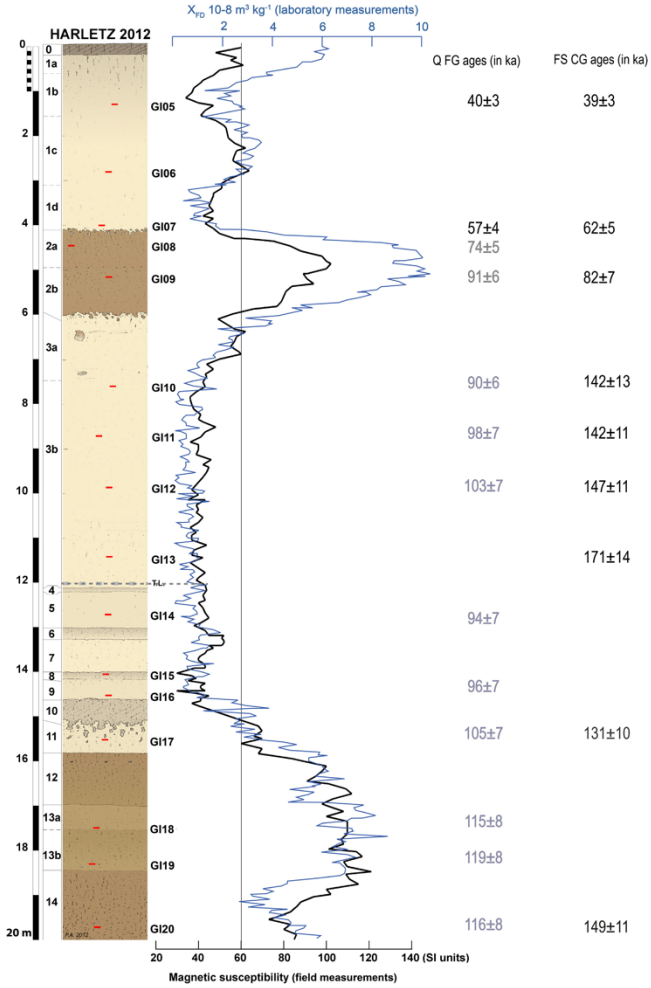

Figure 1: Stratigraphy of the studied loess sequence in Harletz (Bulgaria), with pedosedimentary units presented in Table 1 and magnetic susceptibility data measured in the field (bottom scale) and in the laboratory (top scale). Unit differentiation is based on field observations and was refined by sedimentological and magnetic property data. QFG = quartz fine grain; FSCG = feldspar coarse grain

Palaeoenvironmental and palaeohydrological variability of mountain areas in the central Mediterranean region: A 190 ka-long chronicle from the independently dated Fucino palaeolake record (central Italy)

Mannella G., Giaccio B., Zanchetta G., Regattieri E., Niespolo E.M., Pereira A., Renne P.R., Nomade S., Leicher N., Perchiazzi N., Wagner B.

Quaternary Science Reviews (2019) 210, 190-210.

Proxy records of past climate change spanning beyond the radiocarbon range commonly derive theirchronologies from orbital tuning strategies, thus bounding our spatio-temporal reconstructions to a priori assumptions that cannot be directly tested. Here we present a tephrochronologically constrained framework of past environmental and climatic changes in the central Mediterranean region during the last ca. 190 ka. Our research is based on a high-resolution, multi-proxy study of a sedimentary record (cores F1-F3) retrieved from the Fucino Basin lacustrine succession, central Italy, in 2015. We update the existing tephrostratigraphic framework of the F1-F3 record with the finding of the widespread Campanian Ignimbrite tephra marker layer and produce a robust and independent chronology based on new and published $^{40}Ar/^{39}Ar$ and ^{14}C dating of 17 tephra layers (Fig. 1). Observed palaeoenvironmental changes are tracked in other lacustrine, marine and speleothem records across the Mediterranean and North Atlantic regions via tephrostratigraphic correlations and chronological matching providing a robust assessment of age uncertainties. Results show a complex interplay between local environmental changes and broadscale climatic processes highlighting a strong orbital forcing on glacial-interglacial changes. Along with these major changes we detect prominent millennial-scale variability. During times of intermediate global ice volumes, Mediterranean mountain ecosystems oscillated around an “interglacial” state suggesting that climatic shifts, although large, did not exceed the local environmental tolerance-resilience threshold. Conversely, during periods of large global ice volume, we observe subdued millennial-scale variability with ecosystems operating in a strictly ruled glacial environment.

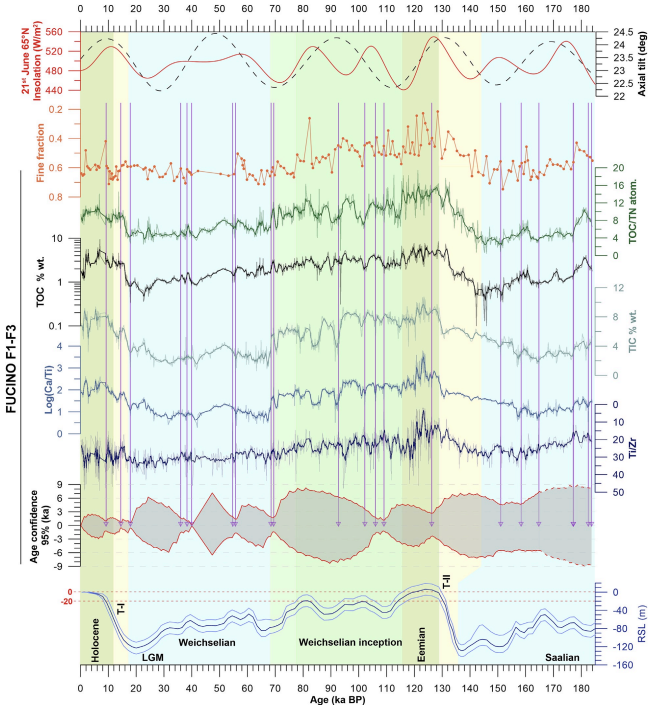

Fig.1 Time-series overview - Fucino F1-F3 proxy time series plotted together with calculations for past Earth's axial tilt and 65_N summer solstice insolation (Laskar et al., 2004)and global Relative Sea Level (RSL) variations (Waelbroeck et al., 2002) as indicative of global ice volume. The two dotted red lines indicate the present day sea level and the -20m threshold, as an indicator of little Northern Hemisphere (NH) ice volumes outside Greenland under interglacial conditions (PAGES, 2016). Ages are at 2σ age uncertainties.

Volcano-tectonic deformation in the Monti Sabatini Volcanic District at the Gates of Roma (central italy) : Evidence from new geochronologic constraints on the Tiber River MIS 5 terraces

Marra F., Florindo F., Jicha B.R., Nomade S., Palladino D.M., Pereira A., Sottilli G., Tolomei C.

Scientific Reports (2019) 9:11496 - doi: 10.1038/s41598-019-47585-8

The accumulation of magma within the Monti Sabatini Volcanic District (MSVD), Italy, coupled with the extensional tectonics of the region, pose both volcanic and tectonic hazards to the city of Rome, located 20 km to the southeast. We combine $^{40}Ar/^{39}Ar$ geochronology of volcanic deposits and a geomorphologic /stratigraphic/ paleomagnetic study of fluvial terraces to determine the recurrence interval and the time elapsed since the last eruption of the MSVD. Moreover, we provide a date for the youngest known eruption of the MSVD and assess the timing of the most recent volcanic phase. Results of this study show :

(i) The most recent eruptive phase occurred between 100 ka and 70 ka;

(ii) the anomalously high elevation of the MIS 5 terrace indicates that it was concurrent with 50 m of uplift in the volcanic area;

(iii) The time since the last eruption (70 ka) exceeds the average recurrence interval (39 ky) in the last 300 ky, as well as the longest previous dormancy (50 ky) in that time span ;

(iv) The current duration of dormancy is similar to the timespan separating the major explosive phase that occurred 590–450 ka

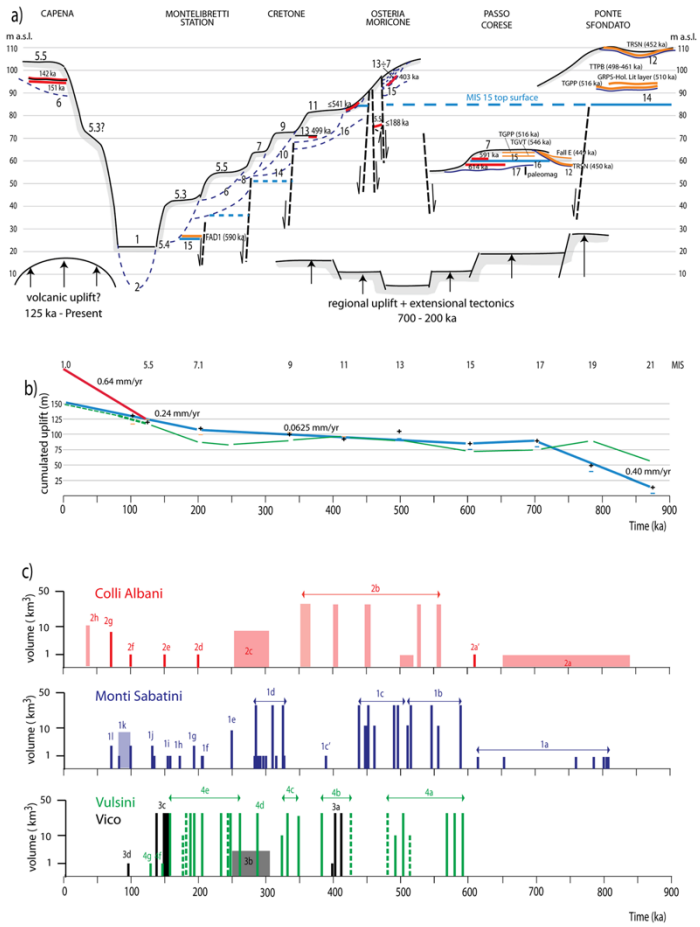

Fig. 1. a) Schematic, composite cross-section showing the morpho-stratigraphical and structural setting of the investigated area. b) Cumulated uplift curve in the time interval 900 ka through Present for the eastern side of the Tiber Valley (blue line) and in the last 125 ka for the western sector (red line). c) Synoptic eruptive histories of the volcanic districts of the Roman Province. Boxes represent eruption cycles, bars represent single events Vertical height is proportional to estimated total erupted volumes in logarithmic scale

The penultimate deglaciation: protocol for Paleoclimate Modelling Intercomparison Project (PMIP) phase 4 transient numerical simulations between 140 and 127 ka, version 1.0

Menviel L., Capron E., Govin A., Dutton A., Tarasov L., Abe-Ouchi A., Drysdale R.N., Gibbard P.L., Gregoire L., He F., Ivanovic R.F., Kageyama M., Kawamura K., Landais A., Otto-Bliesner B.L., Oyabu I., Tzedakis P.C., Wolff E., Zhang X.

Geoscientific Model Development (2019) 12(8), 3649-3685 - doi: 10.5194/gmd-12-3649-2019.

The penultimate deglaciation (~ 138–128 thousand years before present, hereafter ka) is the transition from the penultimate glacial maximum to the Last Interglacial (LIG, ~ 129–116 ka). The LIG stands out as one of the warmest interglacials of the last 800,000 years, with high-latitude climate warmer than today and global sea level likely higher by at least 6 m. Considering the transient nature of the Earth system, the LIG climate and ice-sheet evolution were certainly influenced by changes occurring during the penultimate deglaciation. It is thus important to investigate, with Earth system models, the climate and environmental response to the large changes in boundary conditions (i.e. orbital configuration, ice-sheet geometry and associated meltwater fluxes, Fig. 1) occurring during the penultimate deglaciation.

Here, as part of the working group on Quaternary Interglacials (QUIGS), we propose a protocol to perform transient simulations of the penultimate deglaciation under the auspices of Paleoclimate Modelling Intercomparison Project phase 4. This design includes time-varying changes in orbital forcing, greenhouse gas concentrations, continental ice sheets as well as fresh-water input from the disintegration of continental ice sheets. This experiment is designed for climate models to assess the coupled response of the climate system to all forcings. Additional sensitivity experiments are proposed to evaluate the response to each forcing. Finally, a selection of paleo-records representing different parts of the climate system is presented, providing an appropriate benchmark for upcoming model–data comparisons across the penultimate deglaciation.

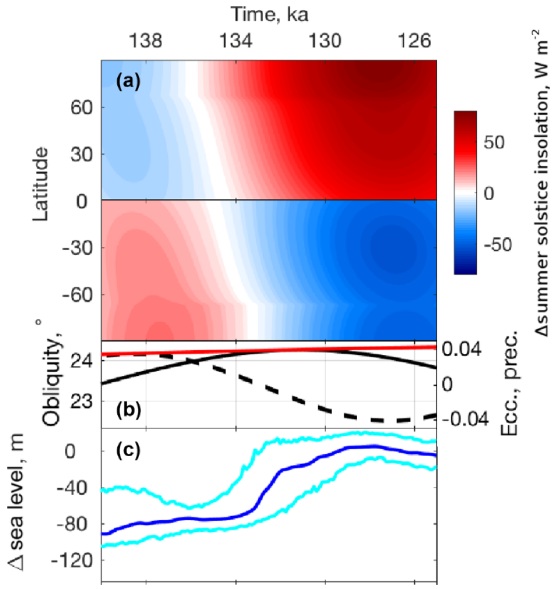

Fig. 1. The penultimate deglaciation: (a) Summer solstice insolation anomalies. Time series of (b) eccentricity (red), obliquity (solid black) and precession (dashed black) (Berger, 1978). (c) Global mean sea- level anomaly probability maximum (blue) including its 95 % confidence interval (cyan) (Grant et al., 2014).

Improving North Atlantic Marine Core Chronologies Using ^{230}Th Normalization

Missiaen L., Waelbroeck C., Pichat S., Jaccard S.L., Eynaud F., Greenop R., Burke A.

Paleoceanography and Paleoclimatology (2019), 34, 1057-1073

Producing independent and accurate chronologies for marine sediments is a prerequisite to understand the sequence of millennial-scale events and reveal potential temporal offsets between marine and continental records, or between different marine records, possibly from different regions. The last 40 ky is a generally well-constrained period since radiocarbon (^{14}C) can be used as an absolute dating tool. However, in the northern North Atlantic, calendar ages cannot be directly derived from ^{14}C ages, due to temporal and spatial variations of surface reservoir ages. Alternatively, chronologies can be derived by aligning Greenland ice-core time series with marine surface records. Yet this approach suffers from the lack of clearly defined climatic events between 14.7 and 23.3 cal ky BP (hereafter ka), a crucial period encompassing Heinrich Stadial 1 and the onset of the last deglaciation. In this study, (i) we assess the benefits of ^{230}Th normalization to refine the sedimentation history between surface temperature alignment tie points and (ii) revisit the chronologies of three North Atlantic marine records. Our study supports the contention that the marked increase in the Greenland Ca^{2+} record at 17.48 ka ± 0.21 ky (1σ) occurred within dating uncertainty of sea surface temperature cooling in the North Atlantic at the onset of Heinrich Stadial 1. This sharp feature might be useful for future chronostratigraphic alignments to remedy the lack of chronological constraint between 14.7 and 23.3 ka for North Atlantic marine records that are subject to large changes in ^{14}C surface reservoir age.

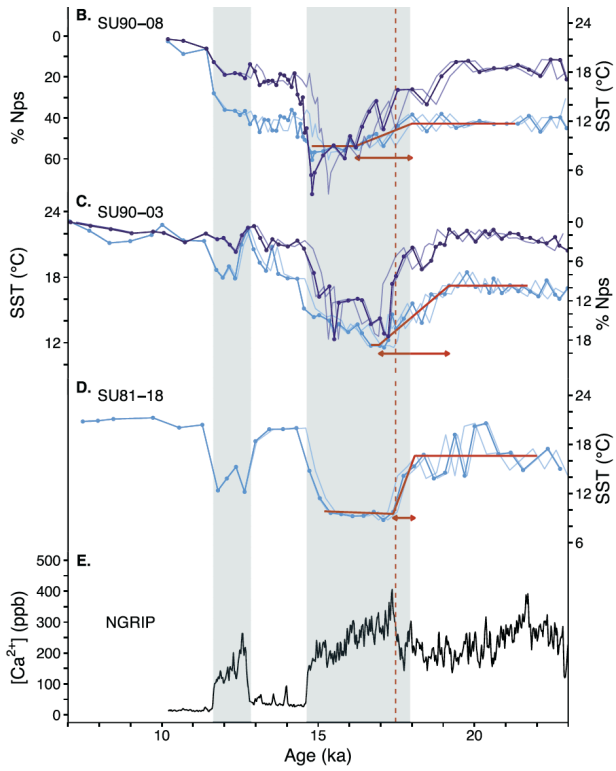

Fig. 1. Sea surface temperature (SST) reconstructions for the cores SU90-03, SU90-08, and SU81-18 compared with NGRIP Ca^{2+} record. (b–d) Summer SST reconstructions (light blue) and %N. pachyderma s. (Nps; dark blue) data for SU90-08 (b), SU90-03 (d), and SU81-18 (e). (e) NGRIP Ca^{2+} record (Seierstad et al., 2014). The thin lines represent the envelope curves obtained when moving the SST alignment tie points within the uncertainties. Precise beginning and end of the cooling observed at the beginning of HS1 are represented by the bold red line. The red vertical dashed line represents the midramp of the increase in NGRIP Ca^{2+} at 17.48 ka.

A biface production older than 600 ka ago at Notarchirico (Southern Italy) contribution to understanding early Acheulean cognition and skills in Europe

Moncel M-H., Santagata C., Pereira A, Nomade S., Bahain J-J., Voinchet P., Piperno M.

Plos One (2019) 14(9): e0218591 – doi : 10.1371/journal.pone.0218591

For the past decade, debates on the earliest evidence of bifacial shaping in Western Europe, The onset and technological strategies for making Large Cutting Tools (LCTs), are often associated with other behavioral changes, such as increased core technology complexity. Current archaeological patterns do not support the existence of transitional industries. Rather, the scant evidence suggests that biface production associated with the management of bifacial volume was widespread around 700 ka. Among the earliest sites, the site of Notarchirico in Southern Italy stands out as one of the most significant examples. 40Ar/39Ar ages and ESR dates recently provided a revised chronology for the whole sedimentary sequence and constrained the archaeological levels between ca. 610 and 670 ka. Five archaeo-surfaces (A, A1, B, D and F) yielded LCTs, including bifaces. In light of this new chronological framework, which is much shorter than previously thought, we propose in this contribution a revision of the bifaces by applying the "chaine opératoire" method for the first time (analysis of reduction processes). The technological analysis shows that hominins had the capacity to manage bifacial volumes, when raw material quality was adequate. Clear differences do not emerge between the different levels in terms of shaping modes or final forms. However, we demonstrate that the oldest level (level F, Fig. 1)), with the richest corpus, lacks flint and displays a higher diversity of bifaces. This ability to manage bifacial and bilateral equilibrium, as well as the diversity of the morphological results, is observed in a few pene contemporaneous sites (700–600 ka), both in the north-western and southern parts of Western Europe. This patterns suggest that hominins mastered well-controlled and diversified biface production, combining intense shaping and minimal shaping, and shared a common technological background regardless of the geographical area, and applied this technology regardless of the available raw materials. The degree of skill complexity of hominins in Western Europe between 700 and 600 ka, the current lack of evidence suggesting "gradual industries" between core-and-flake series and Acheulean techno-complexes, raise numerous questions on the origin of new behaviors in Western Europe, their mode of diffusion, and their association with Homo heidelbergensis or other Middle Pleistocene populations.

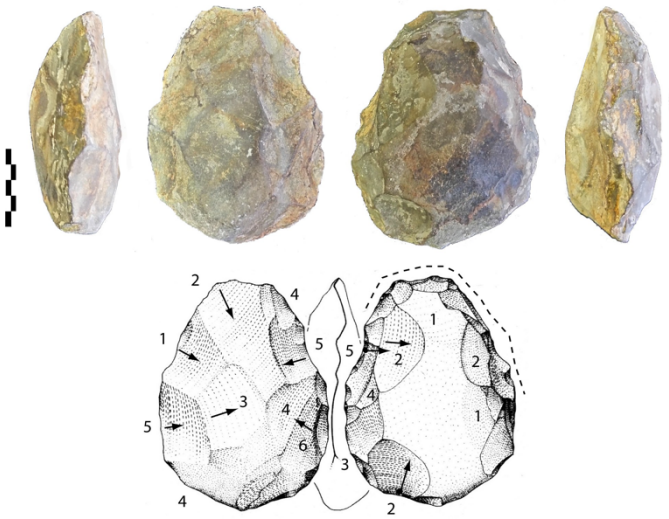

Fig. 1 : Notarchirico Archaeosurface F. Biface on biconvex limestone cobble (more than 670 ka, dated by $^{40}Ar/^{39}Ar$)

Investigations archéobotaniques sur les premiers éleveurs de chevaux au Kazakhstan

Motuzaite-Matuzeviciute G., Lightfoot E., Liu X., Jacob J., Outram A.K., Zaibert V.F., S. Zakharov S., Jones M.K.

Journal of Archaeological and Anthropological Sciences (2019) 11, 6243 - doi : 10.1007/s12520-019-00924-2

Cet article présente les premiers résultats des fouilles du site de Botai (Kazakhstan). Il s'agit d'un campement occupé par des éleveurs de chevaux des steppes d'Asie Centrale durant l'Énéolithique. Les datations au radiocarbone indiquent deux occupations distinctes : entre 3550 et 2700 cal BC puis vers 2000 cal BC. Les résultats d'archéobotanique, fondés sur les vestiges macrobotaniques et sur l'analyse de biomarqueurs moléculaires indiquent que ces populations n'appartenaient pas à un réseau complexe d'échanges de céréales qui ne constituaient pas, par ailleurs, l'alimentation principale. La présence de miliacine suggère que ces populations ont pu cultiver le millet, peut-être après la période d'occupation principale du site.

Le paysage surplombant le site de Botai (Kazakhstan).

The Atlantic Meridional Overturning Circulation as productivity regulator of the North Atlantic Subtropical Gyre

Nave S., Lebreiro S., Michel E., Kissel C., Figueiredo M.O. , Guihou A., Ferreira A., Labeyrie L., Alberto A.

Quaternary Research (2019) 91(1), 399-413

Spatially extensive and intense phytoplankton blooms observed off Iberia, in satellite pictures, are driven by significant nutrient supply by upper-ocean vertical mesoscale activity rather than by horizontal advection by coastal upwelling. Productivity of oligotrophic regions is still poorly depicted by discrete instrumental and model data sets. The paleoproductivity reconstructions of these areas represent the mean productivity over long periods, bringing new insights into the total biomass fluxes. Here, we present paleoproductivity records from the oceanic Tore Seamount region, covering the period from 140 to 60 ka. They show higher nutrient supplies during Termination II, Marine Oxygen Isotope Stage (MIS) 4, MIS 6, and warming transitions of the MIS 5 sub-stages. The highest nutrient content (higher productivity) in phase with tracers of bottom-water ventilation (benthic $\delta^{13}C$, $^{231}Pa/^{230}Th$) establishes a strong linkage with variability of Southern Ocean-sourced waters. Low productivity and ventilation over warm sub-stages of MIS 5 respond instead to North Atlantic Deep Water. Assuming that the Tore Seamount is representative of oligotrophic regions, the glacial-interglacial relationship observed between paleoproductivity and Atlantic Meridional Overturning Circulation strength opens new insights into the importance of estimating the total biomass in these regions. The subtropical gyres might play a considerable role in the carbon cycle over (sub-) glacial-interglacial time scales than previously thought.

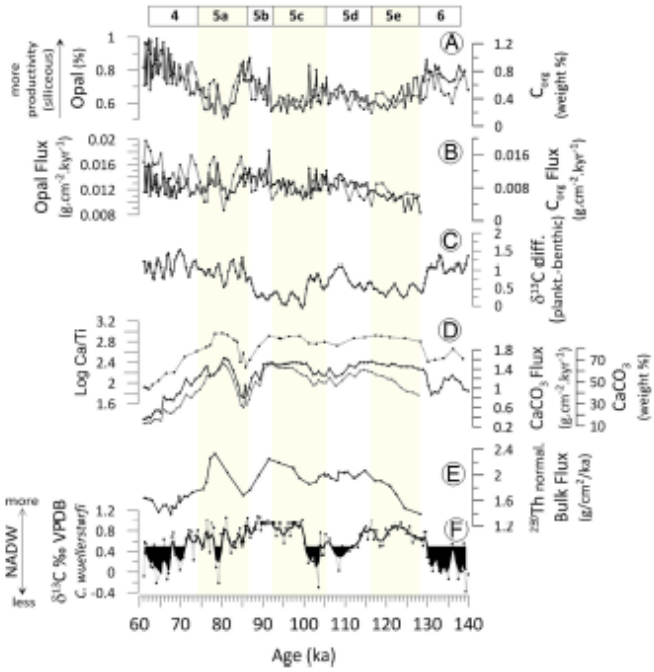

Fig. 1. Productivity proxies from core MD01-2446. (A) Opal content (weight %). Right-side axes are the same parameter ^{230}Th normalized flux (g. cm-2ka-1; bold line). (B) $\delta^{13}C$ difference (G. bulloides - C. wuellerstorfi). (C) Organic carbon (weight %). (D) $CaCO_3$ (weight %). Right-side axes are the same parameter 230Th normalized flux (g. $cm^{-2}ka^{-1}$; bold line). (E) ^{230}Th normalized bulk flux ($g.cm^{-2}ka^{-1}$; Guihou et al., 2010). (F) Benthic $\delta^{13}C$ record..

High-resolution foraminifer stable isotope record of MIS 19 at Montalbano Jonico, southern Italy: A window into Mediterranean climatic variability during a low-eccentricity interglacial

Nomade S., Bassinot F., Marino M., Simon Q., Dewilde F., Maiorano P., Isguder G., Blamart D., Girone A., Scao V., Pereira A., Toti F., Bertini A., Combourieu-Nebout N., Peral M., Bourles D.L., Petrosino P., Gallicchio S., Ciaranfi N.

Quaternary Science Reviews (2019) 205, 106-125.

Understanding millennial and sub-millennial climate variability during past low eccentricity interglacials similar to the Holocene is important for forecasting the evolution of climate and natural variability. The Ideal section (Montalbano Jonico, Southern Italy) studied here provides one of the best records of MIS 19c, the closest orbital analog to the Holocene. This exposed marine series covers Termination IX to the inception of MIS 18 with very high sedimentation rates (i.e. 90-200 cm/ka). We present 1) benthic δ18O and $\delta^{13}C$ records at 90-200 year time-resolution (Fig.1), 2) a new $^{40}Ar/^{39}Ar$ age of 774.1 ± 0.9 ka for tephra layer V4 (Matuyama-Brunhes transitional period) and 3) new calcareous plankton, palynological and authigenic $^{10}Be/^{9}Be$ data. Our new Bayesian depth-age model suggests a 11.5 ± 3.4 ka (95% confidence) duration for the climatic optimum. The δ18O series reveals millennial-scale oscillations (with sharp transitions < 200 years) between ~774.0 and the onset of MIS 18 (~757.0 ka, Fig. 1) with a cyclicity of about 5.4 ka. Spectral analysis and band-pass filtering indicate that these climate oscillations existed throughout the entire MIS 19 period, although they were dampened during MIS 19c, which is chiefly controlled by orbitally-driven insolation. The amplitude of those sub-orbital oscillations increased towards MIS 18 as the climate became drier and cooler. The Ideal section reveals, with unprecedented detail, millennial scale climatic oscillations of MIS 19b-a that have been observed worldwide. They highlight the response of the central Mediterranean area to North Atlantic climatic variation (i.e. oceanic circulation and atmospheric processes related to ice-sheet dynamics) during this low eccentricity interglacial.

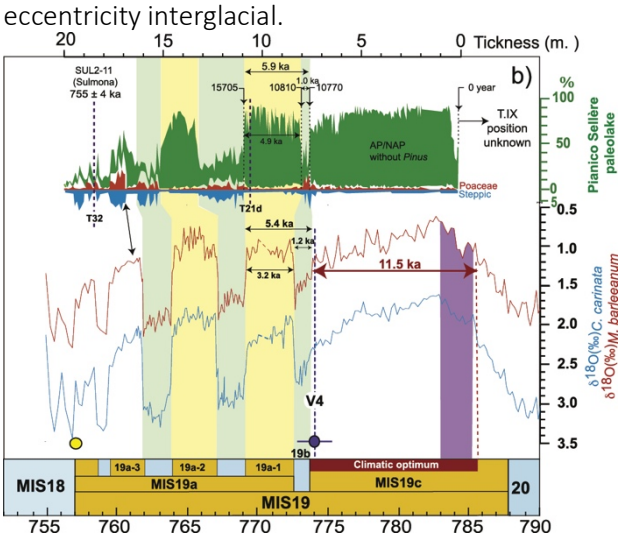

Fig.1 Ideal section δ18O profiles compared with the pollen record from the Pianico-Sellère MIS 19 interglacial (Moscariello et al., 2000; Rossi et al., 2003). The floating varve-based chronology is from Moscariello et al. (2000) and Mangili et al. (2007). (For interpretation of the references to colour in this figure legend, the reader is referred to the Web version of this article.)

Influence of summer sublimation on δD, $\delta^{18}O$, and $\delta^{17}O$ in precipitation, East Antarctica, and implications for climate reconstruction from ice cores

Pang H., Hou S., Landais A., Masson-Delmotte V., Jouzel J., Steen-Larsen H.-C., Risi C., Zhang W.B., Wu S., Li Y., An C., Wang Y., Prié F., Minster B., Falourd S., Stenni B., Scarchilli C., Fujita K., Grigioni P.

JGR Atmosphere (2019) 124(13), 7339-7358
Projet/financement: ERC COMBINISO

In central Antarctica, where accumulation rates are very low, summer sublimation of surface snow is a key element of the surface mass balance, but its fingerprint in isotopic composition of water (δD, $\delta^{18}O$, and $\delta^{17}O$) remains unclear. In this study, we examined the influence of summer sublimation on δD, $\delta^{18}O$, and $\delta^{17}O$ in precipitation using data sets of isotopic composition of precipitation at various sites on the inland East Antarctica. We found unexpectedly low $\delta^{18}O$ values in the summer precipitation, decoupled from surface air temperatures. This feature can be explained by the combined effects of weak or nonexistent temperature inversion and moisture recycling associated with sublimation-condensation processes in summer. Isotopic fractionation during the moisture-recycling process also explains the observed high values of d-excess and ^{17}O-excess in summer precipitation. Our results suggest that the local cycle of sublimation-condensation in summer is an important process for the isotopic composition of surface snow, water vapor, and consequently precipitation on inland East Antarctica.

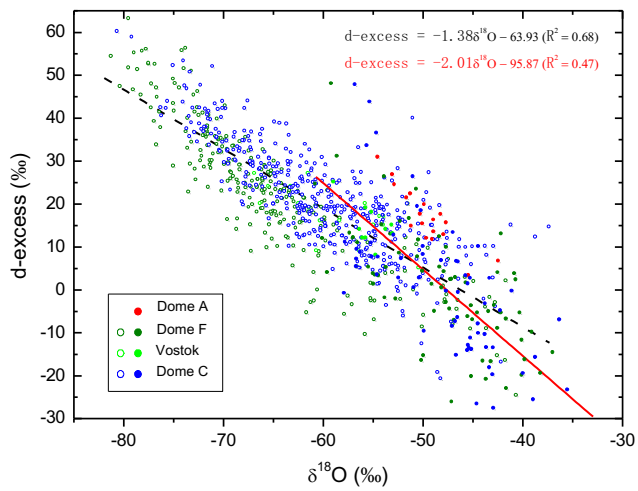

Figure: A comparison of the d-excess/$\delta^{18}O$ relationship in precipitation at Dome A, Dome F, Vostok and Dome C between the warm season (November-January, solid dots and the red line) and the cold season (February-October, open dots and the black dashed line). Analysis of covariance (ANCOVA) indicates that the linear slopes of d-excess/$\delta^{18}O$ during the warm and cold seasons are significantly different.

Radiocarbon and radiocesium in litter fall at Kawamata, ~45 km NW from the Fukushima Dai-ichi nuclear power plant (Japan)

Paterne M., Evrard O., Hatté C., Laceby P.J., Nouet J., Onda Y.

Journal of Radioanalytical and Nuclear Chemistry (2019), 319(3), 1093-1101 - doi : 10.1017/s10967-018-6360-9

Radiocarbon and radiocesium were measured on litter fractions (LF) collected on November 19th, 2011 at 40 km NW of the FDNPP. The ^{137}Cs concentration is much higher in the lower fraction LFb at 226,650 ± 170 Bq kg^{-1} than in the upper fraction LFa at 7290 ± 40 Bq kg^{-1}. From leaf-air ^{14}C comparison, no excess ^{14}C due to the FDNPP accident is detected in LFa deposited in 2010–2011. A significant ^{14}C difference of 1.4% exists between pine needles and deciduous leaves in LFb, which may be due either to post-depositional processes or to a turnover time of 0.5–1 year of stored carbon for deciduous leaves growth.

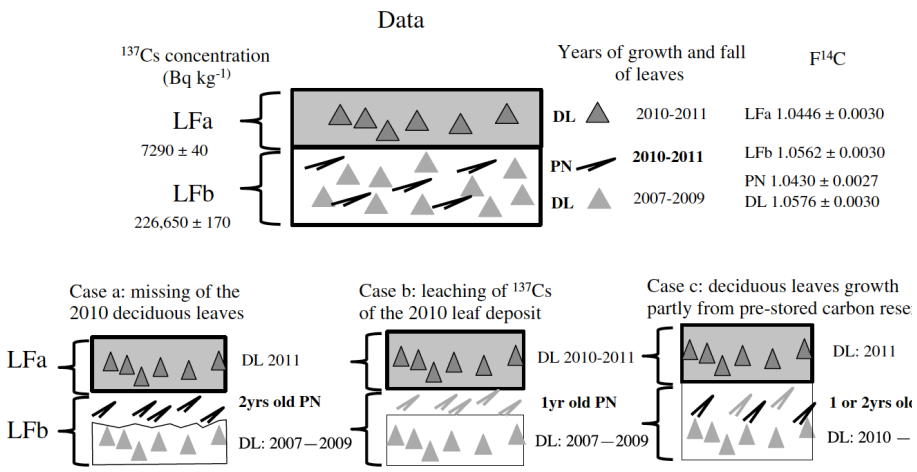

Figure 3 : Schematic description of the litter fall deposition LFa and LFb showing the results of the ^{137}Cs concentration, of the time interval of calibrated ^{14}C of deciduous leaves (DL) and pine needles (PN) and of F^{14}C.

Un méga-puits de carbone et de silice dans les sédiments profonds près du canyon du Congo

Rabouille C., Dennielou B., Baudin F., Raimonet M., Droz L., Khripounoff A., Martinez P., Mejanelle L., Michalopoulos P., Pastor L., Pruski A., Ragueneau O., Reyss J.L., Ruffine L., Schnyder J., Stetten E., Taillefert M., Tourolle J., Olu K.

Quaternary Sciences Review (2019) 222, 105854 - doi : 10.1016/j.quascirev.2019.07.036.

Le cycle du carbone ne connait pas de limite entre les grands compartiments du système Terre et pourtant les flux et leur devenir aux interfaces entre les continents et les océans est encore mal connu. Dans un projet de recherche démarré il y a 10 ans, un groupe de chercheurs, d'ingénieurs et de techniciens emmenés par le LSCE a étudié les lobes terminaux du canyon du Congo à 800 km des côtes africaines par 5000 mètres de fond. Ce groupe pluridisciplinaire comptant des géologues, des géochimistes de l'organique et de l'inorganique, des biologistes- macro et micro, était constitué de groupes de recherches de l'IFREMER-Brest, de l'UPMC-Paris et Banyuls, de l'IUEM-Brest, de l'Univ. Bordeaux, du Georgia Institute of Technology et de l'Hellenic Center for Marine Research. Au cours des deux campagnes océanographiques dédiées à ce projet, nous avons pu explorer en profondeur pour la première fois, les sédiments du complexe terminal des lobes du canyon du Congo vers 5000 mètres de profondeur. Celui-ci est une structure sous-marine gigantesque qui démarre dans l'estuaire du fleuve Congo et se termine dans les abysses à près de 800 km des côtes. Ce canyon draine une partie importante mais mal quantifiée des apports particulaires du Congo.

Les premières observations en Février 2011 faites à l'aide du Robot sous-marin ROV Victor 6000 de l'IFREMER nous ont confirmé que ces sédiments contenaient de grandes quantités de carbone organique : en effet, ils abritent des faunes comme ces bivalves vesicomyidés chimiosynthétiques (Figure 1) qui ne vivent que dans des environnements très réduits typiques des enrichissements en matière organique.

Lors de la deuxième campagne en Décembre 2011, en utilisant des techniques de pointe *in situ* (piège à particules, lander équipés d'électrode ou de chambres benthique, échantillonnage par le ROV Victor), et en les complétant par des mesures en laboratoire sur le type de carbone des sédiments, et sur les taux d'accumulation en utilisant les radionucléides, nous avons pu dresser un bilan du carbone et de la silice depuis les apports du fleuve Congo jusqu'aux lobes terminaux Fig. 2). Celui-ci montre la prédominance des apports par le canyon à la zone des lobes et l'importance de l'enfouissement dans cette zone océanique. On a pu calculer qu'environ 20% du carbone organique exporté par le Congo était enfoui dans cette zone des lobes située à plus de 800km des côtes et que cette zone représentait un puits de carbone organique océanique énorme, 20% du total pour l'Atlantique Sud, au regard de sa surface infime qui ne représente que 0.01% de l'Atlantique Sud. Avec ces lobes termianux, on a donc affaire à des confettis hyper-actifs dans le cycle du carbone qu'il faudra explorer pour comprendre plus en profondeur le cycle du carbone océanique.

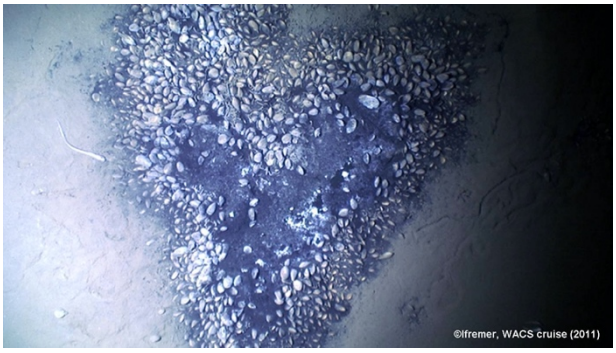

Fig. 1. « Coeur » de bivalves chimiosynthétiques des grands fonds sur sédiments réduits (taille 2m)

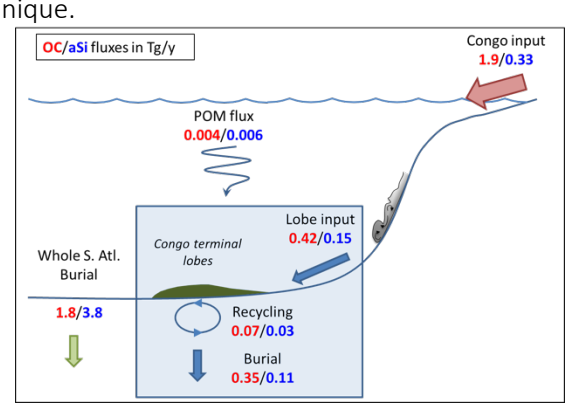

Fig. 2. Bilan de carbone organique (OC-rouge) et de silice amorphe (aSi-bleu) depuis l'embouchure du Congo jusqu'aux lobes terminaux.

Frequency and dynamics of millennial-scale variability during Marine Isotope Stage 19: Insights from the Sulmona Basin (central Italy)

Regattieri E., Giaccio B., Mannella G., Zanchetta G., Nomade S., Tognarelli A., Perchiazzi N., Vogel H., Boschi C., Drysdale R.N., Wagner B., Gemelli M., Tzedakis P.C.

Quaternary Science Reviews (2019) 214, 28-43

Among past interglacial periods, Marine Isotope Stage (MIS) 19 is particularly interesting because its orbital geometry is very similar to that of the present interglacial. Here we present a high-resolution (sub-centennial) multiproxy record covering the ca. 790-770 ka interval, i.e. the interglacial MIS 19c and the ensuing glacial inception of MIS 19b, from a lacustrine sediment sequence retrieved from the Sulmona Basin (central Italy). The record has an independent chronology based on radiometric dating of six volcanic ash layers, and the resulting age model has a mean associated uncertainty of ± 2.6 kyr. Variations in sediment geochemistry and mineralogy are interpreted in terms of past hydrological and temperature changes. Several millennial and sub-millennial events of reduced precipitation are well expressed (Fig. 1). Comparisons with continental and marine records from the mid-latitude and sub-polar North Atlantic suggest a broad spatial expression for the observed events. Events occurring within the interglacial are not clearly associated with changes in marine proxies in the Iberian Margin, although similarities with the record from the sub-polar North Atlantic can be recognized and tentatively linked to changes in local hydrography having a downstream effect amplified by changes in atmospheric circulation. During the glacial inception, changes in the Sulmona record are coherent with changes in North Atlantic records, with drier events likely associated with meltwater-induced intervals of AMOC weakening. An event at ca. 785.6 ka may also reflect oceanic changes caused by freshwater discharges from residual ice-sheets and an outburst flood, similar to the 8.2 ka event in the Holocene.

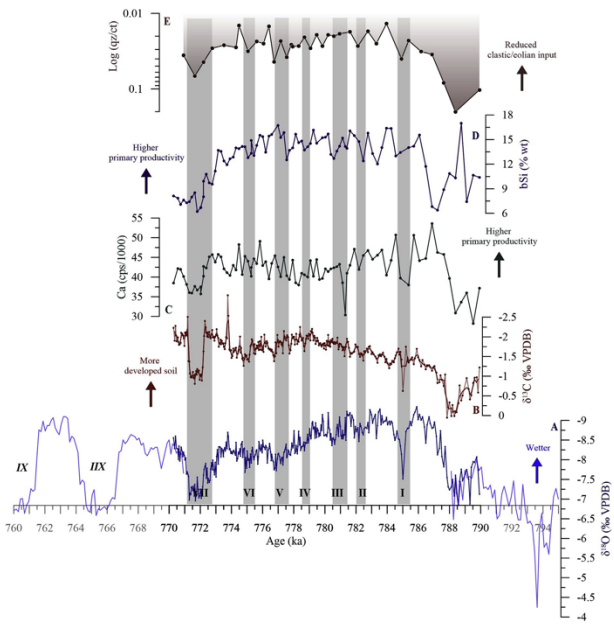

*Fig.1 Sulmona proxy time series presented in this work. A) and B) stable oxygen and carbon isotope composition of bulk lacustrine calcite ($\delta^{18}O$ and $\delta^{13}C$ composition), on A) the lower resolution $\delta^{18}O$ series from Giaccio et al. (2015) is shown as well (light blue line); C) Calcium content (XRF counting*sec); D) Biogenic silica content (% wt); E) Ratio of peak areas of quartz and calcite XRD analyses.*

Pantasma: Evidence for a Pleistocene circa 14 km diameter impact crater in Nicaragua

Rochette P. , Alaç R., Beck P., Brocard G., Cavosie A. J., Debaille V., Devouard B., JourdanF., Mougel B., Moustard F., Moynier F., Nomade S., Osinski G. R., Reynard B., Cornec J.

Meteoritics and Planetary Sciences (2019) 54(4), 880-901.

The circa 14 km diameter Pantasma circular structure (Fig. 1) in Oligocene volcanic rocks in Nicaragua is here studied for the first time to understand its origin. Geomorphology, field mapping, and petrographic and geochemical investigations all are consistent with an impact origin for the Pantasma structure. Observations supporting an impact origin include outward-dipping volcanic flows, the presence of former melt-bearing polymict breccia, impact glass (with lechatelierite and low H_2O,<300 ppm), and also a possible ejecta layer containing Paleozoic rocks which originated from hundreds of meters below the surface. Diagnostic evidence for impact is provided by detection in impact glass of the former presence of reidite in granular zircon as well as coesite, and extraterrestrial $\varepsilon^{54}Cr$ value in polymict breccia.

Two $^{40}Ar/^{39}Ar$ plateau ages with a combined weighted mean age of 815±11 ka (2s; P=0.17) were obtained on impact glass. This age is consistent with geomorphological data and erosion modeling, which all suggest a rather young crater. Pantasma is only the fourth exposed crater > 10 km found in the Americas south of N30 latitude, and provides further evidence that a significant number of impact craters may remain to be discovered in Central and South America.

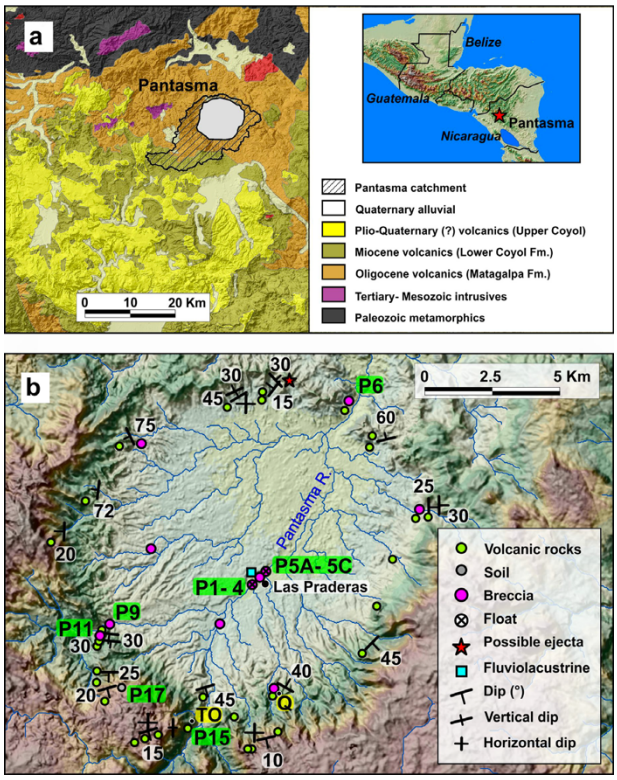

Fig.1 a) Geological map of North Central Nicaragua with the catchment of Pantasma depression (Mapa Geologico Minero de la Republica de Nicaragua, INETER, 1995), modified (Ehrenborg 1996; Elming et al. 2001). Inset: location of the Pantasma structure in Central America. b) Outcrop map of the Pantasma structure with bedding (dip angle in degree, whited) and lithologies indicated on the topography (brown is higher). Bold numbers highlighted in green correspond to rock samples in outcrops, or river bank floats (P1–P5). Torre de oscillation (TO) and Quarry (Q) are indicated (highlighted in yellow). Position of the structure center is 13°22N and 85°57W.

Spatiotemporal patterns of tree growth as related to carbon isotope fractionation in European forests under changing climate

Shestakova T.A. et al., including Daux V.

Glob. Ecology Biogeog. (2019) 28, 1295-1309 - doi: 10.1111/geb.1293

The aim of this paper was to decipher Europe-wide spatio-temporal patterns of forest growth dynamics and their associations with carbon isotope fractionation processes inferred from tree rings as modulated by climate warming.

Location: Europe and North Africa (30–70° N, 10° W–35° E). Time period: 1901–2003. Major taxa studied: Temperate and Euro-Siberian trees.

We characterize changes in the relationship between tree growth and carbon isotope fractionation over the 20th century using a European network consisting of 20 site chronologies. Using indexed tree-ring widths (TRWi), we assess shifts in the temporal coherence of radial growth across sites (synchrony) for five forest ecosystems (Atlantic, boreal, cold continental, Mediterranean and temperate). We also examine whether TRWi shows variable coupling with leaf-level gas exchange, inferred from indexed carbon isotope discrimination of tree-ring cellulose ($\Delta^{13}Ci$).

We find spatial autocorrelation for TRWi and $\Delta^{13}Ci$ extending over a maximum of 1,000 km among forest stands. However, growth synchrony is not uniform across Europe, but increases along a latitudinal gradient concurrent with decreasing temperature and evapotranspiration. Latitudinal relationships between TRWi and $\Delta^{13}Ci$ (changing from negative to positive southwards) point to drought impairing carbon uptake via stomatal regulation for water saving occurring at forests below 60° N in continental Europe. An increase in forest growth synchrony over the 20th century together with increasingly positive relationships between TRWi and $\Delta^{13}Ci$ indicate intensifying impacts of drought on tree performance. These effects are noticeable in drought-prone biomes (Mediterranean, temperate and cold continental).

At the turn of this century, convergence in growth synchrony across European forest ecosystems is coupled with coordinated warming-induced effects of drought on leaf physiology and tree growth spreading northwards. Such a tendency towards exacerbated moisture-sensitive growth and physiology could override positive effects of enhanced leaf intercellular CO_2 concentrations, possibly resulting in Europe-wide declines of forest carbon gain in the coming decades.

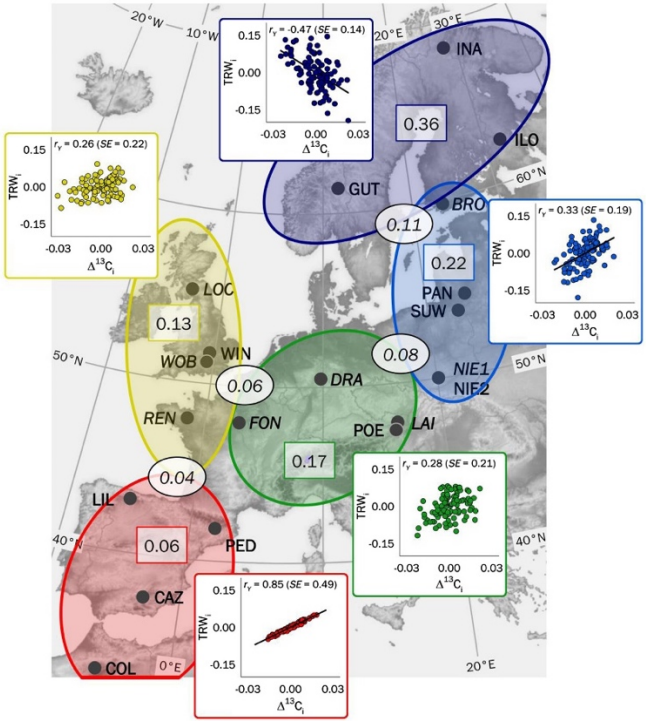

Figure: Geographical distribution of sites, definition of groups of chronologies, synchrony of radial growth, and relationship between TRWi and $\Delta^{13}Ci$ chronologies at the group level across Europe. Each dot identifies a chronology composed of n ≥ 20. Each coloured encircled area identifies a group of chronologies that are separated in pairs up to 1,000 km apart and belong to a particular climate type.

Glacial-interglacial dust and export production records from the Southern Indian Ocean

Thöle L.M., Amsler H. E., Moretti S., Auderset A., Gilgannon J., Lippold J., Vogel H., Crosta X., Mazaud A., Michel E., Martínez-García A., Jaccard S. L.

Earth and Planetary Science Letters 525 (2019) 115716.

Marine sediment cores MD11-3357 (44.68◦S, 80.43◦E, 3,349 m water depth) and MD11-3353 (50.57◦S, 68.39◦E, 1,568 m water depth) were recovered in the vicinity of the Kerguelen Archipelago by the R.V. Marion Dufresne in 2011 (Fig. 1). Core MD11-3357 is located north of the modern Subantarctic Front in the subantarctic Zone (SAZ). The Subantarctic Front is close to the Subtropical Front in this region, forming a very narrow SAZ band. Sediment consists of siliceous and calcareous ooze. Core MD11-3353 is on the modern Polar Front in the antarctic zone (AZ). Sediment mainly consists of siliceous ooze and siliciclastic mud. Age models are based on alignment of reconstructed sea surface temperatures with the EPICA Dome C (EDC) δD record. Vertical particle fluxes were corrected from sedimentary redistribution on the ocean floor using 230Th-normalization.

We observe a high glacial dust input comparable with values from the Atlantic SAZ (Fig. 2). Yet, the offset between Fe and other dust proxies in the SAZ argues for an additional source such as IRDs delivering non-bioavailable iron to SAZ surface waters.

Overall, these results emphasize the potential of Fe fertilization and changes in upwelling intensities in modulating the strength and efficiency of the biological pump. Yet, they also highlight the importance of spatially resolved reconstructions in order to better evaluate regional differences in dust and export production changes needed for a better understanding of glacial carbon sequestration in the Southern Ocean.

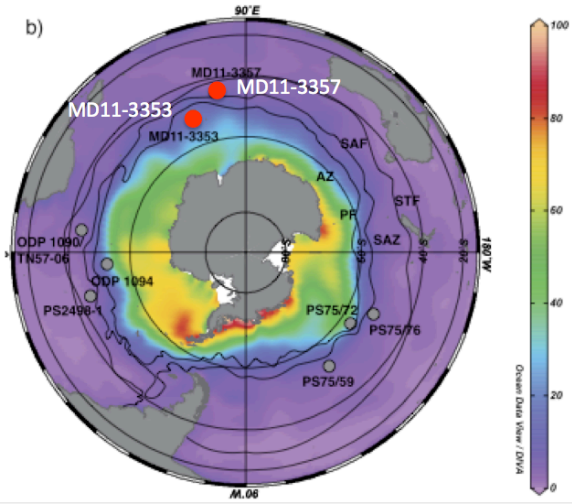

Fig.1: Maps of modern Southern Ocean, with silicate concentration. STF = Subtropical Front, SAF = Subantarctic Front, PF = Polar Front, SAZ = Subantarctic Zone, AZ = Antarctic Zone

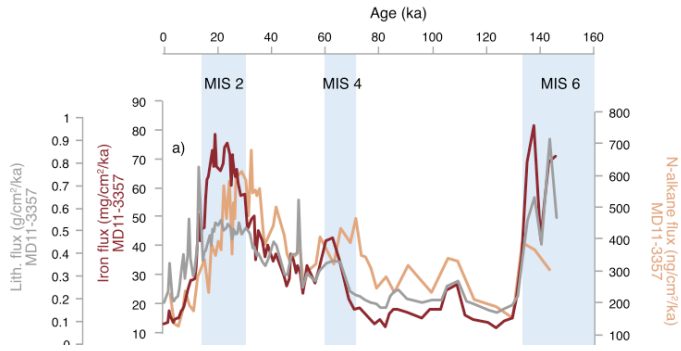

Fig. 2. SAZ (MD11-3357) iron, n-alkane (C25–33) and lithogenic fluxes.

Constraining the age of the last geomagnetic reversal from geochemical and magnetic analyses of Atlantic, Indian, and Pacific Ocean sediments

Valet J-P., Bassinot F. et al.

Earth and Planetary Science Letters (2019) 506, 323-331.

We studied four marine sediment records of the Matuyama–Brunhes geomagnetic reversal from four sites located in the Indian, Atlantic and western Pacific oceans. The results combine paleomagnetic, cosmogenic nuclide beryllium (10Be) and oxygen isotope analyses that were performed on the same samples in order to avoid any stratigraphic bias. The three records from the equatorial Indian Ocean and North Atlantic Ocean did not reveal any offset between the authigenic 10Be/9Be ratio (Be-ratio) peak and the interval of low relative paleointensity (RPI) that characterizes the reversal. The lower and upper limits of transitional directions are also concomitant with the increased atmospheric 10Be production that accompanied the geomagnetic dipole intensity decrease. In contrast, the record from western equatorial Pacific Ocean sediments was found 18 cm below the Be-ratio changes as a result of late magnetization acquisition. At all four sites, maximum 10Be production occurred at the same period soon after the maximum of Marine Isotope Stage 19 (MIS 19) and, therefore, indicates its synchronous worldwide character. Such features are effectively observed from the Be-ratio signals and their relationship with the magnetic transition interval, which further confirms the synchronous character of the transition. Taking all dating uncertainties (1.6 ka between sites and 5 ka for the age model) into consideration, our records suggest a mean reversal age of 772.4 ± 6.6 ka. The age of the transition in the Atlantic Ocean record is closer to 774 ka but this difference is within the limit of significance.

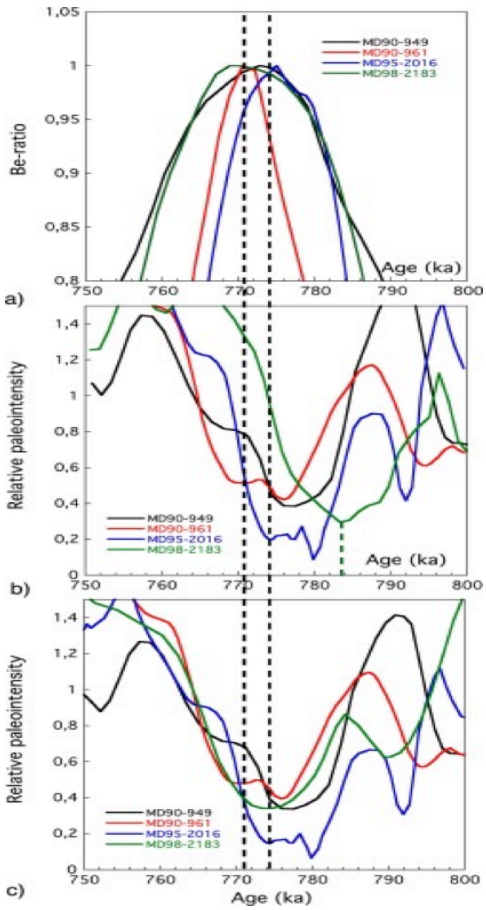

Fig. 1 : Enlarged view of (a) the upper part of the authigenic 10Be/9Be ratio (normalized) changes and (b) lower part of the paleointensity minimum during the reversal as a function of age with the age offset of the RPI signal in core MD98-2183. (c) same as (b) after correcting the RPI signal of MD98-2183 for 20 cm stratigraphic delay with respect to the Be-ratio peak..

Mediterranean winter rainfall in phase with African monsoons during the past 1.36 million years

Wagner B., Vogel H., Alexander Francke, … Nomade S., ….

Nature (2019) 573, 7773, 256-260 – doi : 10.1038/s41586-019-1529-0

Mediterranean climates are characterized by strong seasonal contrasts between dry summers and wet winters. Changes in winter rainfall are critical for regional socioeconomic development, but are difficult to simulate accurately and reconstruct on Quaternary timescales. This is partly because regional hydroclimate records that cover multiple glacial–interglacial cycles with different orbital geometries, global ice volume and atmospheric greenhouse gas concentrations are scarce. Moreover, the underlying mechanisms of change and their persistence remain unexplored. Here we show that, over the past 1.36 million years (Fig. 1), wet winters in the northcentral Mediterranean tend to occur with high contrasts in local, seasonal insolation and a vigorous African summer monsoon. Our proxy time series from Lake Ohrid on the Balkan Peninsula, together with a 784,000 year transient climate model hindcast, suggest that increased sea surface temperatures amplify local cyclone development and refuel North Atlantic low-pressure systems that enter the Mediterranean during phases of low continental ice volume and high concentrations of atmospheric greenhouse gases. A comparison with modern reanalysis data shows that current drivers of the amount of rainfall in the Mediterranean share some similarities to those that drive the reconstructed increases in precipitation. Our data cover multiple insolation maxima and are therefore an important benchmark for testing climate model performance.

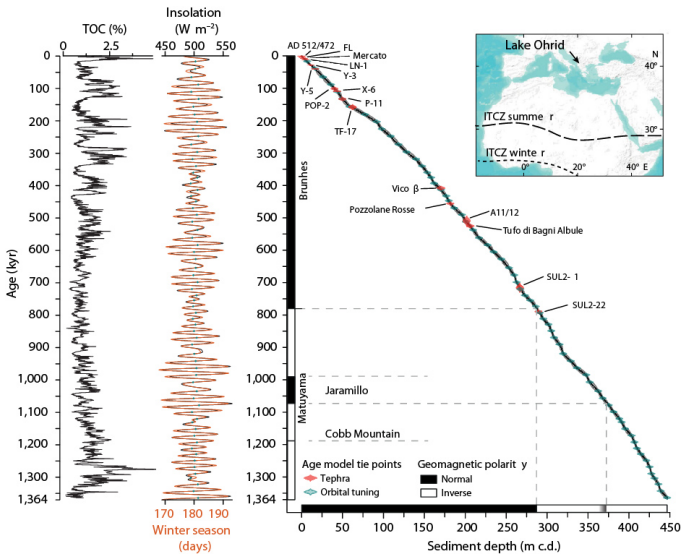

Fig. 1. Chronology and location of the Lake Ohrid DEEP site record. Left to right : total organic carbon (TOC), Winter insolation and lengh of winter season ; DEEP Core age model based on the tephrostratigraphic correlation of the 16 tephra layers to their radiometrically dated proximal deposits (red ellipses) .The map show the Location of Lake Ohrid and the approximate position of the ITCZ ins ummer and winter. m c.d., m composite depth.

A new unspiked K-Ar dating approach using laser fusion on microsamples

Wang F., Shi W.B., Guillou H., Zhang W.B., Yang L., Wu L., Wang Y., Zhu R.

Rapid Communication in Mass Spectrometry (2019) 33, 587-599.

Issues induced by neutron irradiation makes $^{40}Ar/^{39}Ar$ dating inapplicable in some cases. The first issue is 37Ar and 39Ar recoil effects during irradiation that affect fine-grained minerals (<50 µm), such as lunar rocks, glassy groundmass, supergene minerals (e.g., illite, glauconite, Mg-oxide, etc.). The second issue from neutron irradiation is the high radioactivity gain of iron-rich samples such as pyrite, and the third is the production of interference nuclides during irradiation. The inherent drawbacks of conventional K-Ar and current unspiked K-Ar dating make it difficult to assess the reliability of age results.

A new approach is proposed using well-calibrated $^{40}Ar/^{39}Ar$ standard minerals to directly quantify ^{40}Ar, ^{38}Ar and ^{36}Ar. Fish Canyon sanidine (FCs), B4M muscovite and MMhb-1 hornblende, the widely used international standard minerals, were analyzed as unknowns to test the approach. Argon isotope analyses were carried out on a noble-gas mass spectrometer using laser fusion on microsamples (n × 0.01 to n × 0.2 mg). A new isochron – an "inverse isochron" for K-Ar dating – was designed.

FCs and B4M yielded apparent and inverse isochron ages of 28.1 ± 0.1 and 28.0 ± 0.3 Ma, 18.2 ± 0.1 and 18.2 ± 0.5 Ma, which are consistent with the recommended ages, while the MMhb-1 presented lower apparent and inverse isochron ages (510.8 ± 4.8 and 512.3 ± 17.0 Ma) than the recommended ones. The initial argon compositions for the three standard minerals are 299.2 ± 205.3 (FCs), 294.0 ± 16.4 (B4M) and 290.9 ± 203.1 (MMhb-1), agreeing with that of air. The proposed approach potentially overcomes the issues of $^{40}Ar/^{39}Ar$ rising from irradiation and the drawbacks of K-Ar. By using laser fusion on multiple microaliquots from a same sample, this approach can produce accurate and precise K-Ar ages and give an inverse isochron. This new approach may provide an alternate dating method of geochronology based on argon isotopes.

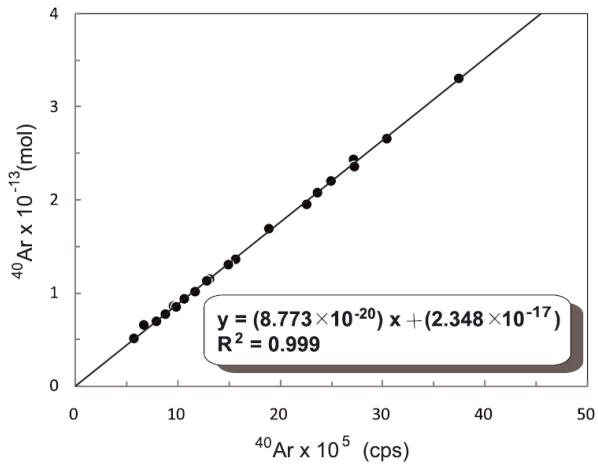

Fig.1 Reference line determined for the Ar content of gas introduced into the IGGCAS Noblesse mass spectrometer and its signal reading. Error bars of 1σ are presented for both 40Arm (in cps) and 40Ar* (in moles) (they are too small to see).*

West Antarctic surface melt triggered by atmospheric rivers

Wille J., Favier V., Dufour A., Gorodetskaya I., Turner J., Agosta C., Codron F.

Nature Geoscience (2019) 338, 1-6

Recent major melting events in West Antarctica have raised concerns about a potential hydrofracturing and ice shelf instability. These events often share common forcings of surface melt-like anomalous radiative fluxes, turbulent heat fluxes and föhn winds. Using an atmospheric river detection algorithm developed for Antarctica together with surface melt datasets, we produced a climatology of atmospheric river-related surface melting around Antarctica and show that atmospheric rivers are associated with a large percentage of these surface melt events. Despite their rarity (around 12 events per year in West Antarctica), atmospheric rivers are associated with around 40% of the total summer meltwater generated across the Ross Ice Shelf to nearly 100% in the higher elevation Marie Byrd Land and 40–80% of the total winter meltwater generated on the Wilkins, Bach, George IV and Larsen B and C ice shelves. These events were all related to high-pressure blocking ridges that directed anomalous poleward moisture transport towards the continent. Major melt events in the West Antarctic Ice Sheet only occur about a couple times per decade, but a 1–2 °C warming and continued increase in atmospheric river activity could increase the melt frequency with consequences for ice shelf stability.

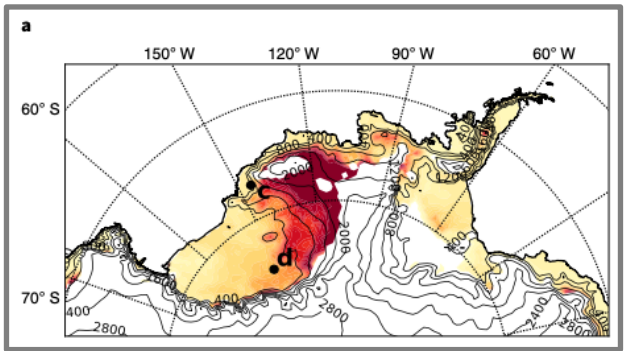

Fig. 1. Surface melt associated with atmospheric rivers (ARs) and average AR life cycle on landfall. (a) The percentage of total surface meltwater from 1979–2017 according to MAR that occurred when an AR made landfall and within 24 h after landfall during summer (December and January).

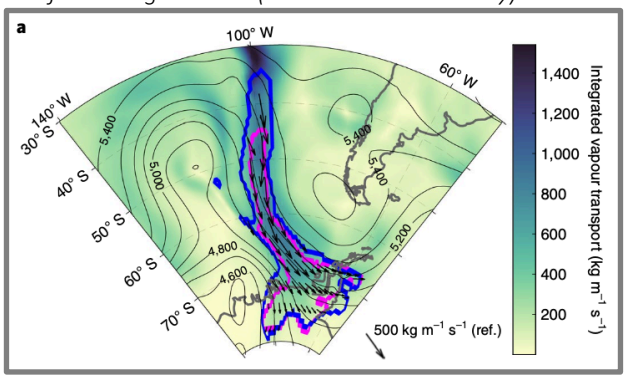

Fig. 2. Atmospheric variables associated with an AR that contributed to the 25–30 May 2016 melt event. The purple contours show the AR shape at the peak of the event at 12.00 (coordinated universal time) on 25 May 2016 with the spatial distribution of integrated vapour transport (IVT) from ERA-Interim. The contours represent the 500 hPa geopotential height contours (m) and the dark blue contour and black arrows represent the AR shape and AR IVT, respectively, according to a precedent Antarctic AR tracking algorithm.

Limited increase in tropospheric ozone since 1850 C.E

Yeung L.Y., Murray L.T., Martinerie P., Witrant E., Hu H.T., Banerjee A., Orsi A., Chappellaz J.

Nature *(2019)* 570*(7760)*, 224, 2019

Tropospheric ozone (O_3) is key component of air pollution and an important anthropogenic greenhouse gas. During the 20th century, proliferation of the internal combustion engine, rapid industrialization, and land-use change led to a global-scale increase in its concentrations, but the magnitude of this increase is not known. Atmospheric chemistry models typically predict an increase in the tropospheric O_3 burden of less than 50% since 1900, while direct measurements made in the late 19th century imply that surface O_3 mixing ratios increased by much more, up to 300%. Improvements in model chemistry have reduced disparities somewhat, but the accuracy and diagnostic power of the measurements remains controversial. Here, we place limits on the 20th-century increase in tropospheric O_3 using a record of the clumped-isotope composition of molecular oxygen ($^{18}O^{18}O$ in O_2) trapped in polar firn and ice. We find that proportions of $^{18}O^{18}O$ in O_2 decreased by 0.03 ± 0.02‰ below their 1590 – 1958 C.E. mean during the second half of the 20th century, implying that tropospheric O_3 increased less than 40% during that time. These results corroborate model predictions of global-scale increases in surface pollution and vegetative stress caused by increasing anthropogenic emissions of O_3 precursors. The radiative forcing due to tropospheric O_3 since 1850 C.E. is likely less than +0.4 W m-2, placing limits on the impact of air-quality regulation as a global warming mitigation strategy.

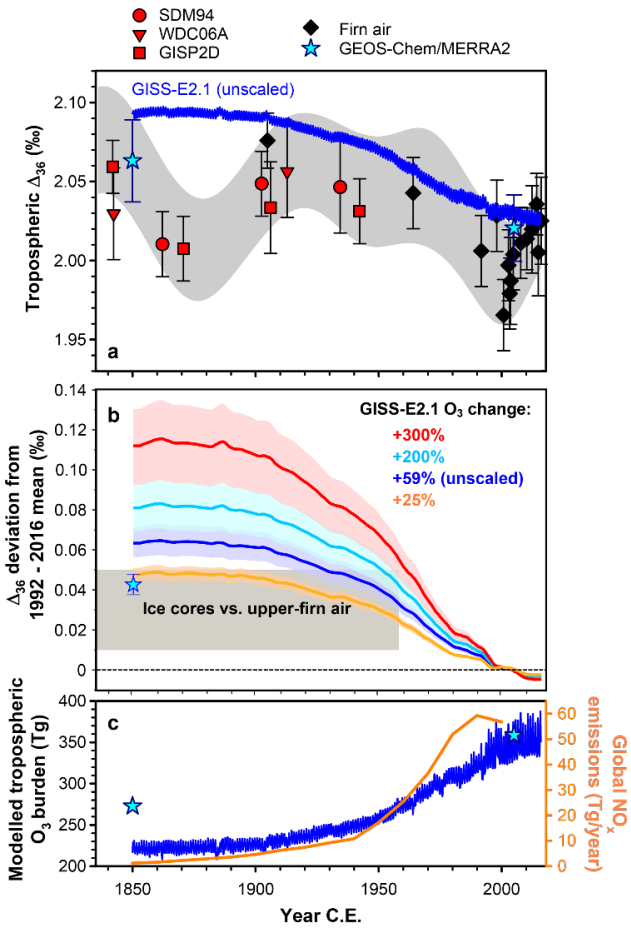

Figure : Measurement-model comparisons for increase in tropospheric O_3 since 1850 C.E. (a) Comparison of best-fit tropospheric history of Δ_{36} values (shaded area representing the 2σ-equivalent uncertainty envelope of the inverse firn/ice model results) with measurements (black and red points). Error bars represent 1 s.e.m. computed using the pooled 1σ uncertainty and the number of replicates for each sample. The firn data point at 1905 C.E. was excluded from best-fit calculations due to potential contamination (see main text), but it is shown here to illustrate general consistency between firn- and ice-core data. Also shown are tropospheric Δ36 predictions for 1850 C.E. and 2005 C.E. derived from the GEOS-Chem/MERRA2 model (cyan stars, with 1σ error bars corresponding to uncertainty in the stratospheric Δ36 input; see Methods) and the mean temporal evolution of the tropospheric Δ_{36} value derived from the GISS-E2.1 model (blue line). (b) Hypothesis tests for the global simulations showing compatibility with the firn- and ice-core data only when the O_3 increase since 1850 C.E. is limited, e.g., +25% for GISS-E2.1. Time-traces are 5-year moving averages and shaded areas represent 1σ uncertainty in the stratospheric Δ36 input. (c) Modeled increase in tropospheric O3 burden from the GEOS-Chem/MERRA2 (cyan stars) and GISS-E2.1 models (blue line), plotted with estimates of historical NOx emissions from ref. 29 (orange line).

… projets de thèse
… projets de post-doctorat

Apport de la géochimie et de la géochronologie à la compréhension de l'usage de l'instrumentarium moderne.

Durier, Marie-Gabrielle

Thèse de doctorat de l'Université Paris Saclay (2019-2021)
sous la direction de C. Hatté et S. Vaiedelich (Musée de la Musique)
Fondation PATRIMA

Le présent sujet de thèse ambitionne de lever les verrous scientifiques liés au positionnement chronologique de l'instrument de musique en ajoutant la datation ^{14}C à la palette d'approches classiquement utilisées et souvent insuffisantes. Au-delà de la poursuite de la construction d'une histoire de l'usage musical et des pratiques d'entretiens, de réparation ou de restaurations qui sont adressées à l'instrument de musique, elles consolideront l'émergence de concerts historiquement documentés.
La géochimie (^{13}C et Sr principalement) apportera des éléments sur les sources des matériaux utilisés.

L'originalité du projet réside dans l'implication de la muséologie, de la caractérisation des matériaux, de la chimie, de la mesure physique et des statistiques bayésiennes. L'apport espéré est donc à la fois méthodologique et expérimental. Le corpus d'instruments sur lesquels seront pratiqués les travaux, sera sélectionné au sein de la collection nationale du Musée de la musique. Ils se composent principalement de deux corpus, les archets anciens, d'une part, les petits instruments (violons et assimilés, luths, guitares.) choisis au regard de l'importante période d'usage dont ils témoignent et le nombre conséquent d'interventions de restaurations qui en sont la conséquence d'autre part. On espère enfin, par le développement d'une nouvelle méthodologie favoriser un intérêt futur de cette approche pour d'autres domaines du patrimoine culturel tel que celui du mobilier.

Le rôle de l'océan et son évolution chimique lors des variations rapides du gaz carbonique de l'atmosphère

Euverte, Romain

Thèse de Doctorat de l'Université de Paris-Saclay (en cours)
Direction : F. Bassinot et E. Michel
INSU/LEFE-SECOAB (E. Michel et F. Bassinot)

En période glaciaire, l'atmosphère contient 30% de dioxyde de carbone en moins que pendant les périodes interglaciaires. Des transferts de carbone importants depuis ou vers l'atmosphère sont observés lors de changements climatiques rapides. Le rôle de l'océan est encore mal contraint car nous manquons de données sur la préservation des carbonates sédimentaires marins et sur l'évolution de la chimie du carbone océanique associée à ces transferts (baisse/augmentation de pH). Nous proposons de reconstruire les variations du cycle océanique du carbone associées aux transferts océan-atmosphère (i) d'un part lors du dernier interglaciaire, plus chaud que l'Holocène avec une calotte Groenlandaise réduite, et (ii) d'autre part lors de la transition vers la période glaciaire caractérisée également par un changement de la circulation océanique. Pour cela, à partir de carotte sédimentaire marines, le doctorant (i) analysera les changements de préservation des carbonates profonds des sédiments océaniques ; (ii) reconstruira les concentrations en ion bicarbonate (associé au pH) de l'océan par la mesure par ICP-MS du rapport Bore/Calcium (B/Ca) des coquilles de foraminifères benthiques, et (iii) étudiera les variations de la production primaire. Ces données lui permettront de préciser les processus océaniques de régulation du dioxyde de carbone de l'atmosphère.

Variations climatiques et variations du cycle hydrologique aux basses latitudes au cours du Quaternaire: une approche combinant modèle et données

Extier, Thomas

Thèse de Doctorat de l'Université de Paris-Saclay (soutenue le 18 Octobre 2019)
Direction : A. Landais et D. Roche
ANR HUMI17

Le climat du Quaternaire est défini par une succession de périodes glaciaires et interglaciaires enregistrées dans les archives climatiques à différentes latitudes. La carotte de glace d'EPICA Dome C fournit un enregistrement haute résolution sur les derniers 800 ka du $\delta^{18}O_{atm}$ (i.e. $\delta^{18}O$ de la molécule d'oxygène de l'air) qui combine les variations passées du cycle hydrologique des basses latitudes et de la productivité de la biosphère. En l'absence du comptage des couches annuelles, ce proxy peut être utilisé comme méthode de datation orbitale des carottes de glace, en lien avec l'insolation au 21 juin à 65°N. Cependant, un décalage de 6 ka entre le $\delta^{18}O_{atm}$ et l'insolation, généralement observé lors des terminaisons glaciaires-interglaciaires, est appliqué sur l'ensemble de l'enregistrement lors de la construction de l'échelle d'âge. Ce décalage et la complexité du signal du $\delta^{18}O_{atm}$ expliquent l'incertitude élevée de 6 ka des carottes de glace, ce qui limite leur interprétation en termes de variations climatiques et environnementales conjointement à d'autres archives. J'ai donc développé une nouvelle chronologie pour les carottes de glace, basée sur le lien entre le δ18Oatm et le δ18Ocalcite des spéléothèmes est-asiatiques, à partir de nouvelles mesures isotopiques permettant d'avoir pour la première fois un enregistrement complet sur les derniers 800 ka à Dome C. Cette nouvelle chronologie permet de réduire les incertitudes par rapport à la chronologie actuelle et d'avoir une meilleure séquence des évènements entre les hautes et basses latitudes. J'ai ensuite développé un modèle simulant la composition isotopique de l'oxygène atmosphérique afin de répondre au manque d'interprétations quantitatives de ce proxy ainsi que pour vérifier son lien avec le $\delta^{18}O_{calcite}$ sur plusieurs cycles climatiques. Pour modéliser le $\delta^{18}O_{atm}$ nous avons dû coupler le modèle climatique de complexité intermédiaire iLOVECLIM avec le modèle de végétation CARAIB. Le $\delta^{18}O_{atm}$ simulé par le modèle couplé sur plusieurs dizaines de milliers d'années confirme que ses variations sont en phase avec celles de l'insolation de l'hémisphère Nord (hormis lors d'évènements de Heinrich) et avec celles du $\delta^{18}O_{calcite}$ via des modifications du cycle hydrologique des basses latitudes, impactant la composition isotopique de l'eau de pluie utilisée par la biosphère terrestre lors de la photosynthèse.

Evolution of heat storage and thermocline structure in the tropical Pacific Ocean and Indonesian Archipelago since the Last Glacial Maximum: New insights from combined paleo-temperature proxies and data/model comparisons.

Pang, Xiaolei

Thèse de Doctorat de l'Université Paris-Saclay (soutenue le 14 Octobre 2019)
Direction : F. Bassinot et S. Sépulcre (GEOPS)
INSU/LEFE-MAGICS (F. Bassinot)

This PhD work is aimed ultimately at improving our understanding of several proxies used for paleo-temperature reconstructions and providing good quality records of temperature changes since the Last Glacial Maximum in the upper ocean from three key areas of the Pacific tropical ocean (eastern and western Pacific, Indonesian Archipelago). The research plan follows a strategy with three main focuses:

(1) The comparison and careful evaluation (coherence with modern hydrographic data, potential calibration problems) of three temperature proxies (foraminifer assemblages, Mg/Ca from different planktonic shells and $\Delta 47$) measured ideally from (i) fresh material (plankton tows, sedimentary traps, water samples) and (ii) from core top material retrieved in the three main geographic area listed above..

(2) The multi-proxy reconstruction of paleo-temperatures on a few, top quality sedimentary records retrieved from our three main target areas in the tropical Pacific. The objectives will be: (i) to get good quality stratigraphic records ($\delta^{18}O$, $\delta^{13}C$) with a very good time control (AMS ^{14}C) down to the last glacial period; (ii) to derive low-resolution, multi-proxy paleo-temperature reconstructions since the LGM; (iii) to perform a special focus on key intervals (ie. LGM, H1, deglaciation events, early and mid-Holocene).

(3) The data will be carefully compared to numerical outputs obtained from the IPSL-CM model (used at LSCE for paleoclimate reconstructions) coupled with PISCES biogeochemical model. Data will be also compared to temperature reconstructions from other models used in PMIP (the international exercise of inter-model comparison). The LGM, early- and late-Holocene are primary interest periods for PMIP and there exists therefore a large set of GCM model runs. In addition, the deglaciation interval is being currently scrutinized by several modeling teams (including LSCE) through transient experiments with global climate models. During the course of the PhD, these transient runs should be available for comparison with temperature changes reconstructed from the deglaciation interval.

The IPSL-CM+PISCES model ouputs will be used to emulate the FORAMCLIM eco-physiological model for a more direct comparison with the foraminifer-based proxy reconstructions (foraminifer assemblages, Mg/Ca from different foraminifer planktonic species). The data model comparison will make it possible (i) to better understand potential causes for proxy discrepancies, and (ii) to help us interpreting our data in terms of heat storage and its evolution through time in response to radiative forcing and changes in the dynamics of the tropical Pacific thermocline. This data/model comparison will also provide the basis for a better evaluation of model capacities to reconstruct past temperature conditions of the tropical oceans.

… développements technologiques
… missions de terrain

Incubateur pour l'étude des flux à l'interface eau-sédiment

Bombled B., Villedieu A., Rabouille C., Brethous L., Lansard B.

En Mai juin 2018 le groupe COOL du LSCE) a réalisé, à bord du navire océanographique Tethys 2 (CNRS-INSU), la mission MissRhoDia 2 au large du Rhône. L'objectif de cette campagne était d'étudier les processus de minéralisation anaérobie de la matière organique (M.O.) dans les sédiments en début d'été, lorsque les transformations de la M.O. déposée au printemps sont encore très intenses. Au cours de cette campagne nous avons effectué, entre autre, des incubations de carottes à bord afin de mesurer les flux totaux d'échange (O_2,

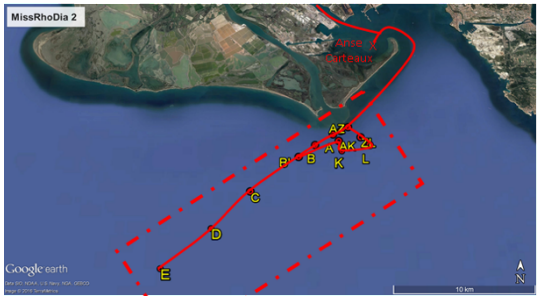

Alcalinité, Carbone inorganique dissous-DIC, , NH_4^+, ...) entre sédiment et eau. Cette manipulation, nouvelle au LSCE, a été rendu possible grâce à la fabrication "maison" d'un incubateur" miniaturisé".

Description :

1- Cryostat pour maintien de la température d'incubation à la température in-situ

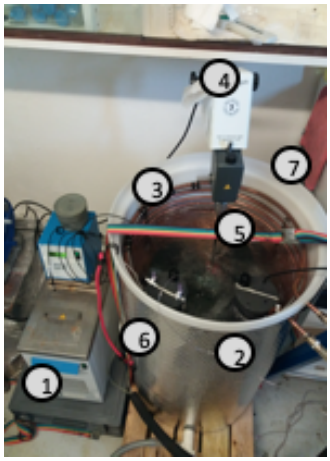

2- Bac d'incubation 100 l avec protection thermique. Capacité : 4 carottes de 9 cm de diamètre

3- Echangeur thermique relié au cryostat. 35 m de tube en cuivre de 1 cm de diamètre.

4- Moteur rotatif

5- Aimant rotatif

6- Carotte avec bouchon permettant une entrée et un prélèvement d'eau, le suivi de la teneur en oxygène et l'homogénéisation de l'eau superficielle

7- Fibre optique pour µ-optode PreSens, pour le suivi de la teneur en oxygène dans l'eau superficielle au cours de l'incubation

Principe :

Lorsqu'un sédiment est isolé de son environnement, on peut mesurer dans l'eau surnageante les effets des flux

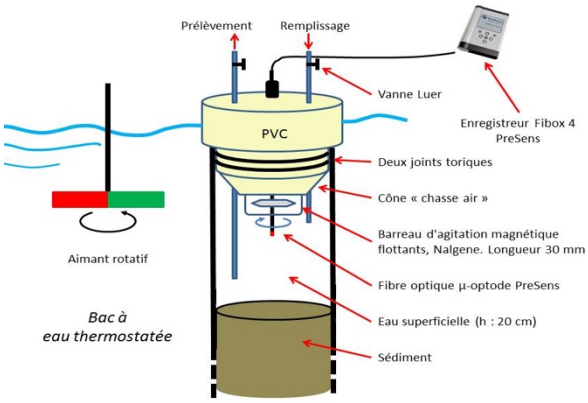

d'éléments chimiques (Alcalinité, DIC, O_2, NH_4^+, ...) échangés entre l'eau et le sédiment qui sont le résultat des

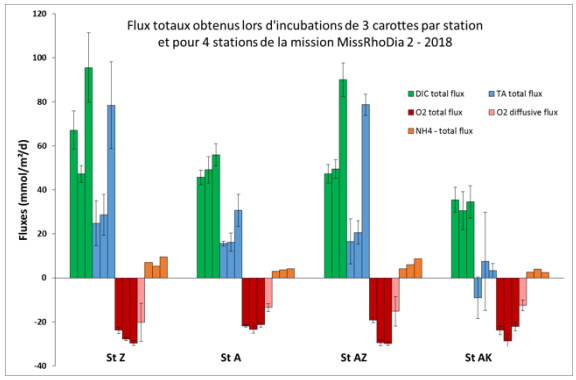

processus biogéochimiques de transformation de la matière dans les sédiments. Ces mesures impliquent des prélèvements, à temps réguliers, ou des suivis de capteurs.

Conclusion :

Ce nouvel incubateur vient renforcer la capacité d'étude du devenir du carbone organique et inorganique dans les milieux aquatiques et plus particulièrement dans les milieux côtiers, les deltas et les estuaires, par le groupe COOL. Par sa petite taille, il permet de palier avantageusement à l'absence d'un Lander pourvu d'une chambre benthique in situ et au fonctionnement possiblement délicat. Lors de la mission MissRhoDia2 le groupe COOL a effectué des incubations de plusieurs heures sur neuf stations et se félicite de la moisson de données originales et uniques que ce dispositif a fournies. A l'avenir nous imaginons l'utiliser lors d'études aussi diverses que celles déjà engagées sur la lagune de Venise ou bien encore dans les mangroves de Guyane, mais également, pourquoi pas, pour l'étude de la respiration de coraux.

Raid EAIIST – mesures isotopiques

Casado M., Leroy-Dos Santos C., Fourré É., Prié F., Landais A., Savarino J., Stenni B.

Mission de terrain, 2019
ANR EAIIST, programme ANTARCTIC-SNOW

Du 5 décembre 2019 au 25 janvier 2020, une équipe franco-italienne parcourt 1318 km en aller-retour au centre du plateau Antarctique, au départ de la station Concordia. Le but est de mieux déchiffrer les archives climatiques et prévoir la hausse du niveau marin.
Le LSCE est en charge sur ce raid des mesures isotopiques de la vapeur d'eau, de la neige de surface et des carottes de glace afin de mieux interpréter les signaux isotopiques dans les carottes profondes à faible taux d'accumulation du plateau Est Antarctique. Dans ce but, M. Casado a installé sur le raid un instrument de mesure isotopique de la vapeur d'eau en continu. Cet instrument a été calibré sur la station côtière de Dumont d'Urville, installé sur le raid scientifique (Figure 1) puis M. Casado a suivi la stabilité des mesures lors du déplacement de la caravane scientifique en assurant le raid scientifique en amont de Concordia, c'est-à-dire pendant 10 jours de conduite entre Cap Prudhomme et la station Concordia. Le système installé (Figure 2) s'est avéré stable vis-à-vis des vibrations. Des données de bonne qualité sont donc attendues au retour du raid en fin d'année 2020.

Fig. 1. Le raid en route.

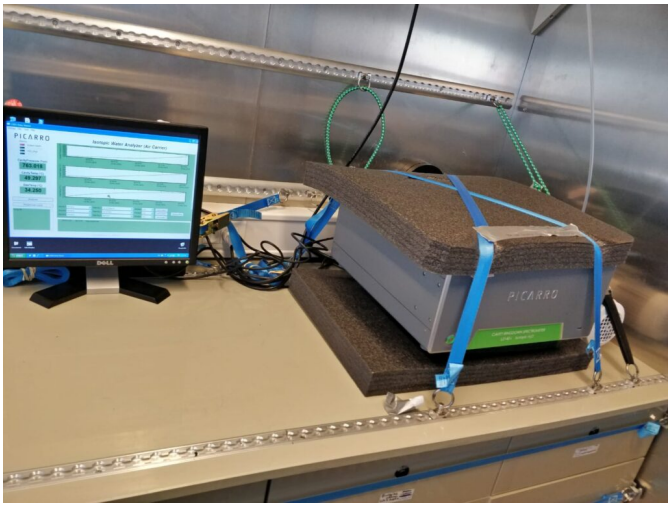

Fig. 2 : Installation de l'instrument de mesure de la composition isotopique de la vapeur d'eau dans la caravane scientifique

Deux missions en Antarctique pendant l'été austral 2018-2019

Leroy Dos Santos C. & Landais A.

Projet/financement: Antarctic-Snow (Fondation Albert 2 de Monaco), EAIIST (ANR) COMBINISO (ERC), NIVO2 et ADELISE (IPEV) ; ADELISE (CNRS)

Lors de l'été austral 2018-2019, Amaëlle Landais et Christophe Leroy Dos Santos ont installé deux instruments de spectroscopie optique sur les sites antarctiques de Dumont d'Urville site côtier) et de Concordia (site isolé sur le plateau Est Antarctique, -54°C en température moyenne annuelle). Ces instruments sont couplés à des générateurs d'humidité spécialement développés et construits au LSCE au premier semestre 2018 pour fonctionner à très basse humidité. Ces instruments vont rester sur place pendant au moins 2 ans et enregistrer en continu la composition isotopique de la vapeur. En parallèle, de nombreux prélèvements de neige de surface, de subsurface et de précipitations sont effectués et analysés au LSCE pour leur composition isotopique.

Le but scientifique est de comprendre la signature isotopique archivée dans les carottes de glace dans ces deux régions de l'Antarctique de l'Est. En effet, en l'absence d'enregistrement météorologique, l'analyse des isotopes de l'eau est l'unique moyen de reconstruire et de comprendre la variabilité climatique et la dynamique du cycle hydrologiques des derniers siècles en Antarctique, une donnée essentielle pour l'évolution du bilan de masse de surface de la calotte Antarctique.

Trois campagnes pilotes d'un mois pendant l'été austral avaient été effectuées avant ce déploiement pour plusieurs années. Elles avaient notamment démontré la faisabilité de telles mesures (Casado et al., 2016), l'enregistrement par les isotopes de l'eau des échanges entre l'atmosphère et la neige de surface sur le site de Concordia (Casado et al., 2018) et l'influence des vents catabatiques sur la composition isotopique de la vapeur d'eau sur le site de Dumont d'Urville (Bréant et al., 2019).

Fig: Christophe et Amaëlle devant le mat de prélèvement à Dumont d'Urville

Développement d'une ligne d'extraction de l'air de la glace pour mesures de 81Kr pour datation absolue de la vieille glace

Prié F., Fourré É, Landais A.

Projet/financement: H2020 BE-OI, franco-russe VOICE

La datation des carottes de glace est essentielle pour fournir des enregistrements de référence du climat et de la concentration en gaz à effet de serre. Cependant très peu de méthodes permettent de dater les carottes de glace de façon absolue, en particulier pour les longues échelles de temps (plusieurs centaines de milliers d'années).

Dans ce cadre, le développement récent de la mesure du 81Kr, élément radioactif avec une demi-vie de 229000 ans, est essentiel. Cependant cette mesure nécessite une instrumentation très lourde (piège magnéto-optique) qui existe actuellement uniquement dans 2 laboratoires au monde. Nous avons construit un partenariat avec l'un de ces centres (Université de Hefei, Chine) pour effectuer ce type de mesure sur de l'air extrait des carottes de glace. A cause de la faible quantité de ^{81}Kr dans l'atmosphère, les quantités de glace nécessaires à cette mesure pour atteindre un niveau de précision sur l'âge absolu de 10% sont énormes: 6 à 10kg.

Nous avons donc développé une méthode permettant d'extraire l'air de grosses quantités de glace (possibilité d'extraire l'air de 20 kg de glace). Ce système a été testé et validé en avril 2019 et appliqué à de la glace du fond des carottes de TALDICE et de EPICA Dome C.

Figure: Système d'extraction de l'air de grosses quantités de glace pour mesure de la composition isotopique du krypton et datation absolue des carottes de glace.

… projets scientifiques

Choix du site de forage pour le forage Beyond EPICA et analyse préliminaire des premiers 120 m

Ritz C., Parrenin F., Landais A., Pantiga A., Minster B., Prié F., Orsi A., Fourré E. and the whole BEYOND EPICA group, 2019

Projet Beyond EPICA

L'objectif du projet Beyond EPICA est l'obtention d'une carotte de glace de 1.5 million d'années dans la zone de la station franco-italienne de Concordia. De nombreux profils radar et suivis d'isochrones ont été effectués au cours des 4 dernières années avec le déploiement d'un dernier radar en début de saison 2019-2020.

Le choix du site de forage a été effectué en fonction de trois critères principaux : absence de mélange stratigraphique d'après les isochrones, absence de fusion à la base de la calotte, résolution maximale autour de 1.5 million d'années.

L'isochrone la plus profonde identifiée est celle de 415 ka. Le site choisi est celui dont la résolution modélisée à 1.5 million d'années est la plus grande (14000 – 15000 ans / an). Il s'agit du site « Patch B / subglacior » (Figure 1).

Un premier forage de 120 m a été effectué sur ce site pendant la saison 2017-2018. Les analyses d'isotopes de l'eau et de composition élémentaires de gaz dans la zone de piégeage ont été effectuées au LSCE pendant l'automne 2019. Ces données (Figure 2) permettent de démontrer que les conditions de température à la surface des derniers 2000 ans sont similaires sur ce site et sur la station Concordia située à 40 km. En revanche, la fermeture des pores à la base du névé se fait sur une épaisseur plus faible sur le site « Patch B / subglacior » que sur le site de Concordia où la carotte de Dome C a été forée. Ce résultat est en accord avec les premières indications d'un taux d'accumulation significativement plus bas sur le site « Patch B / subglacior ».

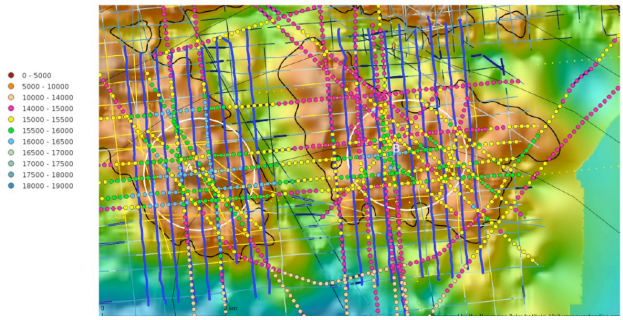

Fig.1: Résolution temporelle au niveau de profondeur correspondant à l'âge A.5 million d'années (modélisation F. Parrenin , IGE)

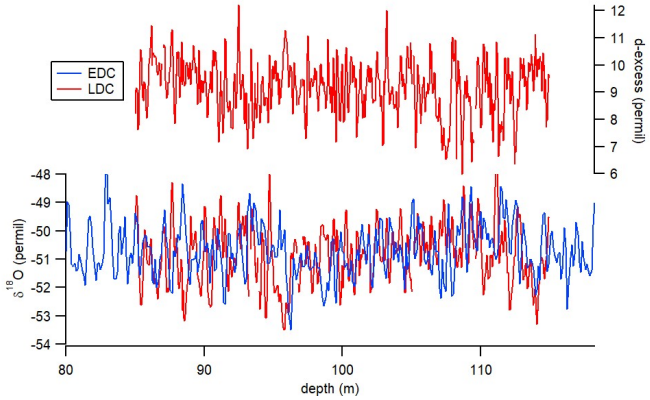

Fig.2: Mesures isotopiques à haute résolution sur la carotte test forée à « Patch B / Subglacior » (LSCE)

CITRON-GLACE : Circulation Intermédiaire dans l'Océan iNdien depuis le dernier maximum GLACiairE

S. Sépulcre (GEOPS) en collaboration avec LSCE (F. Bassinot) et le CEREGE (L. Licari).

projet INSU/LEFE/IMAG0, 2017-2019

La géochimie élémentaire et isotopique des foraminifères benthiques et planctoniques constitue un outil puissant permettant de reconstruire les variations des conditions de surface (foraminifères planctoniques) et de fond (foraminifères benthiques) des océans depuis le Dernier Maximum Glaciaire.

Le projet CITRON-GLACE vise à mieux contraindre le rôle de la circulation océanique dans les modalités de transfert de chaleur et de sel entre basses et hautes latitudes pendant les Terminaisons glaciaire-interglaciaire. Il se focalise autour de la reconstitution de la circulation des masses d'eau intermédiaire de l'Océan Indien depuis le Dernier Maximum Glaciaire.

Ce projet est applique une approche multi-traceurs 1) Assemblages de foraminifères benthiques (niveau trophique, concentration en oxygène) ; 2) $\delta^{18}O$ et δ13C (stratigraphie, salinité, teneur en nutriments) ; 3) Rapports élémentaires (Cd/Ca : nutriments, Mg/Ca : température, B/Ca, Sr/Ca et U/Ca : [CO32-]) ; 4) $\Delta^{14}C$ (ventilation) et 5) εNd (source)

Le projet CITRON-GLACE associe trois laboratoires partenaire (GEOPS, LSCE, CEREGE) et s'appuie sur un travail de thèse en cours (Ms. Ruyfan Ma).

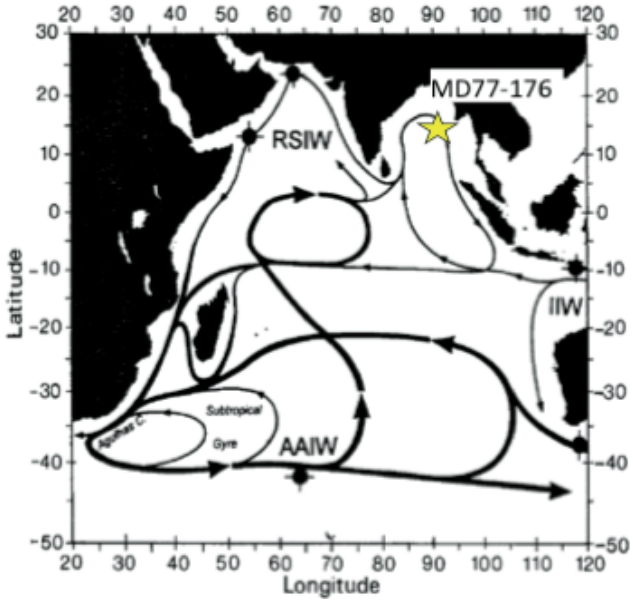

Figure : Localisation de la carotte MD77-176 étudiée dans le cadre du projet CITRON-GLACE.

SECOAB: Cycle océanique du carbone lors du dernier cycle climatique et réponse sédimentaire: l'apport du rapport B/Ca et du $\delta^{13}C$ des foraminifères benthiques

Michel E., Bassinot F., Euverte R., Paillard D., Bouttes N.

Projet INSU LEFE IMAGO - SECOAB (2018-2020)

En période glaciaire, l'atmosphère contient 30% de dioxyde de carbone en moins que pendant les périodes interglaciaires. Des transferts de carbone importants depuis ou vers l'atmosphère sont observés au cours des entrées/sorties de glaciation et lors de changements climatiques rapides. De nombreux mécanismes tant physiques que biologiques et chimiques ont été proposés pour expliquer ces transferts de carbone entre l'océan et l'atmosphère. L'addition de ces mécanismes permet d'expliquer les variations observées du CO_2 atmosphérique mais le manque de connaissances concernant les variations du cycle océanique du carbone ne permet pas de déterminer les mécanismes qui ont réellement joué un rôle au cours du dernier cycle climatique.

L'objectif du projet SECOAB est de documenter les variations de concentrations en $[CO_3^{2-}]$ des eaux profondes en utilisant le traceur B/Ca pour deux séries sédimentaires à fort taux de sédimentation, parfaitement contraintes stratigraphiquement, prélevées dans des zones clés de l'océan : le bassin Pacifique qui représente l'évolution moyenne de l'océan global, et l'océan austral siège d'un bon nombre des mécanismes proposés pour les échanges océans-atmosphère. La comparaison de ces données aux enregistrements $\delta^{18}O$ et $\delta^{13}C$ des foraminifères benthiques (climat, circulation/échange entre les réservoirs), ainsi qu'aux enregistrements de retraçant la variabilité locale de la productivité (ie. teneurs en Barium, en Brome, en Calcium et en Silicium obtenues par mesures XRF) permettra d'améliorer notre connaissance des réorganisations océaniques du cycle du carbone qui accompagnent les échanges océan-atmosphère lors des déglaciations et des entrées en glaciation. Parallèlement, un modèle en boite du cycle océanique du carbone (BoxKit, Paillard et al. 1993, Michel et al. 1995), comportant un module sédimentaire (Russon et al 2010), sera utilisé pour tester les effets temporels conjoints en $[CO_3^{2-}]$ et $\delta^{13}C$ des différents processus physiques et bio-géochimiques proposés pour les variations du carbone atmosphérique. Ces tests permettront d'analyser aisément les effets de plusieurs processus agissant de manière synchrone ou avec des décalages temporels variables. Enfin l'évolution du cycle du carbone océanique ainsi reconstruite pour le dernier cycle climatique pourra être comparée à une simulation avec le modèle de complexité intermédiaire iLOVECLIM qui comporte désormais un compartiment sédimentaire océanique. Ce modèle comporte un cycle du carbone et calcule la distribution de son isotope $\delta^{13}C$. Il sera donc possible de comparer directement données et simulation numérique. Ce projet s'appuie sur la thèse de R. Euverte, (thèse « phare » CEA, 11/2017-2020)

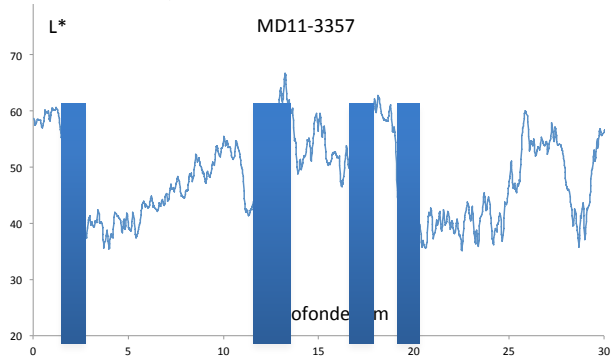

Figure : Carotte sédimentaire de l'océan Austral avec les périodes qui seront étudiées à plus haute résolution

THEMES : THE Mystery of the Expanding TropicS

PI : Valérie Daux

Partners' institutions : LSCE, FR; LOCEAN, FR. IANIGLA-CONICET, AR; Univ. St Andrews, GB; LDEO, USA; UACh, CL. (2018-2020)

More frequent droughts, compared to the historical period, have been recorded during the past 30-40 years in subtropical western South America (SWSA; Fig. 1). Drought has a more direct and immediate impact on humans and ecosystems than temperature changes, but modelling of future hydroclimatic changes is problematic and current climate models have large deficiencies in simulating such variability.

Subtropical climate is largely related to the downward branch of the Hadley Circulation (HC). The descending arm of the HC circulation can be considered the "edge of the tropics". During recent decades, the HC has expanded towards the poles likely in response to anthropogenic global changes, shifting rainfall patterns and broadening the subtropical dry zones, especially in the Southern Hemisphere (SH). Over the last 40 years, this expansion has been estimated to be 1-3° latitude in each hemisphere. These trends in HC expansion are projected to continue through the 21st century. However, the underlying mechanisms of this phenomenon are not well known nor the magnitude of this long-term change. Indeed, several relevant issues, such as the fraction of HC expansion, the causes of the HC broadening (natural, anthropogenic or both), the variability of HC expansion-contraction fluctuations in the past, and the future expansion rates of the subtropical deserts, need to be investigated. The knowledge gaps are partially ascribed to the shortness of observational records documenting changes in large-scale tropical-extratropical atmospheric circulation.

In this context, the overarching aim of the THEMES project is to build a multi-century perspective of HC dynamics using tree-ring records along the America cordillera sector of the SH, extending the analysis of large-scale atmospheric teleconnections beyond the short record provided by instrumental data. The specific objectives are to: (1) Update and develop new tree-ring records along the Andes extending from the outer tropics in the Altiplano (17-23°S), via Central Chile (32-36°S), to northern Patagonia (37-45°S). In addition to traditional ring-width measurements, state-of-the-art techniques in dendroclimatology will be used to develop isotopic and Blue Intensity annual records; (2) Based on these data, provide robust regional reconstructions of hydroclimate and temperature, as well as the latitudinal position and intensity of the HC along SWSA; (3) Characterize the patterns and processes underlying the 20th century amplitude and recurrence of droughts in the subtropical Andes, quantifying the relative importance of the HC expansion upon these events, and (4) Combine instrumental records, reanalysis data, past reconstructions of HC, and ensembles of model simulations to assess the mechanisms underlying changes in hydroclimate induced by the HC for the years 1600 to 2100. By addressing these objectives, THEMES will provide future hydroclimate scenarios that contribute to future socio-economic planning and adaptation strategies in SWSA.

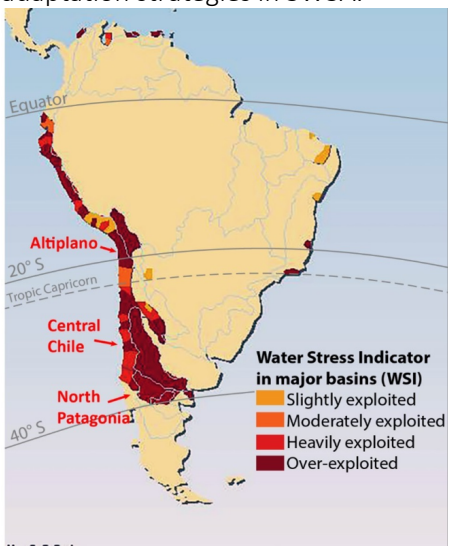

Fig. 1 :The study region Climate change threatens water ressources in the dry subtropics of Western South America to a degree that is probably unmatched anywhere else in the continent. A Water stress Indicator for South America, based on current conditions, shows widespreas stress in much of western Peru, western Bolivia, most northern and Central Chile and the adjacent territories in western Argentina. Source: UNEP (2008)

… prix
… récompenses

Catherine Kissel a reçu la médaille Petrus Peregrinus 2019 de l'Union européenne des géosciences (EGU).

La médaille Petrus Peregrinus 2019 a été décernée à Catherine Kissel pour sa contribution exceptionnelle au paléomagnétisme, appliquée à la compréhension du champ magnétique terrestre, du paléoclimat, de la paléo-océanographie et de l'évolution géodynamique des marges méditerranéennes.

Les travaux de Catherine Kissel couvrent un large éventail d'applications du paléomagnétisme et du magnétisme des roches à l'étude de la tectonophysique, du comportement des champs géomagnétiques, de la paléo-océanographie et du paléoclimat.

Elle a fourni une nouvelle interprétation de l'évolution de la zone de subduction en Méditerranée orientale, inspirant une génération de géologues structuraux. Elle a montré que la courbure de l'arc égéen était un processus rapide et géologiquement récent lié à l'évolution géodynamique de la zone de subduction adriatique.

Elle a également étudié l'évolution du champ magnétique terrestre pendant le Pléistocène supérieur et l'Holocène. Elle a contribué à des études fondamentales sur les excursions géomagnétiques, en particulier sur l'événement de Laschamp, qui est devenu un repère clé dans les sédiments et les carottes de glace.

La chercheuse a ensuite entrepris des études pionnières sur les propriétés magnétiques des sédiments marins pour caractériser les variations des courants océaniques et du climat du passé. Elle a pu déterminer la provenance des sédiments dans la mer de Chine méridionale et dans l'Atlantique Nord. Elle a montré, à partir de l'analyse des propriétés magnétiques des sédiments de carottes des grands fonds marins, que les changements climatiques rapides sont liés aux changements dans la circulation marine des grands fonds. Elle a également utilisé les propriétés magnétiques des sédiments de la baie du Bengale pour décrire comment l'érosion dans l'Himalaya a changé avec le temps et pour extraire des informations sur les moussons.

Elle a dirigé plusieurs grandes collaborations internationales et interdisciplinaires axées sur les reconstructions paléo-environnementales, tout en faisant progresser de nouvelles applications de la minéralogie magnétique et du paléomagnétisme. Au cours des deux dernières décennies, ces collaborations ont englobé une douzaine d'expéditions océanographiques auxquelles elle a participé en tant que scientifique et souvent chef de mission.

Valérie Masson-Delmotte reçoit la médaille d'argent du CNRS

La médaille d'argent du CNRS a été remise à Valérie Masson-Delmotte en novembre 2019.
(article du journal du CNRS)

Climatologue au Laboratoire des sciences du climat et de l'environnement, spécialisée dans l'étude des variations climatiques passées, la compréhension du cycle de l'eau et l'évaluation des modèles de climat. "L'objet de mes recherches est de quantifier les variations climatiques passées, en comprendre les mécanismes et utiliser ces informations pour évaluer les modèles de climat et la confiance dans les projections d'évolutions futures. J'ai notamment participé à deux programmes internationaux qui ont permis de caractériser la variabilité du climat du Groenland au cours des 130 000 dernières années. Nous avons ainsi caractérisé les mécanismes d'amplification polaire et la contribution de la calotte du Groenland au haut niveau marin de la dernière période interglaciaire, en réponse aux variations de l'orbite de la Terre. Beaucoup de questions restent ouvertes pour comprendre l'ensemble des variations climatiques passées, en particulier les changements abrupts et leurs implications pour l'évolution future du climat climat."

Valérie Masson-Delmotte a reçu la médaille Milutin Milankovic (EGU) le 22 octobre 2019.

This medal was established by the Climate: Past, Present & Future Division in recognition of the scientific and editorial achievements of Milutin Milankovic. It is awarded to scientists for their outstanding research in long-term climatic changes and modelling

(article Sciences et Avenir)

Valérie Masson-Delmotte, vice-présidente du groupe 1 du GIEC en 2015, a reçu le 22 octobre 2019 la Milutin Milankovitch Médaille, une récompense annuelle de l'Union européenne des géosciences (EGU) et décernée aux scientifiques pour la recherche en cours dans le domaine du changement climatique à long terme.

… autres valorisations

Quelle histoire se cache dans ces grains de sable ?

Nathalie Picard (avec intervention de Jérémy Jacob)

Ça m'intéresse Août 2019

Dans son numéro d'août 2019, la revue Ca m'intéresse relate la découverte des Mario Wannier et de ses co-auteurs. Dans les sables des plages d'Hiroshima, les auteurs ont identifié des particules exotiques dont ils attribuent l'origine aux matériaux produits par l'explosion de la bombe nucléaire sur la ville d'Hiroshima le 6 août 1945. Jérémy Jacob, chercheur CNRS au Laboratoire des Sciences du Climat et de l'Environnement et spécialiste de l'Anthropocène, a été sollicité pour donner son avis sur cette découverte originale.

Références : Wannier, M.M.A., de Urreiztieta, M., Wenk, H.R., Stand, C.V., Tamura, N., Yuec, B., 2019. Fallout melt debris and aerodynamically-shaped glasses in beach sands of Hiroshima Bay, Japan. Anthropocene 25. DOI:10.1016/j.ancene.2019.100196

QUELLE HISTOIRE SE CACHE DANS CES GRAINS DE SABLE ?

Rien, sur cette plage de carte postale, ne pourrait laisser penser qu'un épisode tragique de l'Histoire s'est joué ici. Rien, si ce n'est quelques grains de sable. Car nous sommes sur la péninsule de Motoujina, dans la baie d'Hiroshima, au Japon. En 2015, alors qu'il étudiait la faune microscopique dans le sable, le géologue Mario Wannier remarqua de singulières particules : des sphères vitreuses aux formes effilées, des grains caoutchouteux… D'où venaient ces débris mesurant à peine 1 millimètre ? Des scientifiques de l'université de Berkeley (Etats-Unis) ont analysé quelque 10 000 échantillons collectés aux alentours d'Hiroshima : tamisage, granulométrie, observation au microscope… Résultat : ils se distinguent des minéraux environnants par leur composition chimique (silice, aluminium, calcium, fer…). Certains ressemblent à première vue à des particules formées lors d'impacts de météorites, mais elles n'ont pas la même composition. D'autres contiennent les mêmes éléments que les matériaux de construction utilisés par l'homme (béton, marbre, brique…). Il s'agit en réalité des traces résiduelles de l'attaque atomique qui a littéralement pulvérisé la ville d'Hiroshima le 6 août 1945 ! Selon les résultats publiés dans *Anthropocene Review* début 2019, ces objets se seraient formés dans le nuage atomique, à haute pression et à des températures supérieures à 1 800 °C, avant de retomber en pluie. Il reste cependant plusieurs zones d'ombre. Ces particules sont-elles radioactives ? Comment se distribuent-elles dans l'espace ? « Prélever une carotte de sédiments dans la baie d'Hiroshima permettrait sûrement de déceler une couche datée de 1945 dans laquelle ces débris seraient concentrés », note Jérémy Jacob, chargé de recherche CNRS au Laboratoire des sciences du climat et de l'environnement. Une étude similaire pourrait être menée dans les environs de Nagasaki, cible, trois jours après Hiroshima, du deuxième bombardement atomique de l'Histoire par les Etats-Unis. N. P.

724 953 impacts de foudre et 296 jours d'orage : 2018 a été l'année la plus **orageuse** en France depuis la création de Météorage il y a trente ans. Avec **60 335 éclairs,** le 6 août 1999 reste la journée record de **foudroiement.**

LA FOUDRE EST-ELLE RADIOACTIVE ?

En février 2017, lors d'un orage, des scientifiques japonais ont réussi à observer un flash de rayons gamma associé à un éclair. Puis d'étonnantes particules de lumière ont surgi : leur énergie témoignerait de la destruction totale des électrons (particule de matière à charge négative) et des positron (« jumeaux » à charge positive), lesquels proviendraient de la transformation d'atomes radioactifs. Preuve que la foudre pourrait déclencher des réactions nucléaires. N. P.

28 QUESTIONS & RÉPONSES AOÛT 2019

Des chercheurs se penchent sur les climats passée pour mieux prédire l'avenir

Sciences et Avenir avec AFP (avec intervention de V. Daux, A. Orsi, C. Hatté, M. Kageyama D. Roche)

Sciences et Avenir (29.11. 2019)

En France, des équipes de recherche, reconnues au niveau international, travaillent sur les climats passés, leur impact sur les écosystèmes et la modélisation des climats.

"Nous sommes obligés d'aller dans le passé"

A Saclay, le bâtiment ICE regroupe 300 personnes du Laboratoire des sciences du climat et de l'environnement (LSCE: CEA/CNRS/UVSQ). Des équipes de pointe, reconnues au niveau international, travaillent sur les climats passés, leur impact sur les écosystèmes et la modélisation des climats. "*Ce qui nous intéresse, c'est de comprendre comment le climat fonctionne*", explique Didier Roche, directeur adjoint du LSCE et chercheur au CNRS. Comme il n'existe des mesures directes que depuis environ 70 ans, "*nous sommes obligés d'aller dans le passé*", poursuit-il. Ils se basent sur des carottages de glace, de sédiments marins ou lacustres, d'arbres...

Dans le cadre d'un projet européen, EPICA (European Project for Ice Coring in Antarctica), une carotte de glace de 3.270 mètres a été extraite de la calotte qui recouvre le continent antarctique, permettant d'établir la teneur de l'atmosphère en dioxyde de carbone et en méthane sur 800.000 ans. La glace offre "*plusieurs traceurs dans une même archive*", indique la paléoclimatologue Anaïs Orsi en présentant des petits glaçons vieux de plusieurs centaines, voire milliers d'années, remplis de petites bulles d'air. "*On peut reconstituer la composition de l'atmosphère", mais aussi grâce aux poussières "s'il y avait beaucoup de feux de forêt en Patagonie" ou "l'aridité en Australie*", détaille la chercheuse au CEA (Commissariat à l'énergie atomique).

Les arbres sont aussi de bons enregistreurs des variations climatiques. "*Ils peuvent nous renseigner sur la température, l'ensoleillement, l'humidité*", expose Valérie Daux, professeure de l'Université Versailles-Saint Quentin en Yvelines. Elle participe à un projet en Patagonie qui permet de remonter dans le temps sur 200 ans grâce aux cernes (anneaux de croissance) d'arbres, des cyprès de Fitzroy, qui projette d'aller jusqu'à 1.000 ans.

Un autre axe de recherche est de voir "*à quelle vitesse un écosystème peut s'adapter à un changement climatique*", en s'aidant du carbone 14, raconte Christine Hatté, chercheuse au CEA.

Avoir des modèles les plus fiables possibles est essentiel face au changement climatique

En parallèle, des scientifiques modélisent les climats du passé, c'est-à-dire qu'ils tentent de les reproduire à partir d'un logiciel très complexe, à partir de certains éléments (atmosphère, océans, hydrologie, végétation...). Ils comparent ensuite leurs modèles aux données récoltées par leurs collègues via les échantillons. "*Nous pouvons regarder si chaque modèle est bon par rapport aux données*", explique Masa Kageyama, directrice de recherche au CNRS, responsable de la modélisation au LSCE. Ceci permet "*de sélectionner les modèles pour le futur*". Avoir des modèles les plus fiables possibles est essentiel face au changement climatique. Les scientifiques français du Centre national de la recherche scientifique (CNRS), du Commissariat à l'énergie atomique (CEA) et de Météo-France participent aux travaux servant de base au GIEC, les experts climat de l'ONU.

Si les émissions se poursuivent au rythme actuel, la planète pourrait se réchauffer de 3,4 à 3,9°C d'ici la fin du siècle, selon le Programme des Nations unies pour l'environnement (PNUE). Et même si les Etats signataires de l'accord de Paris respectent leurs engagements, le mercure montera de 3,2°C. Une hausse de 6 à 8°C par rapport à la période pré-industrielle correspondrait à "*des climats comparables à l'époque des dinosaures (disparus il y a 66 millions d'années) avec des températures très chaudes*" mais la comparaison est difficile et ces climats sont moins bien connus car "*les continents étaient différents et pas à la même place*", dit Didier Roche. Les paléoclimatologues connaissent en revanche mieux les climats qui sévissaient il y a 21.000 ans, quand la température moyenne mondiale était de 3 à 4 degrés plus froide. A cette époque, "*il y avait un kilomètre d'épaisseur de glace à New York, trois kilomètres en Norvège, le niveau de la mer était 120 mètres plus bas*", décrit le chercheur. "*Nous avons perturbé le climat très fortement et sur un temps très court. Plus on continue, plus ça change*", avertit-il.